The role of intrinsic neuronal excitability for Prelimbic network function

Rafael de Sa

université de BORDEAUX

THESIS SUBMITTED FOR THE DEGREE

DOCTOR OF PHYLOSOPHY

UNIVERSITY OF BORDEAUX

DOCTORAL SCHOOL : Life and Health Sciences

SPECIALITY : NEUROSCIENCE

By Rafaël DE SA

The role of intrinsic neuronal excitability for Prelimbic network function

Supervisor : Dr. Andreas FRICK

13/09/2019

Dr. Coutureau, Etienne Bordeaux, FRANCE President
Dr. Pietropaolo, Susanna Bordeaux, FRANCE Reviewer
Prof. Ramaswami, Mani Dublin, IRELAND Reviewer
Dr. Schubert, Dirk Nijmegen, NETHERLANDS Reviewer

Titre : Le role de l'excitabilité neuronale intrinsèque pour les fonctions du réseau pré-limbique

Résumé: Le but de ce travail était de caractériser les propriétés intrinsèques, la morphologie, la connectivité et le profil transcriptomique des neurones pré-limbiques (PL) de la couche 5 exprimant les récepteurs Dopamine 1 (D1R) ou 2 (D2R) chez des souris de type sauvage (WT). Nous avons ensuite décidé d'utiliser la base de données précédente pour déterminer le déficit de ces deux sous-populations dans le modèle de souris *Fmr1*-KO du syndrome de l'X fragile (SXF). Le dernier objectif a été d'étudier une voie neuronale spécifique allant des neurones pré-limbique et qui projettent vers l'amygdale basolatérale. Nous avons déterminé la plasticité qui se produit après la formation de souvenirs de peur.

Dans la première partie de notre étude, nous avons effectué une classification distincte des neurones D1R et D2R WT de la couche 5 PL en fonction de leurs propriétés intrinsèques. Nous avons également déterminé des propriétés morphologiques spécifiques ainsi que des connexions préférentielles de type cellulaire avec d'autres zones du cerveau. L'analyse du séquençage de l'ARNm a révélé plus de 500 gènes différemment exprimés entre D1R et D2R WT divisés en différentes catégories telles que les gènes des canaux ioniques. La création de cette base de données nous a permis de poursuivre notre étude.

Dans la deuxième partie, nous avons déterminé que le déficit des neurones D1R et D2R KO était dû à la perte de la protéine FMRP chez le modèle de souris SXF *Fmr1*-KO. Le SXF est la forme la plus fréquente de retard mental hérité et la plus fréquente d'autisme, conduisant à des déficits d'apprentissage et de mémoire, à un comportement répétitif, à des convulsions et à une hypersensibilité à des stimuli sensoriels (par exemple visuels). La modulation de la dopamine est modifiée dans ce modèle et nous avons voulu caractériser à quel niveau cette modification s'effectue. Nous avons observé des différences de propriétés intrinsèques entre D1R et D2R KO, qui n'étaient pas comparables à celles obtenues entre D1R et D2R WT. Ensuite, nous avons montré des différences entre le même type cellulaire dans les conditions WT et KO. Nous avons également mis en évidence une différence en terme d'expression d'ARNm entre WT et KO avec une surexpression de gènes plus particulièrement chez les souris D1R KO.

Dans la troisième partie, nous avons utilisé le conditionnement contextuel de la peur associé au traçage rétrograde et aux enregistrements éléctrophysiologiques à cellules entières de neurones pyramidaux marqués chez des souris mâles adultes C56BL/6J âgées de 2 à 3 mois. Nous avons montré que les neurones se projetant dans l'amygdale basolatérale présentent des modifications de l'excitabilité neuronale dépendantes de l'apprentissage suite au conditionnement contextuel de la peur. En revanche, l'excitabilité des neurones se projetant au niveau du PL controlatérale ne diffère pas entre les animaux ayant appris et les animaux témoins. Ensemble, ces résultats indiquent que les changements d'excitabilité intrinsèque induits par l'apprentissage ne sont pas généralisés à l'ensemble des neurones du PL mais sont définis par les zones cérébrales où les neurones projettent.

Mots clés : Cortex prefrontal, Dopamine, Canaux ioniques, Syndrôme du X fragile, Mémoire

Title : The role of intrinsic neuronal excitability for Prelimbic network function

Abstract : The goal of this work was the characterization of the intrinsic properties, morphology, connectivity and transcriptome profile of Layer 5 prelimbic (PL) neurons expressing Dopamine 1 (D1R) or 2 (D2R) receptor in wild-type mice. Then, we decided to use the previous database to determine the deficit of these two subpopulations into the Fragile X Syndrome (FXS) mice model *Fmr1*-KO. The last focus have been made in one specific connection which is the prelimbic neurons projecting to basolateral amygdala. We determined the plasticity occurring after fear memory formation.

In the first part of our study, we made a distinct clustering of D1R and D2R WT neurons of the L5 PL area based on their intrinsic properties. We also determined specific morphology properties as well as cell-type preferential connections with other brain areas. RNA sequencing analysis revealed more than 500 genes differently expressed between D1R and D2R WT divided in different categories such as ion channels genes. The creation of this database allowed us to follow to the other part.

In the second part we determined the deficit occurred in D1R and D2R KO neurons due to the lost of FMRP in FXS mice model *Fmr1*-KO. FXS is the most common inherited mental retardation and most frequent genetic form of autism, leading to learning and memory deficits, repetitive behavior, seizures and hypersensitivity to sensory (e.g. visual) stimuli. Dopamine modulation is altered in this model and we wanted to characterize at which level it is altered. We observed differences in intrinsic properties between D1R and D2R KO, which were not comparable to D1R and D2R WT. Then, we showed differences between the same cell-type across WT and KO condition. We also highlighted a difference in term of mRNA expression across WT and KO with an overexpression of genes more especially in D1R KO mice.

In the third part We used contextual fear conditioning together with retrograde tracing and whole-cell electrophysiological recordings of labeled pyramidal neurons in adult 2-3 month old male C56BL/6J mice. We show that neurons projecting to the amygdala display learning-dependent changes in neuronal excitability following contextual fear conditioning. In contrast, the excitability of neurons projecting to the contralateral mPFC does not differ between trained and control animals. Together, these results indicate that learning-induced changes in intrinsic excitability are not generalised across all PL neurons but instead are defined by the neurons' long-range projection targets.

Keywords : Prefrontal cortex, Dopamine, Ion channels, Fragile X syndrome, Memory

Unité de Recherche : [Mécanismes de la plasticité corticale dans les conditions normales et pathologiques, INSERM U1215, Neurocentre Magendie, 146 rue Léo Saignat, 33077 Bordeaux Cedex]

Acknowledgments

It is a pleasure to thank the many people who made the completion of my doctoral degree and this research project possible.

I would like to start by thanking my supervisor Andreas Frick for giving me the opportunity to do a PhD in his lab as well as for his help and guidance throughout this project.

I would like to start by saying that I'm grateful to my supervisor Andreas Frick for giving me the opportunity to do a PhD in his lab, for helping, guiding and supporting me throughout my PhD project. I would like to specially thank all the previous and current team members of the Frick lab: Melanie Ginger, Katy Le Corf, Isabel Del Pino, Arnaldo Ferreira, Rémi Proville, Liangying Zhu, Kamila Castro, Olivier Dubanet , Sourav Ghosh, Arjun A-Bhaskaran, Sreedevi Madhusudhanan, – for their help, for providing a stimulating and fun environment for me to learn and grow. It has been a great pleasure to work in such a friendly environment.

I would like to thank the members of my thesis committee – Pietropaolo Susanna, Ramaswami Mani, Coutureau Etienne and Schubert Dirk for agreeing to evaluate my work.

I wish to thank Csaba Földy and Jochen Winterer and their team members for the fruitful long-term collaboration and their expertise.

I would like to thank Stephane Oliet for the good working conditions within the institute. I thank the administrative and IT staff members for their availability when I needed their help.

I am grateful to all my friends in- and outside the lab for their every-day support and encouragement, the soccer guys and many others, thank you for your moral support.

Above all, I would like to thank my parents and close family for the constant support they gave me during the PhD and for their constant inspiration that led me towards science. Without them I would not have achieved any of this.

List of Abbreviations

1. General Introduction

1.1. The medial Prefrontal cortex (mPFC)

1.1.1. Overview

The medial prefrontal cortex (mPFC) is well known for its role in decision making, error detection (Holroyd et al., 2002), conflict monitoring (Botvinick et al., 2004), executive control (Posner et al., 2007; Ridderinkhof et al., 2004), reward guided learning (Rushworth et al., 2011) and decision making regarding the evaluation of risk and reward (Bechara and Damasio, 2005). The mPFC also plays a key role in memory formation, for example in the consolidation and recall of fear memory (Frankland et al., 2004; Maren and Quirk, 2004; Quirk and Mueller, 2008). One important part of memory formation is the encoding phase. Encoding is the crucial first step to creating a new memory and decades of research in both humans and animals have revealed that mPFC is essential for the encoding (Preston and Eichenbaum, 2013). For example, inactivation of the prelimbic (PrL) part of the mPFC with the voltage-gated Na^+ channel blocker, tetrodotoxin, after fear learning results in reduced fear responses (Corcoran and Quirk, 2007). Other studies have highlighted the role of mPFC in the consolidation of associative memories, showing that interference with mPFC directly after learning disrupts subsequent recall (Tronel and Sara, 2003). In summary, there is strong evidence that the mPFC plays a critical role in short-term, recent and remote memories for a broad range of learning tasks (Lesburguères et al., 2011).

Some studies hypothesized a role of the mPFC in adaptive decision-making, which consists in developing different strategies to make judgments and choices following diverse life situation. Earl Miller and colleagues have suggested that the entire PFC receives a broad range of sensory and limbic inputs which can activate contextually appropriate representations of goals or task rules (Miller, 2000a; Miller and Cohen, 2001). Active maintenance of these goals provides a “top-down” bias signal, which can influence the representation of a specific behavior response in other areas of the brain. They also suggest that feedback of a specific behavior response drives synaptic plasticity in prefrontal cortex, ensuring that the appropriate goal state is enabled in the appropriate context (Miller and Cohen, 2001). Some theories have suggested that the mPFC guides decisions by anticipating emotional outcomes and enacting them as bodily states (Bechara and Damasio, 2005; Fellows, 2007) (Figure 1).

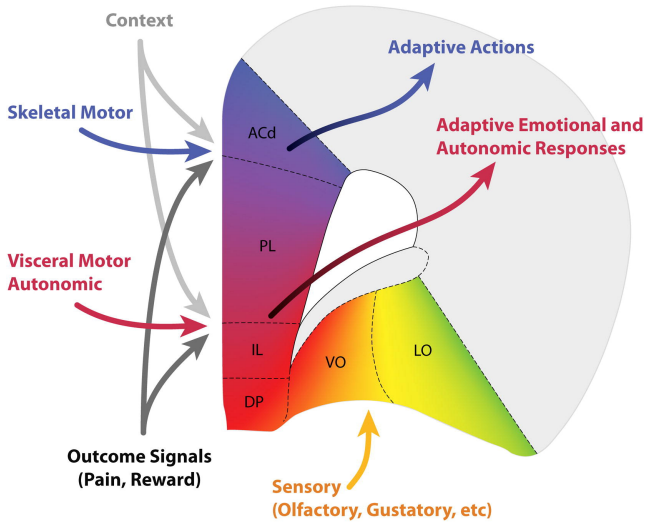

Figure 1: Schematic View of Inputs into, and Functional Roles of Different Regions of the Prefrontal Cortex. The PFC is conceived as a network that maps events within a given spatial and emotional context onto the most adaptive response, which can be either an action or an emotional response, depending on the area of the PFC. All frontal areas are strongly interconnected, meaning that information about actions, emotions, and stimuli is available to all prefrontal areas. (Figure based on Paxinos and Watson, 2007; altered with permission). Abbreviations: ACd, dorsal anterior cingulate; PL, prelimbic cortex; IL, infralimbic cortex; DP, dorsal peduncular cortex; VO, ventral orbital cortex; LO, lateral orbital cortex. Figure from (Euston et al., 2012).

1.1.2. Anatomy and connectivity of the mPFC

The mPFC is a neocortical structure that is divided into four distinct regions from dorsal to ventral: medial precentral cortex (PrCm), anterior cingulate cortex (ACC), prelimbic (PrL) and infralimbic (IL) cortex (Heidbreder and Groenewegen, 2003) (Figure 1). Except for the PFC and the motor cortex, most neocortical regions, for example sensory areas, are divided into six cytoarchitecturally distinct layers (I–VI), starting with layer I just below the pial surface and ending with layer VI bordering the white matter. In the sensory cortices, cells in layers II/III/V/VI contain pyramidal neurons that have apical dendrites projecting to layer I, except for layer VI were some types of cells send dendrites only into layer IV. Layer IV, on the other hand, is largely devoid of pyramidal neurons and is the primary target for sensory input from the thalamus (Miller et al., 2001). The detailed analysis of sensory cortex regions has resulted in a canonical model of cortical circuit organization that has served as a model for cortical circuits in general (Douglas et al., 1989). In this model, layer 4 is the main target of thalamic input. This input is then forwarded to layer 2/3 where it is integrated with inputs arriving from other cortical areas. The activity is next relayed to layer 5 neurons, which are the main source of subcortical projections. Layer 5 neurons innervate those in layer 6, which then close the loop by projecting back to layer 4 and the thalamus. More recent studies have revealed that this view is very simplified and that in fact these neurons also display various patterns of inter- and intralaminar connectivity (van Aerde and Feldmeyer, 2015; Douglas and Martin, 2004; Feldmeyer, 2012; Feldmeyer et al., 2002; Oberlaender et al., 2011; Schubert et al., 2007; Thomson and Lamy, 2007).

The prefrontal cortex (and motor cortex) or rodents has well defined layers I, II/III and V/VI; however, the existence of a discrete layer IV is not clear (Van De Werd et al., 2010). Within layers I, II/III and V/VI, the neuronal organization of the mPFC is similar to that of other neocortical regions. Pyramidal cells are located in layers II/III/V/VI (Yang et al., 1996a), and display a range of firing properties (Wang et al., 2006) similar to those described for other neocortical regions (Connors and Gutnick, 1990). The mPFC also contains a variety of interneuron types (Van De Werd et al., 2010), with the expected distribution of interneuron markers such as morphology, electrical active properties or specific combination of neuropeptides (Markram et al., 2004).

The mPFC is well connected with other subcortical areas to access and mediate processing of diverse information (Figure 2). Indeed, it is reciprocally connected with the basolateral amygdala (BLA), a region critical for emotional learning (LeDoux, 2003). It also communicates reciprocally with the hypothalamus, which controls homeostatic states, such as hunger and thirst, as well as the autonomic and endocrine systems. It sends prominent connections to the dorso- and ventromedial striatum, a brain structure mediating reward, cognition, reinforcement and motivational salience; the periaqueductal gray (PAG) – a region implicated in aggression, defensive behaviour and pain modulation; and to the lateral habenula, an area involved in learned responses to stress, anxiety, pain and reward (Figure 2). The mPFC is also reciprocally connected to a wide-range of neuromodulatory systems including the dorsal raphe, ventral tegmental area (VTA) and locus coeruleus, containing serotonergic, dopaminergic and cholinergic neurons, respectively (Figure 2). Finally, the mPFC receives direct input from the CA1 and the subicular region of the ventral hippocampus (Ährlund-Richter et al., 2019; Hoover and Vertes, 2007; Sesack et al., 1989). Interestingly, a direct return projection exists from the mPFC to the hippocampus (Rajasethupathy et al., 2015). It also exists an indirect way of communication between mPFC and hippocampus which involves the nucleus reuniens (RE) of the midline thalamus as a bidirectional relay structure in the transfer of information (Vertes, 2006; Vertes et al., 2007).

In terms of cortical connections, the mPFC displays very strong intrinsic ipsilateral and bilateral connectivity (Courtin et al., 2013; Gabbott et al., 2005; Hoover and Vertes, 2007; Vertes, 2004; Vertes et al., 2007). Regarding its functional organization, the mPFC seems to possess a dorso-ventral gradient. Whereas ventral regions including the ventral PL and infralimbic (IL) are specialized in autonomic/emotional control, dorsal regions including the AC and dorsal PL are specialized in the control of actions. The connectivity of dorsal and ventral mPFC is very similar with the exception that the dorsal mPFC has weaker connections with the autonomic/emotional centers and stronger connections with motor and pre-motor areas (Euston et al., 2012; Gabbott et al., 2005; Heidbreder and Groenewegen, 2003; Hoover and Vertes, 2007).

Despite the lack of a defined layer 4, the mPFC still displays strong reciprocal connectivity with the thalamus. Indeed, the higher-order mediodorsal nucleus of the thalamus (MD) emerges as the largest input area (Ährlund-Richter et al., 2019).

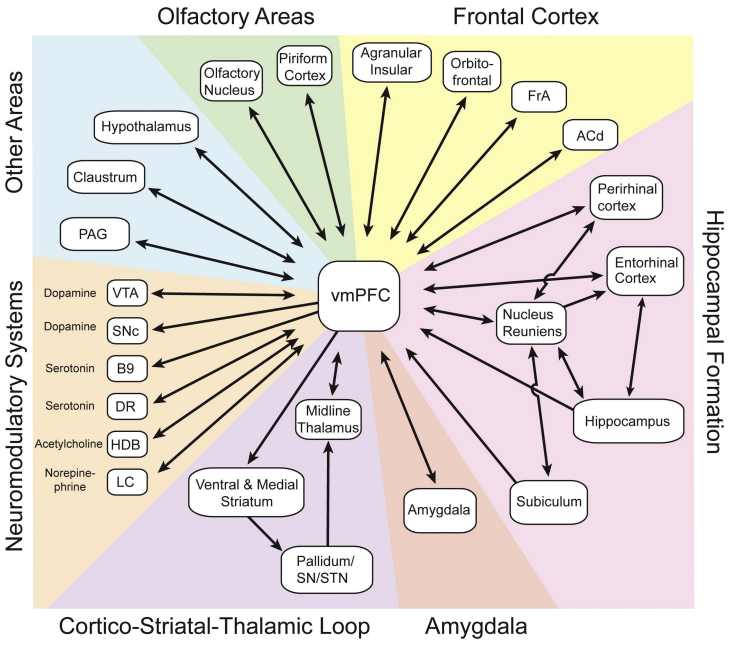

Figure 2: Major Anatomical Connections of Ventral mPFC. Arrows indicate directionality. Connections are derived from recent surveys of efferents and afferents of the mPFC and only the anatomically densest projections are represented. Hence, some potentially important connections, such as those to the lateral habenula, are not shown due to their relative weakness. Abbreviations: ACd, dorsal anterior cingulate cortex; B9, B9 serotonin cells; DR, dorsal raphe; FrA, frontal association cortex; HDB, horizontal limb of the diagonal band of Broca; LC, locus coeruleus; PAG, periaqueductal gray; SN, substatia nigra, STN; subthalamic nucleus, VTA, ventral tegmental area. Figure from (Euston et al., 2012).

1.1.3. Cellular composition

1.1.3.1. Pyramidal neurons

The mPFC contains excitatory neurons (glutamatergic) and GABAergic (γ-aminobutyric acid) inhibitory interneurons (INs) of different classes. The main functionally distinct IN classes express vasoactive intestinal peptide (VIP), somatostatin (SST), or paravalbumin (PV), respectively (Kepecs and Fishell, 2014). mPFC excitatory neurons receive local input from other excitatory neurons, as well as from a variety of INs (DeNardo et al., 2015). INs are assumed to receive local input from neurons of their own subtype, other IN subtypes, and from excitatory neurons (all to different degrees that depends on the IN type). Furthermore, excitatory input, targeting both excitatory and inhibitory neurons, arrives from adjacent mPFC areas (Zingg et al., 2014). For each cortical layer of the mPFC, studies showed different subtypes of pyramidal neurons (van Aerde and Feldmeyer, 2015). Pyramidal neurons have previously been classified mainly based on their electrophysiological properties such as the membrane input resistance, the action potential (AP) firing pattern (regular-spiking, adapting or burst firing), and the AP waveform including the presence of an after-depolarizing potential (Chang and Luebke, 2007; Dégenètais et al., 2002; Yang et al., 1996a).

L2 pyramidal neurons have a very hyperpolarized resting membrane potential (RMP) that sets them apart from pyramidal neurons of other layers of the mPFC. In addition, L2 neurons appear to be a rather homogenous neuron class, with small differences in physiological or morphological parameters. The border between L2 and L3 is remarkably clear within the mPFC. Macroscopically, L2 can be seen as a thin dark band directly below L1 which consists mainly of axons and dendrites and is mostly devoid of cell bodies. At the microscopic level, a decrease in cell density can be observed at the border between L2 and L3. In the mPFC, L2 is only a thin layer, about a quarter of the size of L3 (120µm), consisting of only a couple of "rows" of densely packed pyramidal neurons (van Aerde and Feldmeyer, 2015).

L3 pyramidal neurons of the mPFC have prominent apical dendrites that bifurcate within L1. They can be divided into three main subclasses: thick-tufted regular spiking neurons, thick-tufted adapting neurons, and slender-tufted neurons. The main intrinsic properties differences between these subclasses are the resting membrane potential, rheobase, time constant, sag ratio and firing frequency. The slender-tufted L3 pyramidal neurons can be further divided into those with an adapting and those with a bursting firing pattern (van Aerde and Feldmeyer, 2015).

Pyramidal neurons of L5 are the best-studied cell types of the mPFC, and they have been categorized according to their electrophysiological and morphological properties (Chang and Luebke, 2007; Dégenètais et al., 2002; Wang et al., 2006; Yang et al., 1996a). Morphologically, L5 pyramidal cells can be categorized as "thick-tufted" L5 pyramidal neurons that possess a complex apical dendrite with numerous oblique branches, or "slender-tufted" L5 pyramidal neurons that have a more restricted field span of the apical dendritic tree and less side branches (Wang et al., 2006).

L6 pyramidal neurons are more diverse in their morphological appearance than pyramidal neurons of other layers. L6 pyramidal neurons are ranging from neurons with apical dendrites that spanned all cortical layers and terminated in L1 to small L6 pyramidal neurons with a dendritic tree that was exclusively restricted to L6. Also, the horizontal field span of L6 pyramidal neurons was very diverse: Pyramidal neurons with both the broadest and the smallest field span of all mPFC pyramidal neurons were found in L6. Some L6 pyramidal neurons had inverted apical dendrites pointing towards the white matter. The high percentage of L6 pyramidal neurons with apical dendrites ascending to L1 appears to be a characteristic feature of L6 pyramidal neurons in the mPFC. However, physiologically, L6 pyramidal neurons appeared to be less diverse with respect to their electrophysiological properties. (van Aerde and Feldmeyer, 2015).

1.1.3.2. Interneurons

Studies showed extensive local connections between the mPFC IN types. SST INs receive a considerable fraction of their local input from VIP INs. Accordingly, *in vitro* electrophysiology

experiments have demonstrated that activation of VIP INs primarily suppresses SST INs within the mPFC (Pi et al., 2013). Interestingly, for SST INs the proportion of input from PV INs is similar to that from VIP INs. The existence of IN–IN connections does not *per se* proof the existence of a disinhibitory circuit motif — a connectivity motif, in which an IN subtype inhibits another type of IN, thereby removing an inhibitory break of excitatory neurons (Tremblay et al., 2016). However, disinhibition of projection neuron dendrites through PV suppression of SST INs has been demonstrated in the amygdala, resulting in increased evoked responses of projection neurons (Wolff et al., 2014). mPFC VIP INs are also targeted by local PV INs (Ährlund-Richter et al., 2019).

1.1.4. PL connectivity with the basolateral amygdala (BLA)

The mPFC helps control cognition and emotion (Goldman-Rakic, 1995; Miller, 2000a), as highlighted by the physiopathological consequences of its dysfunction in neuropsychiatric disorders (Egan and Weinberger, 1997). This ability depends on reciprocal circuits between the mPFC and other cortical and subcortical regions. Long-range interactions between the mPFC and BLA are particularly important for emotional control (Burgos-Robles et al., 2009; Herry et al., 2008). These interactions occur through multi-synaptic pathways, or via direct communication between neurons in the mPFC and the BLA.

The mPFC also receives long-range excitatory inputs from many other brain regions (Hoover and Vertes, 2007). To participate in reciprocal circuits, these inputs and local neurons must first be linked by connections inside the same interlaminar space. Excitatory inputs from the BLA and cmPFC densely arborize within superficial layers of the mPFC (Bacon et al., 1996; Sesack et al., 1989). These inputs are poised to directly synapse onto L2 pyramidal neurons whose dendrites sample from these layers (Little and Carter, 2012). This unique anatomy could enable bidirectional communication between these pyramidal neurons and the BLA and cmPFC.

1.1.5.Role of mPFC in memory formation

Stimulation and inactivation studies of the mPFC have established that this region is involved in both fear memory formation and its extinction (Burgos-Robles et al., 2007; Corcoran and Quirk, 2007; Laurent and Westbrook, 2008; Sotres-Bayon and Quirk, 2010), with the IL and PL having distinct roles in these processes (Burgos-Robles et al., 2007). The PL has been implicated in modulating both consolidation and recall of fear memory (Maren and Quirk, 2004; Quirk and Mueller, 2008). Thus, for example, inactivation of the PL with tetrodotoxin after fear acquisition results in reduced fear responses (Corcoran and Quirk, 2007).

Several studies demonstrated an involvement of the mPFC in remote long-term memory. Remote (4 weeks following a behavioural learning task) but not recent (one day after training) memory retrieval was shown to result in increased expression levels of the immediate early genes *c-fos* and *zif268* (Frankland et al., 2004; Maviel et al., 2004), an increased metabolic activity

(Bontempi et al., 1999) and structural changes such as an increase in dendritic spine numbers (Restivo et al., 2009).

It has been suggested that during recent memory retrieval the role of the mPFC is to represent the context, events and responses, while the hippocampus stores the exact mapping between them. In contrast, during remote memory recall, the mPFC might both represent and store the context-event-response mappings, while the hippocampus becomes disengaged (Euston et al., 2012; Frankland and Bontempi, 2005).

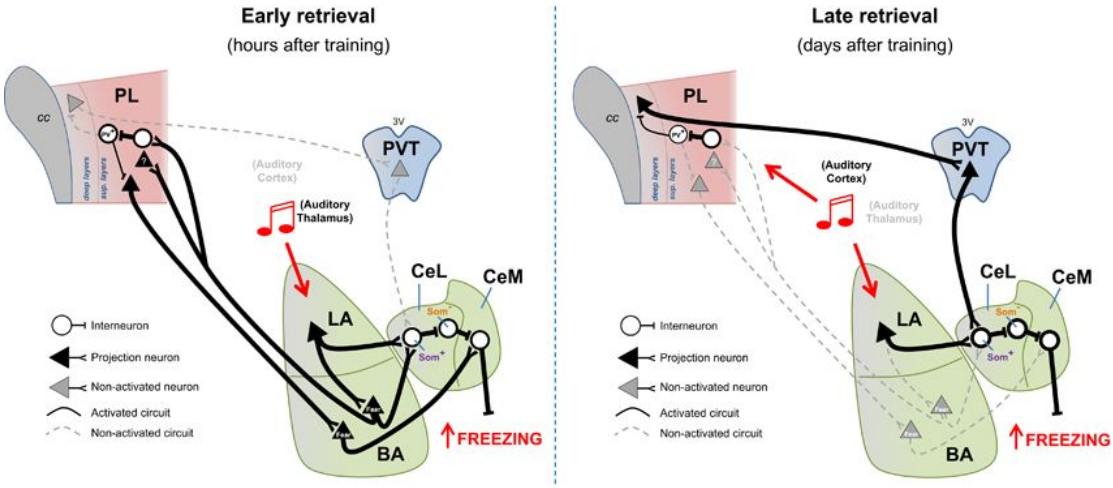

Figure 3: Temporal reorganization of the circuits necessary for retrieval of fear memories. Left – retrieval of fear memories at early time points after conditioning recruits reciprocal activity between the amygdala and PL. During early retrieval, the conditioned tone activates auditory thalamus inputs to LA. Increased activity in LA neurons activates SOM+ neurons in CeL, thereby disinhibiting CeM output neurons that mediate fear responses. Increased activity in LA neurons also activates BA neurons interconnected with PL, thereby allowing a top–down control of fear retrieval. Right – retrieval of fear memories at late time points after conditioning recruits activity in PL neurons projecting to PVT, as well as PVT neurons projecting to CeL. During late retrieval, the conditioned tone activates auditory cortex inputs to both LA and PL. Increased activity in PL interneurons inhibits PV+ interneurons, thereby disinhibiting PL neurons projecting to PVT. Increased activity in PVT neurons activates SOM+ neurons in CeL, and consequently disinhibits CeM output neurons that mediate fear responses. BA, basal amygdala; cc, corpus callosum; CeL, lateral portion of the central amygdala; CeM, medial portion of the central amygdala; LA, lateral amygdala; PL, prelimbic cortex; PVT, paraventricular nucleus of the thalamus; PV+, parvalbumin positive neurons; SOM+, somastotatin positive neurons; SOM–, somatostatin negative neurons; 3 V, third ventricle. Adapted from (Do Monte et al., 2016).

Other studies support the idea that the mPFC plays an active role in memory consolidation. For example, blocking plasticity mechanisms within the mPFC immediately following trace fear conditioning using a selective inhibitor of the mitogen-activated protein (MAP)/Erk kinase (MEK) pathway causes deficits in memory performance when tested 24 or 72 hours later (Runyan et al., 2004). Similar results have been obtained for inhibitory avoidance (Holloway and McIntyre, 2011; Zhang et al., 2011), and the extinction of both fear and drug-related memories (Mamiya et al., 2009; Peters et al., 2009; Sotres-Bayon et al., 2009).

1.1.6. Dopaminergic modulation of the mPFC

Dopaminergic (DA) neurons of the ventral tegmental area (VTA) have been intensively investigated because of their role in encoding motivationally relevant appetitive stimuli. In addition, many studies have implicated DA modulation in aversion and pain (Bromberg-Martin et al., 2010; Budygin et al., 2012). DA neurons of the VTA establish reciprocal projections with the mPFC (Berger et al., 1976; Carr and Sesack, 2000a, 2000b) and play important modulatory roles for the fine-tuning of neuronal activity and for the induction of synaptic plasticity (Durstewitz et al., 2000; Popescu et al., 2016). Behavioral studies have documented the effects of dopaminergic modulation of the mPFC circuits on working memory and attention. Granon et al, (2000) showed beneficial effects on behavioral performance produced by a direct stimulation of prefrontal dopamine function in intact animals (Granon et al., 2000). It has also been shown that optogenetic activation of the VTA DA input into the mPFC elicits anxiety-like behavior (Gunaydin et al., 2014).

Pharmacological studies have shown that blockage of DA D1 receptors in the mPFC disrupts choice behavior guided by working memory (Sawaguchi and Goldman-Rakic, 1994; Sawaguchi et al., 1990). Blockage of DA D1 receptors in the mPFC during retrieval, but not during learning phase selectively disrupted memory-based search behavior in rats (Seamans et al., 1998). Furthermore, it has been proposed that working memory function is optimized when DA D1 receptor occupancy is within a range of 0.1 to 0.2μg/0.5μL of an inverted U-shaped function (Arnsten, 1998; Floresco and Phillips, 2001).

Lesions of the VTA to PL projections impair working memory performance in monkeys (Brozoski et al., 1979) and rats (Simon, 1981). DA D1 but not DA D2 receptor antagonists impair working memory performance when infused into the primate *sulcus principalis* region (part of the brain that connects the dorsolateral and ventrolateral frontal cortex) (Sawaguchi and Goldman-Rakic, 1991) or into the rat PL (Seamans et al., 1998). These findings indicate that D1 receptors strongly shape cognitive performance under the control of the prefrontal cortex in both rat and monkey and are consistent with data showing beneficial effects of the mixed D1/D2 receptor agonist pergolide on a spatial working paradigm in humans (Müller et al., 1998).

Studies suggest that there is an optimal level of mesocortical DA function for mnemonic performance (Arnsten, 1997; Williams and Goldman-Rakic, 1995; Zahrt et al., 1997). There is evidence that an increased cortical DA turnover, sometimes caused by stress or anxiogenic stimuli, is associated with impaired performance in spatial working memory, egocentric spatial processing and inhibition of proactive interference and inappropriate motor responses (Arnsten, 1997; Murphy et al., 1996; Sahakian et al., 1985), similar to the effect of an infusion into PFC of the DA D1 receptor agonist SKF 81297 in rats (Zahrt et al., 1997).

1.1.7. D1 and D2 receptors

1.1.7.1. Overview

DA receptors (DARs) belong to the G protein-coupled receptor family (GPCRs). There are five subtypes of mammalian DARs that are divided in two families according to their structure and biological response. The D1-like family includes D1- and D5 DA receptors (D1R and D5R), while the D2-like DARs family consists of D2, D3 and D4 receptors (D2R, D3R and D4R).

The D1-like dopamine receptor family (D1R-f) is positively coupled to adenylyl cyclase (AC), leading to an increase in the intracellular cyclic 3,5 adenine-monophosphate (cAMP) concentration and the activation of the protein kinase dependent of cAMP (PKA) upon D1R-f activation. In contrast, the D2-like dopamine receptor family (D2R-f) is negatively coupled to AC, resulting in a decrease in cAMP accumulation the ensuing activity of PKA and its effectors following its activation (Arisawa et al., 1983; Forn et al., 1974; Greengard et al., 1999). However, growing evidence suggests that activation of DARs is not only restricted to AC modulation but also other signaling pathways and might act differently depending on the brain area, physiological and/or pathological conditions.

1.1.7.2. D1 Receptors

D1Rs share 80% in the amino acid sequence homology with D5Rs in the transmembrane domains (Civelli et al., 1993; Missale et al., 1998). This family of receptors is widely expressed in the brain, with high densities in striatum or caudo-putamen, nucleus accumbens, substantia nigra pars reticulata (SNr) and olfactory bulb (Wamsley et al., 1989). Lower densities has been reported in the dorsolateral prefrontal cortex, cingulate cortex and hippocampus (Boyson et al., 1986; Cadet et al., 2010). D1Rs play an important role in locomotor activity, reward systems, learning and memory (Graybiel et al., 1994).

Typically D1R activation induces the activation of the AC through the direct activation of guanosine nucleotide-binding proteins (G-proteins), the subunit Gαs of G-proteins induces the conversion of adenosine triphosphate (ATP) into cAMP (Sunahara and Taussig, 2002; Tesmer et al., 1997). cAMP interacts with the regulatory subunits of PKA inducing the release of the catalytic subunits that phosphorylate different substrates (Akimoto et al., 2013; Kim et al., 2006). One of the most studied proteins involved in the regulation of signal transduction pathway mediated by DARs and PKA is the Dopamine and cAMP-regulated phosphor-protein, 32 kDa (DARPP-32). The phosphorylation of DARPP-32 by PKA induces the inhibition of the protein phosphatase-1 (PP1) (Nishi et al., 1999a), while the phosphorylation of DARPP-32 by cyclin-dependent kinase 5 (Cdk5) induces the inhibition of PKA (Bibb et al., 1999; Undieh, 2010) causing a feedback loop in the activation of the PKA. The activation of PKA or the inhibition of PP1 mediated by PKA, may cause changes in the phosphorylation state of several neurotransmitter receptors and as voltage-gated ion channels. These include α-Amino-3-hydroxy-5-methyl-4-isoxazole-propionic acid receptors (AMPA), N-methyl-D-aspartate (NMDA), and Gamma Aminobutyric Acid channel A (GABAA) receptors, as well as L-, N-, P-type Ca^{2+} channels (Roche et al., 1996; Schiffmann et al., 1998; Surmeier et al., 1995). PKA regulates,

either directly or indirectly via DARPP-32, the activity of extracellular signal regulated kinases 1 and 2 (ERK 1/2) that in turn modify protein transcription. A dysfunction in this pathways has been related with the pathophysiological conditions of Parkinson's Disease (Santini et al., 2007) (Figure 4).

D1R activation may elicit an alternate cAMP signaling pathway that is independent of PKA (Undieh, 2010). cAMP activates the Ras superfamily guanine nucleotide exchange factors (GEFs), which are activators of Ras-proximate 1 (Rap1) (Altschuler et al., 1995) that has been involved in cell polarity and migration (Bos et al., 2001; Kawasaki et al., 1998). Rap1 can also activate Mitogen-activated protein kinase (MAPK) signaling implicated in the phosphorylation of transcription factors such as cAMP response element binding protein (CREB) that is involved in the increased or decreased transcription of genes (Neves et al., 2002) (Figure 4).

The D1R family also activates a signal transduction pathway that has been linked to various neuropsychiatric disorders, mediated by a single transmembrane protein calcyon, which promotes the D1Rs interaction with Gαq. As a result, PLC is activated and increases the accumulation of inositol triphosphate (IP3) which, in turn, binds to the IP3 receptors from the intracellular compartments inducing intracellular Ca^{2+} release. Ca^{2+} plays an important role not only in signaling pathways causing the activation of proteins such as protein kinase calcium-dependent (PKC), but also in the modulation of neurotransmitter release via exocytosis. It has been shown that this particular signaling pathways occurs primarily in the prefrontal cortex and calcyon has been found to co-localize with D1Rs in the dendritic spines on pyramidal neurons (Ha et al., 2012). The activation of this pathway in the mPFC is involved in impulsive choice in rats and neuropsychiatric disorders (Loos et al., 2010) (Figure 4).

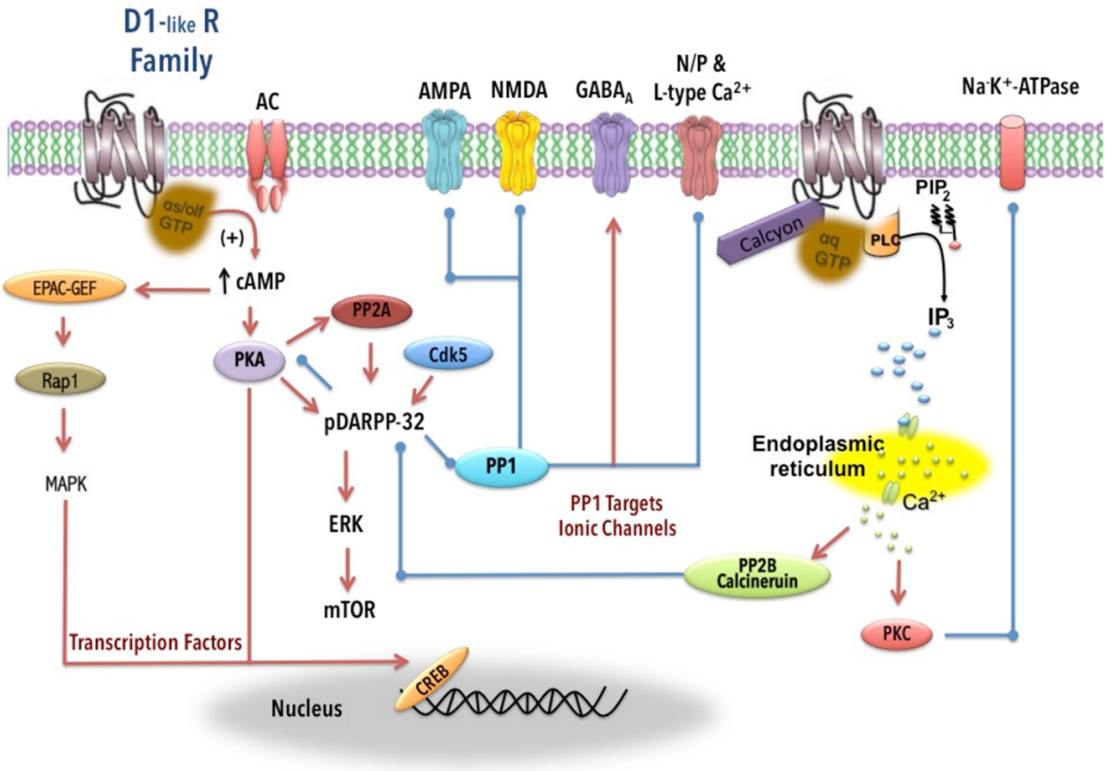

Figure 4: The D1-like DA Receptors Mediated Intracellular Signaling Pathways. DA binding to D1-like DA receptors leads to the activation of different intracellular signaling cascades. Stimulatory effects are indicated with red arrows and inhibitory effects in blue lines ending with a circle. cAMP, 3'-5'-cyclic adenosine monophosphate; αs/olfor αq ATP, active Gα protein; PKA, protein kinase A; DARPP-32, dopamine and cyclic AMP-regulated phosphoprotein, 32 kDa; AC, adenylyl cyclase; PP1, PP2A or PP2B, protein-phosphatase 1, 2A or 2B; PKC, protein kinase C; PLC, phospholipase C; IP3, inositol triphosphate; mTOR, mammalian target of rapamycin; PIP2, phosphatidylinositol 2; Ca2+, calcium; MAPK, mitogen-activated protein kinase EPAC-GEF, guanine-nucleotide-exchange factor of Rap1; Rap1, Ras proximate 1. AMPA, α-Amino-3-hydroxy-5-methyl-4-isoxazolepropionic acid receptors; NMDA, N-methyl-D-aspartate; GABAA, γ-Aminobutyric acid A; CREB; cAMP response element-binding protein. Adapted from (Claudia Rangel-Barajas and Claudia Rangel-Barajas, 2015).

1.1.7.3. D2 Receptor

D2Rs share 75% homology in the transmembrane regions with D3Rs, and 53% identity with D4Rs (Missale et al., 1998). D2Rs are mainly expressed in the striatum, external globus pallidus (GPe), core of nucleus accumbens, amygdala, cerebral cortex, hippocampus and pituitary. D2Rs mRNA also found in the temporal and enthorinal cortex and in the septal region as well in the VTA and SNc in the dopaminergic neurons (Missale et al., 1998) (Figure 5).

The activation of this receptor family typically leads to the inhibition of AC activity (Kebabian and Greengard, 1971), as well as inhibition of PKA and DARPP-32 (Nishi et al., 1999b). However, differences in the functional response and activation of signaling pathways have been observed in receptors from this family, specifically for the D3R subtype. Discrepancies could be due to a differential expression of the AC isoforms, because D3Rs were able to inhibit the AC activity when they were co-transfected with the AC isoform V (ACV) but not with isoform VI (Robinson and Caron, 1997). Furthermore the ACV is widely expressed in dopaminergic-innervated brain regions including the striatum (Cooper, 2003; Cooper et al., 1995). Some studies

suggested that this particular isoform also plays a role in anxiety, depression, abuse drug withdrawal and L-3,4-dihydroxyphenylalanine L-DOPA induced dyskinesia (LID) (Krishnan et al., 2008) (Figure 5).

D2Rs also activate G-protein-coupled inward rectifier potassium (GIRK) channels, which mediate neuronal electrical response (Mark and Herlitze, 2000), through GPCRs coupled to Gαi/o protein and also varying the effects between the receptors of this family. The effect seems to be through the βγ subunits for D2Rs and D4Rs but not D3Rs (Pillai et al., 1998) (Figure 5).

D2Rs are also able to activate cell proliferation-related pathways such as MAPK signaling. The activation of ERK1/2 has been also observed for this signaling pathway. D2Rs and D4Rs also display some differences in the intensity of ERK/MAPK activation compared to D3Rs using highly selective compounds (Beom et al., 2004; Luedtke et al., 2012). On the other hand, the complex GPCRs-β-arrestin also activates ERK/MAPK once the receptor is internalized (Lefkowitz and Shenoy, 2005) (Figure 5).

Stimulation of D2-like receptors activates Akt (protein kinase B PKB) signaling (Brami-Cherrier et al., 2002; Mannoury la Cour et al., 2011). In vitro, D3R activation led to an increase in PKC and PI3K activity (Collo et al., 2008). Specifically, activation of D3Rs enhance the Akt activity, which has been correlated with an increased dendritic arborization in dopaminergic neurons from mouse embryos (Collo et al., 2012). The activation of Akt regulates the activity of the mammalian target of rapamycin (mTOR) and consecutive targets related with synaptic plasticity and cognitive processing (Hoeffer and Klann, 2010). In contrast, the inactivation of Akt (by protein phosphatase 2A PP2A) leads to the activation of the two isoforms of Glycogen synthase kinase-3 (GKS-3α/β). The GSK-3 is a protein kinase abundantly expressed in brain and is involved in signal transduction cascades relevant to neurodevelopment (Peineau et al., 2008). It also regulates proteasome degradation through β-catenin (Doble and Woodgett, 2003), which is involved in neurodegenerative and psychiatric conditions such as Huntington Disorder, bipolar disorder and schizophrenia (Emamian, 2012). A study showed that D3R activates Akt, which in parallel activates, mTOR/p70S6/4E-BP1 signaling, probably mediated by phosphoinositide dependent kinase (PKD). It also causes the inactivation of GSK-3 by Akt-dependent phosphorylation, in medium-sized spiny neurons (MSNs) of striatum and nucleus accumbens (Salles et al., 2013), pathways that have been related with synaptic plasticity, cognitive process, long-term potentiation (LTP) and long-term depression (LDP) (Hoeffer and Klann, 2010). D3Rs also induced the activation of phosphatidylinositol 3-kinase (PI3K) and the atypical protein kinase C (PKCζ) this effect is apparently mediated by βγ subunit of G-proteins and activates MAPK signaling (Beom et al., 2004). Signaling pathways might occur differently in specific brain regions and more important in pathological conditions (Figure 5).

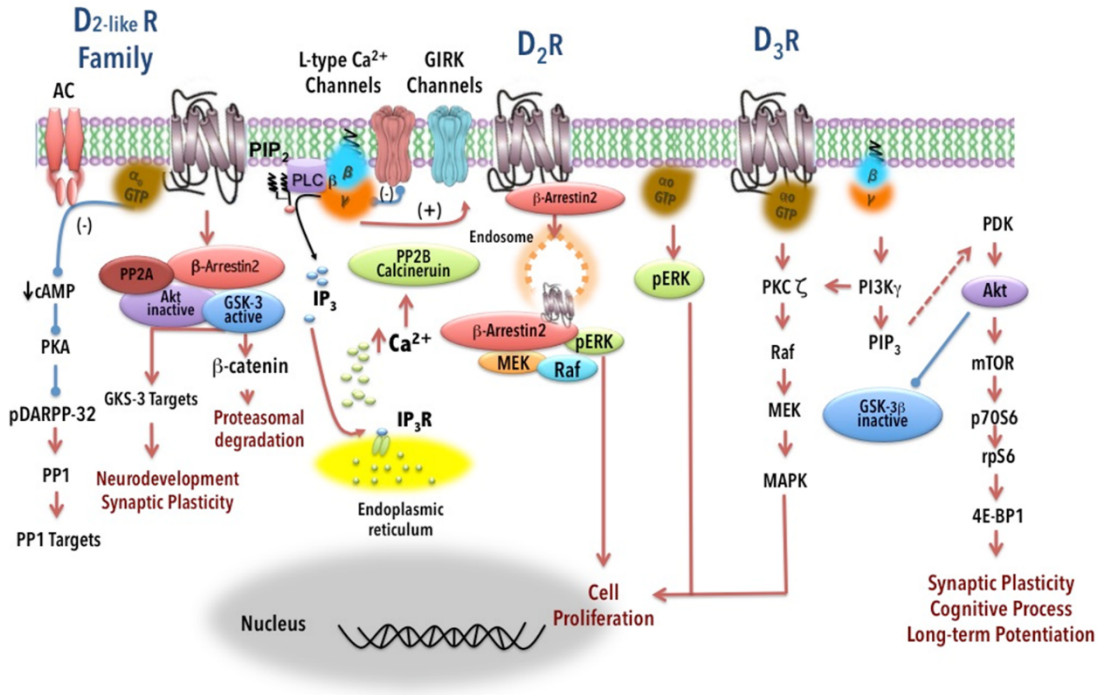

Figure 5: The D2-like DA Receptor Mediated Intracellular Signaling Pathways. Schematic shows the DA mediated effects through D2-like DA receptors that occur by a complex activation of intracellular signals that are related with events such as neurodevelopment, proteasomal degradation, cell proliferation and cognitive process. Stimulatory effects are indicated with red arrows, dashed red arrow indicates plausible activation and inhibitory effects in blue line ended with a circle. cAMP, 3'-5'-cyclic adenosine monophosphate; αi/o ATP, active Gαi/o protein; PKA, protein kinase A; DARPP-32, dopamine and cyclic AMP-regulated phosphoprotein, 32 kDa; AC, adenylyl cyclase; PP1, PP2A or PP2B, protein-phosphatase 1, 2A or 2B; MAPK, mitogen-activated protein kinase; PKC, protein kinase C; Akt, thymoma viral proto-oncogene; GSK-3, Glycogen Synthase Kinase-3; PLCβ, phospholipase C isoform β; PI3K, phosphatidylinositol 3-kinase; PIP2, PIP3, phosphatidylinositol 2 and 3; IP3, inositol triphosphate; Ca2+, calcium ; GIRK, G protein coupled inward rectifier potassium; MEK; Raf,; ERK, extracellular signal-regulated kinase protein kinase; PDK, phosphoinositide-dependant kinase; mTOR, mammalian target of rapamycin; p70S6, p70S6 kinase; rpS6, ribosomal S6 protein; 4E-BP, eukaryotic initiation factor 4E-binding protein 1. Adapted from (Claudia Rangel-Barajas and Claudia Rangel-Barajas, 2015).

1.2. Fragile X Syndrome (FXS)

1.2.1.Overview

In 1943, Martin-Bell described for the first time a familial syndrome of intellectual disability (ID) affecting men, which also showed dysmorphic features and macroorchidism (Martin and Bell, 1943). Subsequently, in 1969 Lubs associated a cytogenetic marker with this syndrome, showing fragility at the terminal end of the long arm of the X chromosome (Xq27.3), leading to the name “fragile X syndrome” (FXS) (Lubs, 1969). In 1991, three research groups independently cloned the fragile X mental retardation type 1 (*FMR1*) gene (Oberle et al., 1991; Verkerk et al., 1991; Yu et al., 1991), which is the cause of FXS. These authors also described for the first time a special mutation called “dynamic mutation”, which consists of a CGG triplet expansion that increases from generation to generation. During the following decade, geneticists tested a large number of patients for this mutation, leading to the discovery of new human diseases caused by dynamic mutations. After further studies, Hagerman et al described a

neurological disease related to the *FMR1* premutation that was named fragile X-associated tremor/ataxia syndrome (FXTAS) (Hagerman et al., 2001). Finally, since 2007 the spectrum of the clinical phenotype associated with the *FMR1* premutation has continuously widened.

FXS is the most common cause of inherited ID (1%-2% of all ID) and the leading monogenic cause of autism spectrum disorders (ASD). FXS is a neurodevelopmental disorder that causes a range of problems including learning disabilities and cognitive impairment. Relative strengths in cognitive performance are frequently reported for vocabulary capacity, visuo-perceptual abilities, and the processing and recall of simultaneous and meaningful information. In contrast, consistent deficits have been reported for verbal short-term memory visuo-spatial memory, linguistic processing, selective and divided attention, and the processing of sequential and abstract information (Dykens et al., 1987; Maes et al., 1994; Munir et al., 2000). The hallmark physical characteristics of FXS patients include post-pubertal macroorchism, a long face, hyperextensible joints, and prominent ears. The *FMR1* gene is inherited as an X-linked dominant trait with a reduced penetrance of 80% in males and 30% to 50% in females. The incidence is variable depending on the population gender, but affects approximately 1 in 4000 males and 1 in 7000 females worldwide (Lozano et al., 2016). Females that are heterozygous for the full mutation allele have a 30% chance of having a normal intelligence quotient and a 25% chance of having ID with an IQ < 70; nonetheless, they can present learning deficits and emotional difficulties (Tolmie, 2002).

FXS results from an inactivation of the FMR1 gene. While the clinical manifestations of FXS have not varied since the first descriptions of the syndrome, the implication of the Fmr1 gene in autism and ASD has gained great relevance in later years. Approximately 30% to 50% of FXS patients meet the full criteria of the Diagnostic and Statistical Manual of Mental Disorders-4th edition-Text Revision (DSM-IV-TR) for Asperger Syndrome (AS), with 60% to 74% fulfilling the criteria for ASD. Over 90% of individuals with FXS display some form of atypical behavior which are characteristics of autism including difficulties in social interaction (McCary and Roberts, 2013), and approximately 2% to 5% of all the diagnoses of ASD are related to FMR1 gene mutation (Schaefer and Mendelsohn, 2008).

1.2.2.Fragile X mental retardation type 1 gene

In most cases the molecular basis of FXS is a dynamic mutation: a CGG trinucleotide repeat expansion located in the untranslated region of the first exon of the *FMR1* gene leading to a hypermethylation of the CGG repeats and the adjacent CpG island (Oberle et al., 1991; Verkerk et al., 1991; Yu et al., 1991). The Fmr1 gene is located on the X chromosome and spans 17 exons and 40 kb of genomic DNA. It transcribes an mRNA of 3.9 kb. The translated protein is called "fragile X Mental retardation protein" (FMRP), which is necessary from early stages of life (Pieretti et al., 1991).

In the general population the number of CGG repeats is polymorphic, presenting from 6 to 44 CGGs, and the adjacent CpG island, which acts as a promoter, is non-methylated. Alleles harboring 6 to 44 CGGs are considered normal and remain stable upon transmission. The next class is premutation alleles that exhibit CGG repeat lengths between 55 to 200 CGGs. In this situation, the Fmr1 gene is also transcribed and translated, and the CpG island is non-methylated. However, premutation carriers have normal or slightly reduced synthesis of FMRP and increased levels of mRNA (2- to 8-fold more than normal alleles), and these individuals are asymptomatic for FXS. Premutation carriers have a risk of having affected offspring as the number of CGGs is unstable and tends to increase with each cellular division. Moreover, people carrying premutation alleles are at risk of developing some disorders such as FXTAS and emotional disorders, among others.

Finally, when the CGG number is greater than 200 repeats, these alleles are in the full mutation range. The CpG island and the repeats themselves are methylated, and this methylation switches off the gene, blocking transcription and the production of FMRP. Male individuals with the full mutation are always affected FXS related symptoms, while only 30% to 50% of females carrying the full mutation are affected due to the X-inactivation phenomena induced by the presence of two X chromosomes. The clinical manifestations of FXS may vary according to the presence of this mosaicism, different methylation levels of the fully mutated allele or of X-inactivation leading to differential FMRP expression within tissues.

More than 25% of patients show a premutation-full mutation mosaicism caused by the somatic instability of the full mutation in early embryogenesis. Methylation mosaicism can also be observed in large expansions with incomplete or null methylation. These mosaicisms allow the expression of some FMRP and, in some cases, have been associated with milder ID in males or full mutated males who display normal phenotypes referred to as high-functioning males (Pretto et al., 2014).

In up to 98% of cases, FXS is due to a CGG repeat expansion which is always inherited, but any other *FMR1* mutation leading to a loss-of-function of the gene may also cause FXS or an FXS-like phenotype. Point mutations or deletions affecting the Fmr1 gene are responsible for up to 1% to 2% of FXS cases. These mutations can be *de novo* or inherited from a carrier mother (Myrick et al., 2014). It has been suggested that patients with a clinical FXS-like phenotype but not carrying the full mutation should be screened for *FMR1* mutations.

1.2.3.Fragile mental retardation protein (FMRP)

In adult human tissues, FMRP was found to be a broadly, but not ubiquitously expressed protein, particularly abundant in neurons, where it is principally localized in the perikaryon and in the proximal part of axons and dendrites (Devys et al., 1993; Feng et al., 1997a). In the mouse, FMRP expression starts at day 2 of gestation. In general, during early and intermediate embryonic development (0–14 days), FMRP is ubiquitously expressed, similarly to adult tissues.

During late embryonic stages (15–19 days) and in newborn animals, FMRP shows a specific pattern of expression, mainly in tissues from ectodermal origin, like brain, hair follicles, sensory cells, and adrenal medulla. This pattern of protein expression is consistent with results of *in situ* hybridization in human embryonic and foetal tissues (Abitbol et al., 1993; Agulhon et al., 1999).

FMRP is an RNA binding protein associated with polyribosomes. A clue for the function of FMRP was given by the finding that FMRP contains motifs (two KH domains and one RGG box) characteristic of other RNA binding proteins (Siomi et al., 1993). Indeed, FMRP is able to bind RNA *in vitro*, with preference for poly(U) and poly(G) RNA homopolymers (Adinolfi et al., 1999; Ashley et al., 1993). FMRP-ribosome association is sensitive to low levels of RNAse, which removes the mRNA link without disturbing ribosome assembly (Corbin et al., 1997; Feng et al., 1997b). These findings led to the conclusion that FMRP is part of a ribonucleoproteic complex linked to polyribosomes via mRNA.

FMRP is regulated by posttranslational modifications. Phosphorylated FMRP stalls ribosomal translocation and inhibits translation, whereas dephosphorylation of FMRP upregulates translation (Ceman et al., 2003; Coffee et al., 2012). Bidirectional regulation of FMRP phosphorylation by the S6 kinase and protein phosphatase 2A (PP2A) in response to activity provides a potential link between synaptic stimulation and local protein translation in the dendrites (Santoro et al., 2012).

FMRP is well positioned to be a key regulator of synaptic plasticity for three main reasons. First, the protein is found in dendritic spines (Antar et al., 2004; Feng et al., 1997b; Weiler et al., 1997), important postsynaptic sites of plasticity induction and maintenance. Secondly, FMRP regulates dendritic mRNA translation (Bassell and Warren, 2008; Garber et al., 2006), which is required for multiple forms of plasticity (Sutton and Schuman, 2006). Finally, FMRP itself is dynamically regulated by activity: experience and synaptic activation can trigger its local translation and rapid degradation, in addition to the posttranslational regulation mentioned above. Multiple experimental manipulations associated with synaptic plasticity have been shown to increase FMRP levels, including exposure to an enriched environment, a complex learning task, and pharmacological activation of group 1 metabotropic glutamate receptors (mGluRs) (Irwin et al., 2000; Todd et al., 2003; Weiler et al., 1997). Importantly, FMRP is synthesized rapidly, on the same time scale (10–30 minutes) as the induction of stable synaptic plasticity (Gabel et al., 2004). In hippocampal cultures, activity- and mGluR-dependent increases in dendritic FMRP may result from increased trafficking of existing FMRP, rather than *de novo* FMRP synthesis (Antar et al., 2004, 2005; Dictenberg et al., 2008). Either way, FMRP is an ideal candidate to be involved in regulating synaptic plasticity because of its rapid, transient rise in dendrites following well-characterized plasticity induction paradigms, as well as its role as an inhibitor of translation.

While many forms of translation-dependent synaptic plasticity are abnormal in *Fmr1* KO mice, other forms of hippocampal plasticity, including NMDAR-dependent LTD and early-phase LTP, are normal (Li et al., 2002; Paradee et al., 1999). These observations suggest that FMRP regulates plasticity mainly in its role as a regulator of translation. However, removal of FMRP has also been shown to affect some forms of synaptic plasticity that do not require *de novo* translation, such as early-phase LTP in other brain areas, including the cortex and amygdala (Li et al., 2002; Paradee et al., 1999). Some of these effects could be explained by FMRP modulation of protein synthesis-dependent plasticity thresholds; however it seems likely that many represent end-stage consequences of altered synaptic development in the *FMR1* KO.

Long-lasting synaptic potentiation and depression have long been considered potential neural correlates of learning and memory. In conjunction with FMRP's role in synaptic plasticity in multiple brain areas, FMRP is also important for a wide range of behavioral learning tasks in mice. *FMR1* KO mice show deficient amygdalar trace fear memory (Zhao et al., 2005), cerebellar learning (Koekkoek et al., 2005), inhibitory avoidance learning (Dölen et al., 2007), and have difficulties with a prefrontal cognitive learning task (Krueger et al., 2011). Drosophila mutants lacking FMRP also have impaired long-term memory (Bolduc et al., 2008). Overall, learning and memory deficits in the *FMR1* KO mouse are a likely behavioral consequence of abnormal synaptic plasticity.

1.2.4.FMRP and regulation of intrinsic excitability

The amino terminus domain of FMRP is capable of supporting protein-protein interactions which can directly regulate properties of ion channel proteins, such as the (potassium) K+ channels Slack and BK (Brown et al., 2010; Deng et al., 2013), while the carboxyl-terminus domain is able to directly interact with calcium (Ca2+) channels (Ferron et al., 2014). FMRP can therefore potentially influence neuronal excitability through multiple mechanisms: by regulating translation of a diverse array of proteins that indirectly set neuronal excitability, and through a translation-independent role by interacting directly with a number of membrane ion channels to alter cellular excitability (Figure 6).

Assays of RNA binding combined with analysis of mRNA translational profiles altered in *FMR1* KO mice have revealed a wide variety of pre- and postsynaptic targets of FMRP that are normally involved in regulating neuronal excitability (Brown et al., 2001; Darnell et al., 2011; Miyashiro et al., 2003). Quantitative proteomic analysis of cortical neurons cultured from *FMR1* KO mice directly confirmed that the levels of many pre- and postsynaptic proteins are affected by loss of FMRP (Liao et al., 2008), including many proteins affecting membrane excitability, ionic homeostasis, AP generation and propagation, neurotransmitter release, and postsynaptic receptor signaling (Figure 6).

A number of K^+ channels that function at the resting potential have been identified as FMRP targets (Darnell et al., 2011), suggesting possible changes in intrinsic membrane

properties. Abnormally elevated intrinsic membrane excitability has been observed in layer (L) 4 excitatory cortical neurons of *FMR1* KO mice, due to an increase in input resistance and decrease in cell capacitance (Gibson et al., 2008). In contrast, the resting membrane potential is normal in excitatory hippocampal neurons and in L5 pyramidal neurons in entorhinal cortex of young *FMR1* KO mice (Deng et al., 2013). Also, all intrinsic excitability parameters, including input resistance, membrane time constant and threshold potential are unaffected in the soma of L5 pyramidal neurons in somatosensory cortex of *FMR1* KO animals (Desai et al., 2006; Zhang et al., 2014). Similarly, analysis of neurons derived from FXS human embryonic stem cells (Telias et al., 2013), which provide an interesting perspective into human neuron dysfunction, have found that passive membrane properties are similar to those from neurons derived from control subjects (Figure 6).

Recent measurements of intrinsic excitability in the distal dendrites of cortical L5 pyramidal neurons of *FMR11* KO mice found significant differences in resting membrane potential, input resistance, and the membrane time constant, all of which are consistent with a hyperexcitable state of the dendritic membrane in *FMR1* KO mice (Zhang et al., 2014). Moreover, back-propagating APs have larger amplitudes and evoke greater calcium influx in the dendrites of *FMR1* KO neurons (Routh et al., 2013; Zhang et al., 2014). The abnormal excitability of dendrites has been linked to the altered expression of several ion channels, including reduction in Kv4.2 (Gross et al., 2011; Lee et al., 2011; Routh et al., 2013), BK channels (Zhang et al., 2014) and altered expression of HCN1 channels (Brager et al., 2012; Zhang et al., 2014). Notably, the changes in dendritic properties caused by FMRP loss appear to be brain region specific. For instance, HCN1-channel expression is increased (and input resistance reduced) in dendrites of hippocampal neurons of *FMR1* KO mice (Brager et al., 2012), which is opposite to what is observed in the dendrites of cortical L5 neurons (Zhang et al., 2014). These findings emphasize the non-uniformity of excitability changes caused by FMRP loss, which affects intrinsic membrane excitability in a brain region-, cell type- and compartment-specific manner (Figure 6).

The changes in excitability and AP properties have been observed predominantly in excitatory pyramidal neurons. The true impact of these defects on the circuit excitability ultimately depends on the combination of changes in excitatory neurons and inhibitory GABAergic interneurons. So far there is little evidence for altered excitability of inhibitory neurons in FXS mice. One study found no alterations in intrinsic excitability and AP properties in L4 fast spiking interneurons (Gibson et al., 2008). Further studies of different subpopulations of inhibitory interneurons and at different developmental time points are clearly needed to determine how the interplay of cellular changes in excitatory and inhibitory neurons impact circuit hyperexcitability in FXS.

Voltage-gated Ca^{2+} channels (VGCCs) are expressed in axons (predominantly N-, R-, P/Q-and T-types) and in dendrites (mainly the L-type) to regulate excitability, synaptic transmission and various forms of plasticity. mRNAs coding for the pore-forming subunits of most major VGCCs have been found among FMRP targets (Brown et al., 2001; Darnell et al., 2011; Miyashiro et al., 2003). L-type VGCCs are often localized to dendrites and spines where they contribute to synaptic plasticity. Major changes in dendritic Ca^{2+} channels are triggered by loss of FMRP, such as the striking absence of any L-type VGCC activity in spines of prefrontal cortex (Meredith et al., 2007) and reduced mRNA for L-type Ca^{2+} channels in several brain regions (Chen et al., 2003) (Figure 6). These alterations have been linked to changes in the threshold for the induction of spike timing-dependent synaptic plasticity in *FMR1* KO mice (Meredith et al., 2007).

1.2.5.Non-canonical role of FMRP

A number of synaptic FMRP actions arise from direct protein-protein interactions between FMRP and some ion channels, independently of FMRP's traditional role in translational regulation (Brown et al., 2010; Deng et al., 2013; Ferron et al., 2014; Myrick et al., 2015a). Initial evidence for direct modulation of ion channel function by FMRP came from studies by Kaczmarek and colleagues which demonstrated that FMRP interacts directly with the sodium-activated K^+ channel Slack, and modulates its gating in the auditory brainstem (Brown et al., 2010). The N-

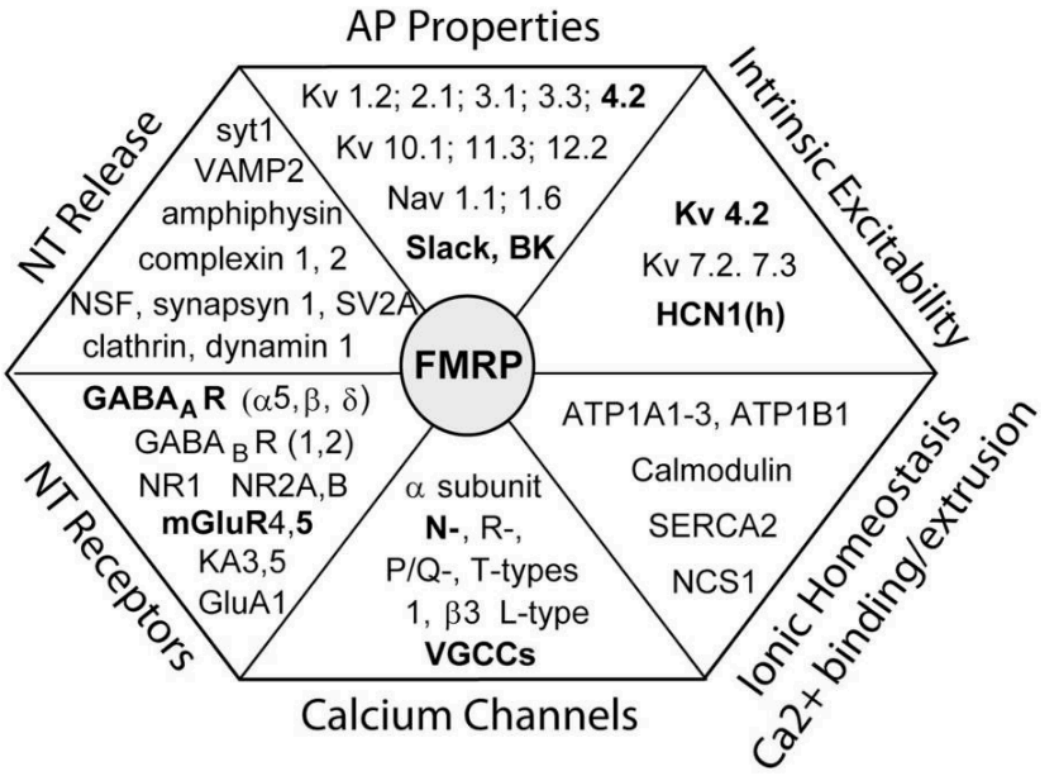

Figure 6: FMRP regulation of neuronal excitability: molecular and cellular mechanisms. Chart representing various aspects of neuronal excitability affected by FMRP loss and corresponding changes in the absence of FMRP in expression of proteins regulating these processes. Interactions that have been functionally validated and demonstrated to have an effect on excitability in Fmr1 KO mice are shown in BOLD. Figure adapted from (Contractor et al., 2015).

terminal aa1-298 fragment of FMRP, which lacks ability to interact with ribosomes, is sufficient for this interaction. Slack channels play major roles in excitability in many brain regions by regulating adaptation of firing during sustained activity and by setting a high temporal accuracy of APs, essential in many forms of sensory processing (Kim et al., 2014a). Mutations in the Slack channel have been linked to childhood seizures and severe forms of intellectual disability (Kim and Kaczmarek, 2014), implicating altered activity of this channel in the absence of FMRP as an important contributor to excitability defects in FXS (Zhang et al., 2012).

FMRP also regulates excitability of hippocampal and cortical pyramidal neurons by directly modulating another K^+ channel, the BK channel (Deng et al., 2013; Myrick et al., 2015a). Owing to their dual voltage- and Ca^{2+} dependence, BK channels influence excitability by controlling the AP duration and the AHP during sustained firing, thereby regulating both neurotransmitter release efficiency and the neuron's ability to generate high-frequency spiking (Contractor, 2013). Loss of FMRP reduces BK channel activity and causes excessive AP broadening, leading to elevated presynaptic Ca^{2+} influx and increased glutamate release during repetitive activity in both hippocampal and cortical pyramidal neurons (Deng et al., 2013). This study determined that FMRP regulates BK channel activity by interacting with the channel's auxiliary β4 subunit, which explains its reduced Ca^{2+} sensitivity in the absence of FMRP. This interaction is necessary for FMRP regulation of AP duration since FMRP-dependent AP broadening could not be induced in mice lacking BK β4 subunit. Together these findings suggest that FMRP regulation of AP duration is translation-independent; indeed, the excessive AP broadening in *FMR1* KO mice can be rapidly rescued and mimicked in the absence of protein synthesis (Deng et al., 2013).

The translation-independent role of this FMRP function in FXS excitability defects has been revealed in a study of an *FMR1* missense mutation R138Q, which is in the KH0 RNA binding domain of FMRP, and was found in a patient with a partial FXS phenotype (Myrick et al., 2015b, 2015a). This patient has a history of global developmental delay, intellectual disability, and intractable seizures, but no other features typical of FXS. While the R138Q mutation was found to preserve the canonical mRNA binding and translation-regulation capabilities of FMRP, the mutation rendered FMRP unable to modulate AP duration in both hippocampal and cortical pyramidal neurons (Myrick et al., 2015a). The R138Q mutation also almost fully abolished the interaction of FMRP with the BK channel β4 subunit. This finding provides further evidence for the role of FMRP-BK channel interactions in regulation of the AP properties and suggests that this translation-independent function of FMRP is linked to a specific subset of FXS phenotypes.

Another non-canonical aspect of FMRP's effects on excitability is that it directly binds to presynaptic N-type VGCCs and regulates their surface expression (Ferron et al., 2014). Unlike the interactions of FMRP with the Slack and BK channels, there is no effect of FMRP loss on N-type channel activity. This interaction of FMRP also differs from interactions with other channels in that it is mediated by the carboxyl-terminal domain, rather than the amino-terminus of FMRP

(Ferron et al., 2014). Loss of this interaction has a major impact on neurotransmitter release in dorsal root ganglion neurons, expanding the known range of FMRP functions that affect excitability and neurotransmitter release. Loss of direct protein-protein interactions of FMRP with ion channels is therefore emerging as a major contributor to excitability defects in FXS.

1.2.6.Learning and memory deficit in FXS

A majority of individuals with FXS exhibit intellectual impairment, which can range from mild to severe. Studies showed a larger hippocampus in individuals with FXS (Kates et al., 1997; Reiss et al., 1994) and functional deficits in the hippocampal domain in subjects with FXS (Cornish et al., 1998, 1999) would suggest that any fear task, spatial navigation or associative memory task requiring the hippocampus would show a deficit. Further, while individuals with FXS have normal amygdala and prefrontal cortex volumes, they have altered behavioral responses to tasks requiring the amygdala (Kim et al., 2014b), frontal lobe (Mazzocco et al., 1992) and prefrontal cortex (Kwon et al., 2001).

Therefore, decades of research characterizing the cognitive abilities of individuals with FXS predict that deficits in a FXS mouse model should occur in short-term (visual) memory, visual-spatial abilities, sequential information processing, executive function and attention (Cianchetti et al., 1991; Freund and Reiss, 1991; Maes et al., 1994).

1.3. Role of neuronal intrinsic excitability in mPFC function

1.3.1.Overview

Learning and memory are most frequently studied as a change in the efficacy of synaptic transmission. However, it is now clear that learning can also induce non-synaptic forms of plasticity such as changes in the intrinsic excitability of a neuron. Intrinsic plasticity can be defined as a change in the neuron's electrical properties, which are determined by ion channels expression in the membrane of neurons. These changes are induced by various neuromodulators, activity patterns, disease states, or learning paradigms (Disterhoft and Oh, 2006; Frick and Johnston, 2005; Magee, 2008; Mozzachiodi and Byrne, 2010; Szlapczynska et al., 2014; Zhang and Linden, 2003). These changes are mediated by a change in the properties and/or expression level of a wide range of voltage-gated Na^+, Ca^{2+}, K^+ hyperpolarization-activated and cyclic nucleotide-gated (HCN) channels, as well as voltage-independent ion channels present in the neuronal membrane (Migliore and Shepherd, 2002; Nusser, 2012). The exact kinetics and expression levels of these channels are characteristic for a given neuronal type and its sub-cellular compartments (e.g. soma versus dendrites). Any changes in the biophysical properties and/or distribution of these channels will alter the excitability of the neuronal membrane (Frick and Johnston, 2005). Intrinsic plasticity can take place anywhere along the cellular membrane

causing a neuron-wide change in excitability, or it can occur locally and remain restricted to individual dendritic branches. Changes induced in the somato-dendritic compartment typically affect the integration and propagation of synaptic inputs whereas those occurring in the axon modulate action potential properties (AP) and synaptic transmission.

The study of intrinsic plasticity is particularly useful in the context of learning and memory because it can potentially affect a wide range of neuronal functions including the presynaptic release of neurotransmitters, the way synaptic inputs are integrated in the dendrites, the AP output at the AP initiation site, the active back-flow of information into the dendrites, calcium signaling and numerous signaling pathways. Additionally, it has been suggested that it serves as a mechanism for metaplasticity, homeostatic regulation of neuronal activity, memory allocation or it even acts as part of the memory trace itself (Benito and Barco, 2010; Chen et al., 2006; Disterhoft and Oh, 2006; Frick and Johnston, 2005; Frick et al., 2004; Mozzachiodi and Byrne, 2010; Xu et al., 2012; Zhang and Linden, 2003; Zhou et al., 2009).

1.3.2. Ion channels involved in regulating intrinsic excitability

Neurons contain a vast number of different ion channels, which play an important role in shaping the excitability of the neuron. Ion channels are pore-forming membrane proteins and are the most fundamental excitable elements in the neuronal membrane. They are specifically responsive to incoming stimulation such as membrane potential change, neurotransmission and neuromodulation, chemical signaling or mechanical deformation, to name just a few. When ion flux occurs across the membrane, it has an immediate effect on the membrane potential leading to the activation of voltage-sensitive ion channels. Ion channels are present in membranes of all cells and play a critical role in regulating many aspects of their function. For example they are responsible for shaping the cell's resting membrane potential (RMP), controlling the flow of ions across the neuronal membrane including the messenger Ca^{2+} ions, regulating the electrical signals generated by the cell as well as controlling the cell's volume (Hille, 2001). The quest for investigating the distribution and properties of voltage-gated ion channels can be dated back to the 1950s. That is when Alan Hodgkin and Andrew Huxley first described a model that could accurately predict the shape of an AP that is generated and propagated along the squid giant axon (Hodgkin and Huxley, 1952). Since then electrophysiological and molecular studies unveiled the complex distribution patterns and properties of various families of ion channels in the neuronal membrane (Catterall et al., 2012; Lai and Jan, 2006; Migliore and Shepherd, 2002). Below I provide a brief overview of the voltage-gated ion channels that are present in mammalian pyramidal neurons of the neocortex.

Voltage-gated ion channels fall into a number of broad categories based on their selectivity for certain ions, for example K^+, Na^+, Ca^{2+} (Kv, Nav, Cav, respectively) channels, and non- selective cation channels activated by hyperpolarisation (i.e. hyperpolarisation activated and cyclic nucleotide-gated channels, HCN). All mammalian voltage-gated ion channels contain

one or four transmembrane pore-forming proteins. More specifically, Nav and Cav channels are formed by a single α-subunit (Nav) or α1-subunit (Cav) containing four transmembrane repeats (domains I-IV), whereas Kv and HCN are formed by four α-subunits, each with a single domain. In the case of Kv and HCN channels, the four α-subunits can co- assemble to form both homo- and heterotetrameric pore-forming subunits, increasing their molecular diversity (Lewis and Chetkovich, 2011; Luján, 2010). Each domain comprises six transmembrane segments (S1-S6). The S4 segment in each domain detects changes in membrane potential whereas segments S5 and S6 and the re-entrant pore loop between them form the lining of the pore. These pore-forming subunits are associated with auxiliary subunits (α2, β, γ or δ), as well as a range of other molecules, such as scaffolding proteins, which serve to modulate the channels' properties or their subcellular location. Differential splicing, the formation of heteromers and additional post-translation modifications further extend the diversity of voltage-gated ion channels (Luján, 2010; Migliore and Shepherd, 2002; Vacher et al., 2008).

1.3.2.1.Nav channels

Nav channels mediate a fast depolarising inward current and thus are the primary channels responsible for the generation and propagation of APs in the axon (Hodgkin and Huxley, 1952) as well as the back-propagation of APs into the dendrites (Stuart and Sakmann, 1994; Stuart et al., 1997a, 1997b). They also allow for the generation of Na^+ mediated dendritic spikes and the non-linear integration of synaptic potentials (Larkum et al., 2007, 2009; Stuart et al., 1997a). In mammals, nine genes are known to encode the α-subunits of Nav channels - Nav1.1 to Nav1.9. Of the nine known Nav family members, four subunits (Nav1.1, 1.2, 1.3 and 1.6) are expressed in the rodent/human brain (Golding et al., 2001; Trimmer and Rhodes, 2004).

The Nav1.2 subunits are expressed specifically in the main axon and its terminals and are thought to be the major channels underlying AP propagation as well as important regulators of neurotransmitter release in the terminals (Westenbroek et al., 1989). Nav1.1 and Nav1.3 show a somato-dendritic distribution, with Nav1.3 having the highest expression levels in the embryonic and early postnatal brain. Finally, Nav1.6 is present both in the somato-dendritic compartment and in the axon (Golding et al., 2001; Trimmer and Rhodes, 2004). Nav channels are sensitive to modulation by a large number of neurotransmitters, which have been shown to alter their function. For example, phosphorylation of Nav channels has important functional consequences as it can result in a reduction of Na^+ currents or the long inactivation of Na channels in the dendrites. This mainly occurs via the phosphorylation of the α-subunits by the cAMP (cyclic adenosine monophosphate), dependent protein kinase A (PKA) and protein kinase C (PKC) or dephosphorylation by the Ca^{2+} regulated phosphatase calcineurin and protein phosphatase (Cantrell and Catterall, 2001; Frick and Johnston, 2005; Spruston and Johnston, 1992).

Although the majority of the current generated by Nav channels is fast, Nav channels can also generate a persistent noninactivating or slowly inactivating current INaP (Crill, 1996; Kiss, 2008). This current constitutes only a small fraction of the transient Na^+ current but it has significant physiological consequences.

1.3.2.2.Cav channels

Cav channels are important regulators of neuronal excitability. They are expressed in the somata, dendrites and axon terminals. They mediate Ca^{2+} influx into the cell following membrane depolarisation and play an active role in the amplification of incoming synaptic signals, generation of dendritic Ca^{2+} spikes, the activation of Ca^{2+} gated K^+ channels, signalling resulting from back-propagating APs and synaptic plasticity. Cav channels also mediate a range of intracellular processes such as Ca^{2+} dependent enzyme activation, gene transcription and neurotransmitter secretion (Catterall, 2011; Vacher et al., 2008). For those reasons, Cav channels create an important link between neuronal excitability, physiological events within the cell and synaptic plasticity. Cav channels can be classified into three families — Cav1-3 — giving rise to five different channel types: L-type (Cav1), P/Q-type (Cav2.1), N-type (Cav2.2), R-type (Cav2.3) and T-type (Cav3) (Lai and Jan, 2006).

Cav1 or L-type channels are expressed in the somata and dendrites where they play an important role in somato-dendritic signalling. They require a strong depolarization for their activation (high-voltage activated), conduct large currents and display slow inactivation kinetics. On the other hand, Cav3 or T- type channels are activated at much more negative membrane potentials, have small single channel conductance, inactivate rapidly and deactivate slowly. They play a role in regulating Ca^{2+} permeability around RMP and AP firing. Finally, Cav2 require a high voltage for activation and display fast deactivation kinetics and moderate to slow inactivation kinetics. Apart from playing a role in somatodendritic Ca^{2+} influx they also regulate fast neurotransmitter release from presynaptic terminals (Catterall, 2011; Trimmer and Rhodes, 2004; Vacher et al., 2008). Cav channels are modulated by phosphorylation, G-proteins and by Ca^{2+} itself (Catterall, 2000).

1.3.2.3.TRP channels

Members of the TRP (Transient Receptor Potential) superfamily of channels share the common features of six transmembrane segments, varying degrees of sequence homology, and permeability to cations. Despite these similarities, TRP channels are highly unusual among the known families of ion channels in that they display an impressive diversity of cation selectivities and specific activation mechanisms. Perhaps most amazing is that a single TRP channel can be activated through seemingly disparate mechanisms. In many cases, TRPs can be considered as multiple signal integrators, as the response to one input is modified by another. Nevertheless, a common thread among the superfamily is that TRP channels play critical roles in the responses

to all major classes of external stimuli, including light, sound, chemicals, temperature, and touch. TRP channels also imbue individual cells with the ability to sense changes in the local environment, such as alterations in osmolarity (Venkatachalam and Montell, 2007).

TRP channels are expressed and function in a great variety of multicellular organisms, including worms, fruit flies, zebrafish, mice, and humans. The TRP superfamily is broadly divided into groups 1 and 2, which are themselves divided into seven subfamilies (Montell, 2005). The separation of the group 1 and 2 TRPs is based on sequence and topological differences. The group 1 TRPs consist of five subfamilies: the classical or TRPC, TRPV, TRPM, TRPA, and TRPN subfamilies. The two subfamilies TRPP and TRPML comprise the group 2 TRPs, which are distantly related to the group 1 TRPs. The TRPP and TRPML proteins share sequence homology over the transmembrane segments and contain a large loop separating the first two transmembrane domains (Venkatachalam and Montell, 2007).

The mechanism(s) through which a given TRP is activated and regulated cannot be predicted reliably on the basis of its subfamily assignment. For example, thermally activated TRPs belong to members of the TRPV, TRPM, and TRPA subfamilies, while regulated exocytosis stimulates cation influx via several TRPC, TRPV, and TRPM channels. However, in some cases there are similarities among subfamily members, as all TRPC channels are activated through pathways coupled to stimulation of phospholipase C (PLC). The recurring theme is that most TRP channels are activated through a diversity of mechanisms (Venkatachalam and Montell, 2007).

The TRP superfamily of channels participates in a diversity of functions in both excitable and nonexcitable cells. However, a recurring theme is that TRP channels have critical roles in sensory physiology. These include sensory roles in the broadest sense. TRP channels are not only essential in allowing animals to sense the outside world, but also allow individual cells to sense their local environment.

1.3.2.4.K^+ channels

K^+ channels are the most important negative regulators of intrinsic excitability and are the largest and most diverse ion channel group. In general, K^+ channels play an important role in dampening neuronal excitability by providing outward or inward rectifiers currents. Their exact functional role depends on their specific biophysical properties such as activation/inactivation kinetics, voltage-dependence of activation (Yuan and Chen, 2006). There are over 100 genes in the mammalian genome encoding K+ channel α- and auxiliary subunits (Gutman et al., 2005; Yuan and Chen, 2006). K^+ channels can be subdivided into several groups based on their pore-forming α-subunits – voltage-gated (Kv), Ca^{2+} activated, inward rectifying (Kir3/GIRK) and two-pore (K2P) channels. In contrast two Kv and Ca^{2}+ activated K^+ channels, K2P and Kir3 are formed by four and two transmembrane domains respectively (Luján, 2010). A study showed than increasing Kir3 activity rescued all hippocampal deficits induced by Amyloid-β due to the

restoration of excitability values in the hippocampus CA3–CA1 synapse (Sánchez-Rodríguez et al., 2017). This study suggests a role in plasticity of Kir3 channel.

1.3.2.5.Kv channels

Kv channels represent the largest and most diverse group of voltage-gated ion channels (Luján, 2010; Vacher et al., 2008). The mammalian Kv α-subunits are encoded by approximately 40 genes, which can be grouped into 12 families Kv1-Kv12 (Gutman et al., 2005). The prototypic Kv subunits were categorised into 4 families (Kv1-Kv4) based on their Drosophila homologues Shaker, Shab, Shaw, Shal. More recently, α-subunits forming Kv5-Kv12 subfamilies have been discovered. Consequently, the genes encoding the α-subunits are known under these names: Shaker/Kv1/KCNA; Shab/ Kv2/KCNB; Shaw/Kv3/KCNC; Shal/Kv4/KCND; Kv5/KCNF; Kv6/KCNG; Kv7/KNCQ; Kv8/KCNV; Kv9/KCNS; Kv10/KCNH; Kv11/KCNH; and Kv12/ KCNH.

The expression pattern of Kv1 is limited mainly to the axon and nerve terminals, Kv2 and Kv4 show a somato-dendritic distribution, whereas Kv3 is expressed both in the axonal and somato-dendritic compartments. Kv7 expression is mainly axonal, with some accounts of also somato-dendritic localisation. Information about the subcellular distribution of Kv5-6 and Kv8-12 is limited. Depending on their activation kinetics, Kv channels can be categorised into transient (Kv1.4, Kv3.3-Kv3.4, Kv4), sustained (Kv1.1-Kv1.3, Kv1.5-Kv1.6) or delayed rectifying channels (Kv2, Kv7).

One of the most studied K^+ channel is the rapidly activating and inactivating dendritic A-type K^+ channel (Kim et al., 2007; Yang et al., 2015). Most of our knowledge about this channel and the current it generates comes from studies on the hippocampus and neocortex. In these brain regions the A-type K^+ current is generated predominantly by Kv4.2 and Kv4.3 subunits with some contribution from Kv1.4 (Norris and Nerbonne, 2010). These currents regulate AP repolarisation, repetitive firing, synaptic integration and AP backpropagation (Cai et al., 2004; Chen et al., 2006; Frick et al., 2003; Grewe et al., 2010; Johnston et al., 2003). Kv4.2 is regulated by a number of intracellular signalling pathways and kinases, including PKA, PKC, MAPK (Mitogen – activated protein kinase) and CaMKII (Ca^2+/calmodulin – dependant protein kinase) (Rosenkranz et al., 2009; Schrader et al., 2002). The activation of PKA, PKC and MAPK by various neuromodulators results in a decrease of the A-type K^+ channel activity (Hoffman and Johnston, 1998, 1999; Yuan et al., 2002), whereas CaMKII activation alters the channel's surface expression (Varga et al., 2004).

Kv7 channels are delayed rectifiers with slow kinetics, which are activated at subthreshold levels and play a role in maintaining the RMP and reducing neuronal excitability. Kv7 channels underlie the M-type current, a slowly activating and inactivating current that is modulated by G-proteins. The main subunits underlying the M-type current are Kv7.2 and Kv7.3. M-type K^+ channels play a critical role in controlling the subthreshold membrane excitability, the generation of theta-frequency oscillations, the regulation of interspike intervals and the neuron's

responsiveness to synaptic inputs (Guan et al., 2011; Wang et al., 1998). Moreover, Kv7 channels regulate the dynamics of neuronal firing (Peters et al., 2005; Rogawski, 2000) and have been shown to contribute to the generation of fast AHP (fAHP) occurring after a single AP (Brown and Passmore, 2009; Santini and Porter, 2010). Kv7 channels are also readily phosphorylated. PKA activation for example, enhances M-type currents, whereas the activation of tyrosine kinase results in a slow inhibition of Kv7.2/Kv7.3 expression.

Kv1 channels that are expressed mainly in the main axon and its terminals, and are likely to be the channels generating the dendrotoxin sensitive D-type K^+ current. D-type K^+ current is a fast-activating, slow-inactivating current that plays a role in controlling the AP threshold, waveform, firing frequency, presynaptic neurotransmitter release and synaptic efficacy (Bekkers and Delaney, 2001; Guan et al., 2007a; Kole et al., 2007; Shu et al., 2007).

Kv1, Kv2 and Kv7 channels all contribute to regulating the biophysical properties of the somata of neocortical pyramidal neurons. Out of these three, Kv2 channels account for the largest K^+ current of the somatic compartment — up to 60% of the total Kv current activated by large depolarizing voltage steps (Guan et al., 2013). Kv2 channels activate slowly at depolarized membrane potentials (Guan et al., 2007b) and due to their slow kinetics their major role is to regulate repetitive firing in reducing it (Guan et al., 2013; Johnston and Narayanan, 2008; Malin and Nerbonne, 2002).

Kv3 family members display rapid activation kinetics at voltages more positive than -10 mV and very rapid inactivation kinetics. Their functional role is to facilitate sustained high firing frequencies by enabling fast AP repolarization. They are therefore highly expressed in fast-spiking neurons, such as neocortical or hippocampal interneurons (Vacher et al., 2008).

1.3.2.6.Ca^{2+} activated K^+ channels

Ca^{2+} gated K^+ channels are activated by an increase in the intracellular concentrations of Ca^{2+} and voltage changes. Their opening curtails calcium transients and causes membrane hyperpolarisation and a decrease in neuronal excitability. The main Ca^{2+} activated K^+ channels expressed in the brain are the small-conductance voltage-insensitive K^+ channels (SK), with a single channel conductance of 2-20pS, and the big-conductance K^+ channels (BK), which are activated by both intracellular $Ca2^+$ and voltage and have a single channel conductance of 200-400pS (Sah and Faber, 2002). SK channels are formed by three subunits SK1-SK3 and they are sensitive to apamin and bicuculline, which distinguishes them from BK channels that are insensitive to these drugs (Luján, 2010; Sah and Faber, 2002; Wei et al., 2005; Yuan and Chen, 2006). BK channels play a role in rapid repolarization of APs and the fAHP, which lasts 2-5 milliseconds and occurs immediately after a single AP. Also, M-type and A-type currents are thought to contribute to fAHP. The fAHP plays a role in AP repolarization and therefore AP width, and controls spike frequency adaptation (Disterhoft and Oh, 2006; Faber and Sah, 2003; Yuan and Chen, 2006). SK channels on the other hand are thought to underlie the medium AHP

(mAHP) currents that occur after a single AP or a burst of APs. The mAHP has a much slower decay time than the fAHP and lasts from 50-200 milliseconds (Stocker et al., 2004). In addition to fAHP and mAHP, the AHP can also have a third slow component (sAHP) that typically occurs after a burst of APs and decays over the course of seconds. The exact Ca^{2+} activated K^{+} channel underlying this conductance has not yet been identified (Andrade et al., 2012; Disterhoft and Oh, 2006).

In the cortex, SK channels respond to the Ca^{2+} induced Ca^{2+} release triggered by the activation of muscarinic receptors (Gulledge et al., 2007; Yamada et al., 2004) or metabotropic glutamate receptors (Hagenston et al., 2008). In the prefrontal cortex the block of SK channels improves working memory (Brennan et al., 2008). In L5 pyramidal neurons of the mPFC, SK channels-mediated hyperpolarization followed by a prolonged depolarization that respectively decreased and increased neuronal excitability through an interaction with NMDA (N-methyl-D-aspartate) receptors and Cav channels (Faber, 2010). Both SK and BK channels are present in the soma and dendrites of pyramidal cortical neurons (Benhassine and Berger, 2005; Sailer et al., 2004; Sausbier et al., 2006). SK1 and SK2 are highly expressed in the neocortex with SK3 showing higher expression levels in the subcortical regions (Stocker et al., 2004).

1.3.2.7.HCN channels

HCN channels differ from other voltage-gated ion channels as they are activated by hyperpolarisation and deactivated by depolarisation. They belong to the superfamily of K+ channels, however, they are non-selective cation channels enabling flux of a mixed K+/Na+ current. This hyperpolarisation-activated current is called *I*h. HCN channels are directly modulated by cAMP. Because HCN channels can generate rhythmic activity in neurons and cardiac cells, they are often referred to as 'pacemaker channels'. Ih plays a wide range of important functions in neurons: they contribute to the RMP, act as resonance conductors, suppress temporal and spatial summation of synaptic inputs and decrease the efficacy of backpropagating AP. Most of HCN activity results in a reduction of dendritic excitability. However, Ih also causes rebound depolarisations following membrane hyperpolarisations that contribute to the generation of dendritic plateau potentials or spikes (Lewis and Chetkovich, 2011; Luján, 2010).

HCN channels are composed of four subunits HCN1-HCN4. The functional properties of these channels are determined by the subunits that form them. For example, HCN1 subunits respond much faster to hyperpolarising potentials and display faster activation kinetics than HCN2-4. Out of all the subunits, HCN4 require the strongest hyperpolarisation and are the slowest to activate. On the other hand, HCN4 subunits are very sensitive to the presence of cAMP, whereas the responsiveness of HCN1 to cAMP is minimal. cAMP activity shifts the voltage activation of HCN channels to more depolarised potentials, which enhances their activation at RMP. In the neocortex, the two major subunits responsible for generating Ih are HCN1 and HCN2

and they show a non-uniform gradient of distribution increasing in density with distance from soma. HCN3 and HCN4 subunits are more concentrated in subcortical regions. HCN channels are also, although to a lesser degree, expressed in the axon (Kole et al., 2006; Migliore and Shepherd, 2002; Notomi and Shigemoto, 2004; Pape, 1996; Robinson and Siegelbaum, 2003).

1.4. Cell classification

Cells have traditionally been categorized based on location within an organism, their structure, function or even developmental history. Neuronal classification remained a dominant theme in neurobiology over the past half-century as a physiological and molecular methods matured and mechanistic, to be valued over projects. The development of a cellular taxonomy will facilitate our understanding of how the brain works or, in diseases, fails to work properly.

What are the relevant properties? The four main categories are morphological, physiological, molecular and connectivity (Fishell and Heintz, 2013; Petilla Interneuron Nomenclature Group et al., 2008; Sanes and Masland, 2015) (Figure 7). The morphological properties of neurons, dendritic and axonal shapes and branching patterns have been the most informative; however, features such as soma size and spine density are also used. The physiological properties of neurons include biophysical properties and the action potential firing pattern and rate. Of the many molecular properties that can be considered, the most useful are protein composition and mRNA composition (Figure 7). A fourth category of properties, connectivity, is equally relevant but is harder to assess and is therefore less often used.

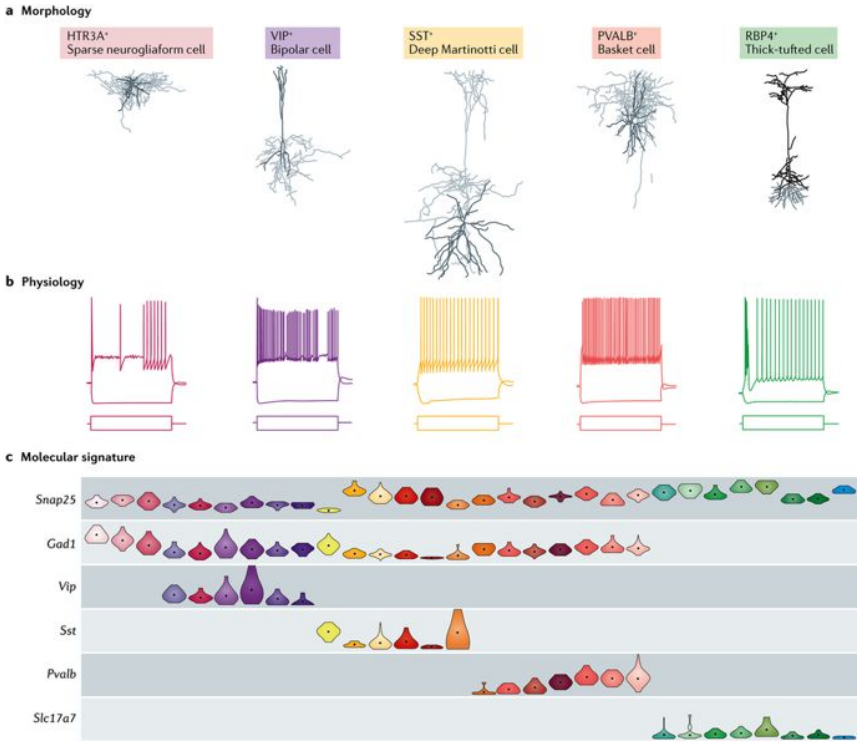

Figure 7: Neurons can be classified using morphological, physiological and molecular criteria. a, Representative examples of five subclasses of cortical neurons obtained from brain slices. The cells were filled with biocytin, stained and imaged following patch clamp recording (**b**). For the four interneurons on the left, the dendrites are shown in dark grey and the axons in light grey. **b,** Differential electrophysiological responses of the five subclasses of neurons shown in part (**a**) to square pulses of current in patch clamp recordings. **c**, Differential molecular signatures of the five subclasses of cortical neurons illustrated in part (**a**) derived from single-cell RNA-sequencing data. The violin plot shows the collective gene expression profile for each gene of all the cells in a type (cluster). The smallest discrete clusters of cells are defined as types and the aggregates of types that share common features as classes or subclasses. Each transcriptomic cell type is shown as a column of data points with the same color. Figure adapted from (Zeng and Sanes, 2017).

New methods for sparse labelling and high-throughput light-microscopic imaging have fueled efforts to assess neuronal morphologies, including entire axonal and dendritic arbours, in both fruitflies and mice. A key advance has been the generation of many cell type-specific transgenic lines driven by *cis*-regulatory elements in isolation or in a genomic context (Harris et al., 2014; Taniguchi et al., 2011). These and other tools — e.g. viral tools (Haberl et al., 2015) — are being used to collect whole-brain catalogues of morphologies (Economo et al., 2016; Gong et al., 2013). In addition, recordings from, and morphological reconstructions of, thousands of neurons from cortical brain slices have been used to classify them into hundreds of morpho-electrical types (Frick et al., 2008; Markram et al., 2015; Oberlaender et al., 2011; Radnikow and Feldmeyer, 2018).

A series of important advances in single-cell genome-wide molecular profiling techniques that have occurred over the past decade are benefiting cell-type classification efforts (Shapiro et al., 2013; Trapnell, 2015). These advances include improvements in methods used to assess the genome, transcriptome, proteome and epigenome of single cells. These methods

demonstrate vastly improved sensitivity compared with the previous generation of techniques. These previous approaches typically require as input hundreds to millions of cells, revealing only an average reading across cell populations. For developmental biology, where individual cells make decisions about their fate, these ensemble measures provide only limited information, as individual cellular measurements are lost.

At this time, the most mature, scalable and useful technique for molecular profiling of cell type diversity is single-cell RNA sequencing (scRNA-seq). This method is easily amenable to automation and, if applied at a sufficiently large scale, could drive a first 'complete' cell-type classification. To perform scRNA-seq, investigators dissociate cells from tissues and isolate them by manual picking, microfluidics or fluorescence-activated cell sorting. Subsequently, RNA is converted to cDNA, which is amplified and sequenced. A number of studies have used this approach to identify and classify cell types in a collection of neural tissues (Földy et al., 2016; Poulin et al., 2016; Svensson et al., 2017).

Satisfactory cell-type classification requires the collection of morphological, physiological, molecular and possibly connectional categories (Figure 7). This is best accomplished by collecting two or more data types from the same cells. This was common in earlier studies: for example, dye filling of neurons was performed following intracellular recording, and immunohistochemistry was performed on green fluorescent protein (GFP)-labelled cells. More recently, in Patch-seq, cellular contents are extracted following patch clamp recordings and subjected to scRNA-seq (Cadwell et al., 2016; Földy et al., 2016; Fuzik et al., 2016). This combination provides rich data but is restricted to small numbers of cells.

1.5. Aims of this study

Objective 1: Establish the molecular and intrinsic excitability signature of L5 pyramidal neurons mediating D1/D2 modulation within PL.

To achieve this, we combined electrophysiological whole-cell recordings from L5 pyramidal neurons in acute slices of the PL part of the mPFC with single-cell RNA sequencing, morphological, and connectivity analysis. Electrophysiological recordings revealed different intrinsic properties of L5 pyramidal neurons. The *Fmr1*-KO mice presented a deficit in some intrinsic properties of both subpopulations D1R and D2R type. Accordingly, principal component analysis enabled the categorization into two neuron types, resembling the D1R and D2R type described in the literature. To further explore the molecular underpinnings of these differences, we performed single-cell RNA sequencing of the recorded neurons. Transcriptome analysis revealed significant differences in the expression level of >500 gene products (out of 14000 RNAs detected) for D1R and D2R comparaison, belonging to many different functional categories. We also showed a significant differences in the expression level of >1500 and >1100 gene

products for D1R WT *versus* D1R KO and D2R WT *versus* D2R KO, respectively. For example, differences in the intrinsic excitability correlate with a differential ion channel expression pattern. Importantly, 109 gene products were exclusively expressed in either one or the other neuron type, including transcription factors and risk genes for disease, providing potential candidates for cell-type specific genetic targeting and disease prediction, respectively.

Objective 2: Probe the functional role of intrinsic excitability plasticity in PL-L5 pyramidal neurons of the neurons belonging to the class of D1-type neurons and projecting to the basolateral amygdala, in long-term memory formation.

We first tested if contextual fear conditioning induces plasticity of the intrinsic excitability in L5 pyramidal neurons of the PL that are projecting to the basolateral amygdala (BLA), and the time course of this form of plasticity. To address this, we used electrophysiological whole-cell recordings in acute slices of the PL either 1 to 4 or 10 to 15 days after the learning task . While we observed a change in the intrinsic excitability during the early phase of memory formation, there was no significant plasticity observed at the later phase. To investigate a causal role between intrinsic excitability plasticity and long-term memory formation, we used a pharmacogenetic approach to manipulate the excitability of PL–BLA L5 pyramidal neurons at the same time intervals following learning where intrinsic excitability plasticity was either present or not, and tested memory retrieval during remote time points. Reducing the excitability of these neurons 1 to 7 days following learning reduced remote memory performance, while increasing their excitability had the opposite effect. In contrast, no change in remote memory performance was observed following manipulation during the later time period. These findings suggest causality between the intrinsic excitability plasticity of PL L5 neurons projecting to the BLA and long-term memory formation.

2. Results

2.1. Molecular and intrinsic excitability profiles of L5 pyramidal neurons D1R and D2R type

The following manuscript describes experiments leading to better understand the functional role of two subpopulations of L5 pyramidal neurons into the PL area involved in memory formation via two different streams of DA modulation.

Manuscript N°1

Manuscript in preparation for submission

Single-cell RNA and electrophysiological profiling of D1+ and D2+ principal neurons of the prefrontal cortex

R. De Sa[1], D. Lukacsovich[3], J. Winterer[3], K. Le Corf[1], M. Ginger[1], C. Földy[3], A. Frick[1,2]

[1]Inserm u1215, Neurocentre Magendie, Bordeaux 33077, France

[2]University of Bordeaux, Bordeaux 33077, France

[3]University of Zurich, CH-8006 Zurich, Switzerland

Abstract

Among the hallmark phenotypes reported in individuals with fragile X syndrome (FXS) are deficits in attentional function, inhibitory control, and cognitive flexibility, a set of cognitive skills thought to be associated with the prefrontal cortex (PFC). However, despite substantial clinical research into these core deficits, the PFC has received surprisingly little attention in preclinical research, particularly in animal models of FXS. In our study, we decided to focus on neurons expressing D1 or D2 receptor and characterized them by electrophysiology, morphology, connectivity and transcriptomic profiling in WT and *Fmr1*-KO mice. Electrophysiological recordings revealed different intrinsic properties of L5 pyramidal neurons. The *Fmr1*-KO mice presented a deficit in some intrinsic properties of both subpopulations D1R and D2R type. Accordingly, principal component analysis enabled the categorization into two neuron types, resembling the D1R and D2R type described in the literature. To further explore the molecular underpinnings of these differences, we performed single-cell RNA sequencing of the recorded neurons. Transcriptome analysis revealed significant differences in the expression level of >500 gene products (out of 14000 RNAs detected) for D1R and D2R comparaison, belonging to many different functional categories. We also showed a significant differences in the expression level of >1500 and >1100 gene products for D1R WT *versus* D1R KO and D2R WT *versus* D2R KO, respectively. Importantly, 109 gene products were exclusively expressed in either one or the other neuron type, including transcription factors and risk genes for disease, providing potential candidates for cell-type specific genetic targeting and disease prediction, respectively.

Introduction

During higher-order executive tasks, the medial prefrontal cortex (mPFC) exerts top-down control, coordinating activity in downstream networks via extensive connections to cortical and subcortical targets (Miller, 2000b; Narayanan and Laubach, 2006). This top-down control of PFC neurons is tuned by several neuromodulators, including acetylcholine, serotonin and dopamine (DA). DA modulation in the PFC modulates a number of higher cognitive functions, such as working memory (Seamans and Yang, 2004), relaying motor commands and gating sensory input (Ott and Nieder, 2019). Indeed, dysfunction of the DA modulatory system of the

mPFC has been implicated in cognitive and behavioral impairments associated with Tourette's syndrome, post-traumatic stress disorder, attention-deficit hyperactivity disorder, and schizophrenia (Bonilha et al., 2008; Bremner et al., 1999; Casey et al., 2007; Lewis and González-Burgos, 2008; Marsh et al., 2007; Shin et al., 2004). DA alters the intrinsic excitability of neurons via DA 1 (D1R) or 2 (D2R) receptor (Seamans and Yang, 2004), but the nature of the modulation depends on the brain area (Wang and O'Donnell, 2001; Ceci and Borsini, 1999; Rozenkranz and Johnston, 2006), downstream signaling (Seaman and Yang, 2004) and the activity of the surrounding network (Gulledge and Jaffe, 2013).

A primary source of output from the mPFC occurs via layer V pyramidal neurons. Neuromodulation of synaptic inputs of pyramidal neurons possessing D1R or D2R (Law-Tho et al., 1993; Couey et al., 2007; Wang et al., 2008; Kruse et al., 2009) and their intrinsic properties have been characterized, with some conflicting results (Gulledge and Jaffe, 1998; Gulledge and Stuart, 2003; Yang and Seamans, 1996). One potential explanation for these discrepancies may be the diversity of layer V pyramidal neuron types. In several neocortical regions, layer V pyramidal neurons have distinct interconnectivity, morphology, and firing patterns depending on their long-range projection targets (Brown and Hestrin, 2009; Molnár and Cheung, 2006; Morishima and Kawaguchi, 2006; Otsuka and Kawaguchi, 2008). Another explanation comes by the fact that pyramidal neurons have different sets of DA receptors, D1R, D2R and a combination of both. Then, we also have a difference in the modulation of intrinsic excitability depending on which receptors are activated (Claudia Rangel-Barajas and Claudia Rangel-Barajas, 2015). Single-cell RNA sequencing combined with electrophysiological recordings and morphological analysis provides a tool for detailed profiling of D1R and D2R pyramidal neurons and thus identification of distinct cell types.

Fragile X syndrome (FXS) is the most common form of inherited mental retardation with a variety of phenotypes including impaired cognitive ability, working memory, autistic behavior, and increased incidence of epilepsy (Dykens et al., 1987; Maes et al., 1994; Munir et al., 2000). Most commonly, FXS is caused by silencing of the *fmr1* gene encoding for the fragile X mental retardation protein, FMRP (Bell et al., 1991). A *Fmr1* KO mouse model was reported to show similar phenotypes and is frequently used to study the neurobiological underpinnings of the disease (The Dutch-Belgian Fragile X Consortium, 1994).

FMRP is known to interact with at least 800 different mRNAs. In addition, recent studies show that FMRP interacts with different voltage-gated ion channels via direct protein-protein interaction (Gross and Bassell 2011; Brown and Kaszmarek, 2010; Strumbos and Kaszmarek 2010; Deng et al., 2013). Considering the role of ion channels in determining the intrinsic excitability of neurons, these findings raise the possibility of an altered intrinsic excitability phenotype in *Fmr1* KO neurons. Furthermore, dopaminergic modulation of synaptic transmission was found to be altered in *Fmr1* KO mice (Wang and Zhuo, 2008). Experimental evidence further

supported the hypothesis that dopaminergic signaling in FXS is disrupted (Wang et al., 2008), raising the possibility that the modulation of ion channels is also altered in these mice.

Here, we combined electrophysiological recordings with single-cell RNA sequencing (RNAseq) and morphological analysis to identify and characterize D1R- and D2R layer 5 pyramidal neuron types within the pre-limbic (PL) part of the mPFC. Our data represent the first single-cell transcriptome analysis from electrophysiologically and morphologically defined layer 5 pyramidal neurons of the mPFC. We find several characteristic differences in the intrinsic properties of these neuron types that are correlative of differences in their ion channel gene expression profiles. The quantification of expressed genes shows that D1R/D2R neurons can be characterized by the differential expression of >500 genes divided into different categories (ion channels, cell adhesion molecules, transcription factors, receptors, …). The comparison in gene expression between D1R WT and D1R KO neurons reveals more than 1500 genes with a differential expression and more than 1100 genes between D2R WT and D2R KO neurons. Another interesting fact, is that D2R WT cell-type showed an overall high expression of different genes and might be more prone to disease based on the highest expression of autism risk genes. However, D1R KO cell-type seems more impacted by the lost of FMRP leading to an over expression of different genes. Our data lays the foundation for a biologically relevant analysis of how cell type-specific neuronal gene expression may sculpt neural circuits. Further, this study could also lead to a generation of mice model targeting D1R or D2R pyramidal neurons into layer 5 PL area and could also provide a potential therapeutic target for FXS.

Materials and Methods

Brain slice preparation

Electrophysiological experiments were performed on layer (L) 5 pyramidal neurons in acute prelimbic cortex (PrL) slices from male (P28-35) C57Bl/6J mice. Mice were anesthetized with a lethal dose of isoflurane (absence of foot-pinch reflexes), and intracardially perfused with ice-cold cutting solution containing (in mM): 2.5 KCl, 25 $NaHCO_3$, 7 $MgCl_2$, 1.25 NaH_2PO_4, 1 $CaCl_2$ and 240 Sucrose (pH 7.4; 300-310 mOsm). Coronal slices (300 µm thick) were prepared using a vibratome (VT1200, Leica, Germany) in ice-cold cutting solution, and then incubated at 37°C for 30 min in artificial cerebrospinal fluid (aCSF) containing (in mM): 125 NaCl, 25 $NaHCO_3$, 25 D-glucose, 2.5 KCl, 1.25 NaH_2PO_4, 2 $CaCl_2$, 1 $MgCl_2$, 1 ascorbic acid and 4 pyruvic acid (pH 7.4; 300-310 mOsm). Both solutions were saturated with carbogen (5% CO_2/95% O_2). For electrophysiological recordings, brain slices were placed in a submerged chamber and superfused with aCSF at a rate of 3-5 ml/min.

Electrophysiology

PrL-L5 pyramidal cells were visualized by infrared gradient contrast using an upright microscope (Carl Zeiss Axio Examiner.D1), fitted with a 63X/1.0 numerical aperture water-immersion objective. Whole-cell patch-clamp recordings were performed from the cell bodies using borosilicate glass pipettes with filaments (Harvard Apparatus, GC150F-7.5, 1.5 mm OD, 0.86 mm ID, 7.5 cm length). Pipettes (open tip resistance 4-6 MΩ) were filled with a standard intracellular solution (in mM): 135 K- gluconate, 10 HEPES, 10 Phosphocreatine-Na, 4 KCl, 4 ATP-Mg, 0.3 Na-GTP (pH 7.3 adjusted with KOH, 290-300 mOsm). Signals were sampled at 50 kHz acquisition rate and low-pass filtered at 3 kHz using a Multiclamp 700B amplifier (Axon Instruments, Inc.). Current-clamp recordings were obtained in continuous single-electrode current-clamp mode, and capacitance and bridge were compensated for. Access resistance was monitored throughout, in the range of 15 – 30 MOhm, and recordings were terminated if the value was above 30 MOhm or increased by >15%. Recordings were also terminated if the initial resting membrane potential changed by >5 mV. All experiments were performed at room temperature and in the presence of the following synaptic blockers (in μM): 10 Gabazine ($GABA_A$ receptor), 3 NBQX (AMPA receptor) and 50 DL-APV (NMDA receptor). All chemicals were purchased from Sigma or Tocris.

Identification of Cell Types

Cells were identified based on soma location and passive/active membrane properties including action potential (AP) firing properties. For the recordings that were combined with RNA sequencing, we did not use any labeling method that could potentially interfere with the RNA quality. Thus, *post hoc* morphological or immunohistochemical analyses were performed on a different set of recordings. Biocytin-filled neurons were processed using standard procedures (see Frick et al., 2008). Briefly, slices were fixed at 4°C for 2 h in phosphate buffer (PB) containing 4% paraformaldehyde (PFA), then incubated overnight at 4°C in 0.5% Triton X-100, 3% Bovine Serum Albumin (BSA), 4% Normal Goat Serum (NGS) solution containing Streptavidin-Alexa Fluor 488 (Molecular probes). Slides were embedded using Mowiol (Sigma-Aldrich). Neurons were reconstructed using the Neurolucida system (MBF Bioscience) with a 100×oil-immersion objective.

Single cell RNA collection

To avoid any impact of the whole-cell recording on the number of detected gene transcripts, we kept the duration of the electrophysiological recording time to <10 min. After recording, the cytosol of individual L5 pyramidal neurons was aspirated through the patch pipette and collected in 1 μl of buffer (10x collection buffer). Cell collection microtubes containing cell collection buffer were stored on ice until they were used for cDNA preparation. Although the aspirated cytosol may have contained some of the genomic DNA, our choice of

cDNA preparation, which involved poly-A selection virtually eliminated the possibility of genomic contamination in the RNAseq data.

cDNA Preparation and Library Preparation for Next-Generation Sequencing

Single-cell mRNA sequencing was performed using the Clontech's SMARTer Ultra Low Input RNA Kit for Sequencing. Briefly, after collecting the cytoplasm in buffer, the samples were briefly spun, snap frozen on dry ice, and stored at −80 °C until further processing. As a next step, RNA was converted into cDNA, harvested and analyzed using the automated fragment analyzer by Advanced Analytical. Only cells that had a cDNA concentration higher than 0.05 ng/µl were selected for library preparation. Library preparation was performed using Nextera XT DNA Sample Preparation Kit (Illumina) as described in the protocol. Following library preparation, cells were pooled and sequenced in an Illumina NextSeq500 instrument using 2 × 75 paired end reads on a NextSeq high-output kit (Illumina).

Processing of mRNA Sequencing Data

After demultiplexing the raw reads into single-cell datasets, we used Prinseq to remove short reads (-min_len 30), to trim the first 10 bp on the 5′-end (-trim_left 10), to trim reads with low quality on the 3′-end (-trim_qual_right 25), and to filter low complexity reads (-lc_method entropy \-lc_threshold 65). We used FASTQC to determine overrepresented sequences and removed those using cutadapt (-e 0.15 –m 30). We then used Prinseq to remove orphan pairs less than 30 bp in length followed by removal of Nextera adapters using Trim Galore (–stringency 1). Remaining reads were aligned to the mm10 genome with STAR using the following options (–outFilterType BySJout \–outFilterMultimapNmax 20 \–alignSJoverhangMin 8 \–alignSJDBoverhangMin 1 \–outFilterMismatchNmax 999 \–outFilterMismatchNoverLmax 0.04 \–alignIntronMin 20 \–alignIntronMax 1000000 \–alignMatesGapMax 1000000 \–outSAMstrandField intronMotif). Then, in each sample, aligned reads were converted to counts for every gene using HTSeq (-m intersection-nonempty \-s no).

Labeling of projections from PL-L5 pyramidal neurons to BLA/VTA/Thalamus

For injection of retrograde tracers to label projections from the PL to other brain regions, mice were anesthetized with isoflurane (1.5-2%) and held in a stereotaxic apparatus (David Kopf Instruments, Tujunga, CA). The scalp was incised and retracted, and head position was adjusted to place bregma and lambda in the same horizontal plane. Small burr holes were drilled in the skull above the BLA (1.45mm posterior to bregma, 3.5mm lateral to bregma, -4.2mm ventral to the skull surface), VTA (-3.16mm posterior to bregma, 0.6mm lateral to

bregma, -4.2mm ventral to the skull surface) or Thalamus (-1mm posterior to bregma, 0.5mm lateral to bregma, -3mm ventral to the skull surface). A 10 µl Hamilton syringe mounted to a infusion pump (UltraMicroPump, World Precision Instruments) was used to deliver 300, 200 and 200 nl, respectively, of Cholera toxin subunit B (CtB) Alexa Fluor conjugates 555 (CtB 555; C22841, Molecular Probles). Once the infusions were complete the skull was closed and the skin sutured (Ethilon 5-0, FS-3 Needle, F2413, Ethicon). The skin was treated locally with Betadine (10%, MedaPharma) for local disinfection. The mice were then rehydrated through intraperitoneal injections of 0.2-0.3 ml of saline. The mice were left to recover on a heating pad. Once awake they were injected subcutaneously with an analgesic Buprenorphine (0.01-0.05 mg/kg, Axience). The mice were allowed to recover for one week before any further experimentation. All these mice were then used for electrophysiological recordings to determine the cell-type (D1- or D2-type) projecting to these 3 different areas.

Electrophysiology Analysis

Electrophysiology data were acquired using Axograph (John Clements), and analyzed using Axograph as well as custom written routines in Python. Action potential (AP) threshold was determined as the membrane potential at which the voltage rise exceeds 10 mV/ms. AP amplitude was measured as peak of the action potential from baseline, and AP half-width was determined as the width of the AP at 50% of the maximum voltage amplitude from baseline. To determine input resistance (Rn), a current-voltage (I/V) plot was created, and the slope of the curve was measured near the resting membrane potential (membrane potential changes to current injections in the range from -20 pA to +20 pA). Rheobase values were defined as the minimum current injection that elicited an AP. The voltage sag was measured by giving current pulses from -200 pA to -50 pA during 800 ms. Sag response was determined by the ratio between the voltage response at the steady-state and the voltage response at the peak after the long hyperpolarizing current pulses. To compare the voltage sag between different neurons, the voltage deflection (the steady-state hyperpolarization during the current injection) was approximately 10 mV. Action potential firing accommodation was quantified as the ratio of the inter-spike interval (ISIs) of the first and that of the last pair of APs during a train of ten APs. The resonance frequency was measured using sinusoidal current injections of constant amplitude (30 pA) and linearly increasing frequency in the range from 0 to 20 Hz within 20 s. The impedance amplitude profile (ZAP) was determined by taking the ratio of the fast Fourier transform of the voltage response to the fast Fourier transform of the current injection. The ZAP plot was then fitted with 5-7 exponential fits and the resonance frequency was defined as the peak of the exponential fit. The amplitude of the somatic after- depolarization (ADP) was measured as the difference in the RMP and the maximum voltage deflection 10 ms after the peak of the last AP of a train of three APs.

Morphological Analysis

To aid cell type identification and to quantify differences in the morphology of recorded D1- vs D2-type neurons, we measured their cell body diameter and dendritic parameters. The following dendritic properties were extracted using Neurolucida explorer (MBF Bioscience): Number of primary dendrites, total dendritic length, surface area and volume, ratio of the total dendritic length to the total dendritic surface area, highest dendritic order segment, average tortuosity of dendritic segments (defined as the ratio of the length of the segment over the straight-line path between its extremities), and number of dendritic nodes. In addition, we performed a Sholl analysis (Sholl, 1953) to describe differences between neuronal arborization. The length of the dendritic arborization that could be enclosed within a 100 µm radius circle around the cell body, between 100 and 200 µm radii, between 200 and 300 µm radii, and outside a 300 µm radius was systematically extracted.

Protein-Protein Interaction (PPI) Analysis

For protein interaction analysis of the statistically different expressed gene transcripts, we used Molecular Interaction Search Tool (MIST), which is an integrated resource for mining gene and protein interaction data (https://fgrtools.hms.harvard.edu/MIST/). To determine the gene position and the size of the mouse chromosome we used files coming from http://www.informatics.jax.org/downloads/reports/index.html. Concerning the genes belonging to the Autism Spectrum Disorder risk genes list, they have been determine by a specific database on https://gene.sfari.org/. Circa plots for visualization of mRNA-correlated interactions were generated using Circa software (http://omgenomics.com/circa/).

Statistics

Summary data are shown as box plots, with individual data points (circles), median (white line), interquartile range (box), and min – max range (whiskers). Significance was defined as $p < 0.05$ (*) and determined using the nonparametric Wilcoxon-Mann-Whitney two-sample rank test or the Wilcoxon signed rank test for paired data (when appropriate), neither of which makes assumptions about the data distribution. Principal component analysis (PCA) was applied to determine the relative correlation between the two cell types, using the electrophysiological properties of each cells recorded. This analysis is a dimensionality reduction method that uses transformations to project a high-dimensional set of data into a lower dimensional set of variables, called principal components (PCs). The extracted PC values contain important information from the data, revealing its internal structure in a way that best explains its variance. PCs are ranked according to the percentage of total variance in the data they explain. PC1 explains the maximal total variance found within the data. The subsequent PC values represent

the remaining variation, without being correlated with the preceding components. Python has been used to realize the PCA.

Results

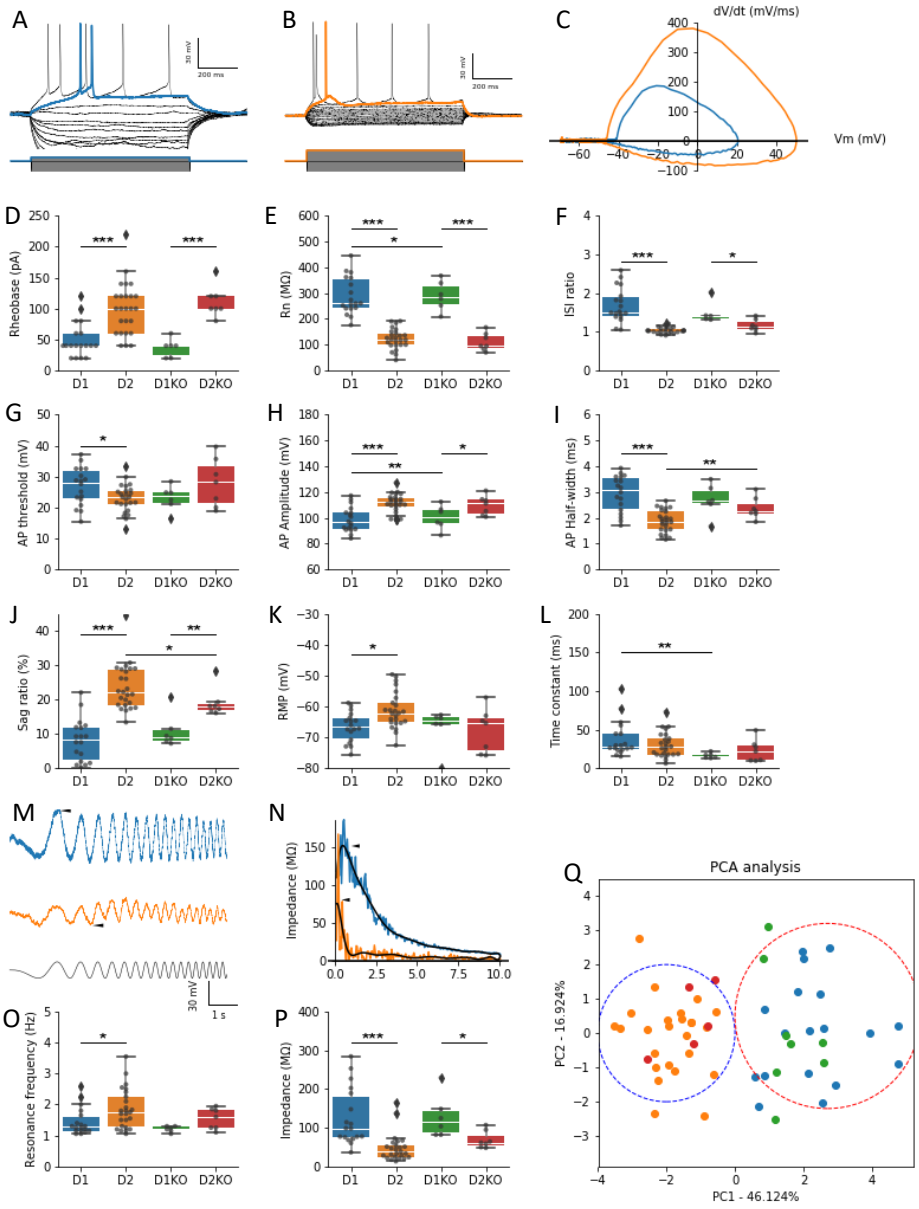

Fig 1: Intrinsic properties difference between D1R and D2R WT and *Fmr1*-KO. (A) and (B) Representative traces from D1R (blue) and D2R (orange) L5 pyramidal neurons in response to an I/V curve steps. The D1R/D2R colored responses represent the rheobase for comparison. (C) Example traces of minimum dV/dt of the first Action Potential (AP) (D1R: blue, D2R: orange). Group data showing difference in Rheobase (D), Input resistance (E), Interspike interval ratio (F), AP threshold (G), AP amplitude (H), AP half -width (I), Sag ratio (J), resting membrane potential (RMP) (K) and time constant (L) change between D1R and D2R types in WT and KO mice. (M) Representative traces from D1R (blue) and D2R (orange) L5 pyramidal neurons in response to a resonance frequency step. (N) Example traces of impedance (Mohm) over frequency (Hz) (D1R: blue, D2R: orange). Group data showing difference in resonance frequency (Hz)(O) and impedance

(Mohm)(P) change between D1R and D2R types in WT and KO mice. (Q) Representation of a PCA analysis allowing a clustering of the different cell types following the mice condition based on the electrophysiological properties (Blue: D1WT, orange: D2WT, green: D1KO and red: D2KO). D1R WT neurons are displayed in blue (n=18), D2R WT in orange (n = 25), D1R KO in green (n= 8) and D2R in red (n= 5). Data are mean ± SEM, *P<0.05, ** P<0.01, *** P<0.001.

Distinct electrophysiology properties between D1R and D2R pyramidal neurons into PL in WT mice

Previous studies showed that mPFC L5 pyramidal neurons form a heterogeneous population that can be distinguished based on their dendritic morphology and electrophysiological parameters. Seong and Carter (2010) showed that mPFC L5 pyramidal neurons can be subdivided in two subpopulations of neurons expressing dopamine receptor 1 (D1R) or not (D2R). Based on these findings, we decided to focus more our study into the PL cortex. Using whole-cell patch-clamp recordings (Fig1A,B), we observed a lot of difference into the intrinsic properties highlighted by the phase plot (Fig1C-P). The rheobase is higher for D2R than D1R cells suggesting a hypoexcitability of D2R cells (D1R= 50 ± 6.71 pA, n=18; D2R= 100 ± 8.49 pA, n=25; $P < 0.001$) (Fig1C). We found a highly significant difference in input resistance (R_N) (D1R= 288.61 ± 17.18 MΩ, n=18; D2R= 123.04 ± 7.77 MΩ, n=25; $P < 0.001$) (Fig1E) and voltage sag (D1R= 8.24 ± 1.46, n=18; D2R= 23.67 ± 1.33, n=25; $P < 0.001$) (Fig1J), as predicted by Seong. Therefore, the latter study observed a significant more hyperpolarized RMP in the D1R group, which we also found (D1R= -66.64 ± 1.12 mV, n=18; D2R= -61.25 ± 1.16 mV, n=25; $P < 0.05$) (Fig1K). For D1R cells, we showed an ISI ratio between the second and the last interval higher than D2R cells suggesting an accommodation during long stimulation (D1R= 1.68 ± 0.10, n=18; D2R= 1.04 ± 0.01, n=25; $P < 0.001$) (Fig1F). Then, we determined significative difference in AP parameters, which could explain an easier implication of one type *versus* another one during plasticity formation during a specific behavior. AP threshold is higher for D1R than D2R suggesting a higher number of Na^+-K^+ pump on D1R membrane (D1R= 26.86 ± 1.43 mV, n=18; D2R= 22.89 ± 0.9 mV, n=25; $P < 0.05$) (Fig1G). D1R presents lower AP amplitude than D2R (D1R= 98.74 ± 2.28 mV, n=18; D2R= 111.46 ± 1.63 mV, n=25; $P < 0.001$) (Fig1H). We also observed a higher AP half-width for D1R than D2R, which suggests a difference in K^+ or T-type calcium channel expression (D1R= 2.94 ± 0.17 ms, n=18; D2R= 1.87 ± 0.09 ms, n=25; $P < 0.001$) (Fig1I). Then, we also wanted to characterize the resonance frequency and the impedance associated of D1R and D2R (Fig1 M-P). We found a higher resonance frequency for D2R than D1R (D1R= 1.44 ± 0.10 Hz, n=18; D2R= 1.85 ± 0.13 Hz, n=25; $P < 0.05$) (Fig1O). In contrast, impedance was higher for D1R than D2R (D1R= 125.95 ± 17.35 MΩ, n=18; D2R= 47.80 ± 7.1 MΩ, n=25; $P < 0.001$) (Fig1N, P). These two last findings suggest a difference in H- or calcium-current between D1R and D2R. To finish, we decided to perform principal cluster analysis (PCA) (Fig1Q). These data showed two different groups based on their electrophysiological properties. Once the WT mice

characterized, we decided to go through the *Fmr1*-KO mice to determine if these intrinsic properties difference between D1R and D2R are still present.

Fmr1-KO mice show altered intrinsic properties of D1R and D2R pyramidal neurons in L5 of the PL

Somatic whole-cell recordings revealed that D1KO and D2KO pyramidal neurons present two intrinsic properties (rheobase and R_N) with the same significative difference than WT. D1KO showed lower rheobase than D2KO (D1R= 35 ± 5 pA, n=8; D2R= 107.27 ± 6.19 pA, n=5; $P < 0.001$) (Fig1D). As WT mice, *Fmr1*-KO mice showed a higher R_N for D1KO than D2KO neurons (D1R= 285.05 ± 17.94 MΩ, n=8; D2R= 116.25 ± 11.29 MΩ, n=5; $P < 0.001$) (Fig1E). Then, four others intrinsic properties (AP amplitude, ISI ratio, sag ratio and impedance) were still showing significative difference but less than WT. AP amplitude was higher for D2KO than D1KO (D1R= 102.81 ± 3.2 mV, n=8; D2R= 112.63 ± 2.37 mV, n=5; $P < 0.05$) (Fig1H), as well as the voltage sag (D1R= 11.61 ± 1.19, n=8; D2R= 18.04 ± 1.63, n=5; $P < 0.01$) (Fig1J). ISI ratio presented a higher value as for WT mice for the D1KO neurons (D1R= 1.44 ± 0.09, n=8; D2R= 1.18 ± 0.05, n=5; $P < 0.05$) (Fig1F). D1KO showed higher impedance than D2KO neurons (D1R= 96.43 ± 11.09 MΩ, n=8; D2R= 65.32 ± 6.46 MΩ, n=5; $P < 0.05$) (Fig1P). Based on these intrinsic properties, we also performed PCA analysis allowing us to cluster the *Fmr1*-KO cell-type.

Then, we decided to compare each cell-type between the two conditions (WT and *Fmr1*-KO) to determine a potential deficit between the cell-types. We found three intrinsic properties different (R_N, AP amplitude and time constant) between D1R WT and D1R KO and two intrinsic properties different (AP half-width and voltage sag) between D2R WT and D2R KO. We hypothesized than these differences could be due to ion channel gene expression changes between the subpopulations.

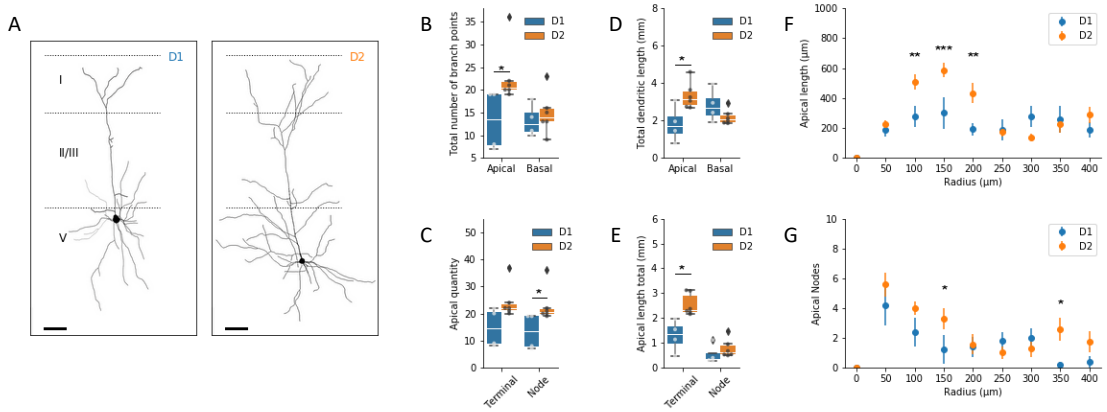

Fig2: Morphological difference between D1R and D2R WT. (A) Neurolucida reconstruction of D1R (left, n=5) and D2R (right, n=7) L5 pyramidal neurons. Scale bars = 50 µm. (B) Summary of total number of branch points in the apical and

basal dendrites of D1R (blue) and D2R (orange) neurons. (C) Summary of terminal and node quantity in the apical dendrites of D1R (blue) and D2R (orange) neurons. (D) Summary of total dendritic length (mm) in the apical and basal dendrites of D1R (blue) and D2R (orange) neurons. (E) Summary of apical length in terminal and nodes of D1R (blue) and D2R (orange) neurons. (F) and (G) Sholl analysis of apical dendritic length (µm) and nodes quantity, respectively of D1R (blue) and D2R (orange) neurons. Significance is indicated by *.

Morphology properties characterization in WT mice

To a better characterization, we also decided to determine the morphology of D1R and D2R WT. After electrophysiology recordings of the intrinsic properties, we filled D1R and D2R L5 pyramidal neurons with biocytin and analyzed them using confocal microscopy and neurolucida software (Fig2A). We found that the apical dendrites of D1R neurons were smaller and less complex than D2R neurons in terms of total number of branch points (D1R = 13.25 ± 3.33, n = 5; D2R = 23 ± 6.63, n = 7; $P < 0.05$) (Fig2B) while none difference was observed in the basal dendrites. Still in apical dendrites, the nodes quantity was also smaller in D1R than in D2R suggesting bigger back propagation in D2R neurons, which correlates with the HCN1 gene higher-level expression (D1R = 13.6 ± 5.8 mm, n = 5; D2R = 24.4 ± 5.8 mm, n = 7; $P < 0.05$) (Fig2C). Dendritic length was less in the D1R apical dendrites than in D2R (D1R = 1.9 ± 0.8 mm, n = 5; D2R = 3.5 ± 0.7 mm, n = 7; $P < 0.05$), while none difference was observed in the basal dendrites (Fig2D). We observed a higher apical length in the terminal dendrites of D2R type than D1R advising higher probabilities of input received by D2R cells (D1R = 14.75 ± 3.64 mm, n = 5; D2R = 24.33 ± 2.6 mm, n = 7; $P < 0.05$) (Fig2E). Then, we decided to focus our sholl analysis on two parameters (apical length and apical nodes quantity). We observed a significative difference in apical length inside 100 until 200µm from the soma between D1R and D2R (Fig2F). For apical nodes quantity, the significative differences were in 150µm and 350µm from the soma between D1R and D2R. Together, these results indicate that L5 pyramidal neurons expressing D1R and D2R represent a morphologically distinct set of cells into PL area and that the main differences occur into the apical part of the neurons.

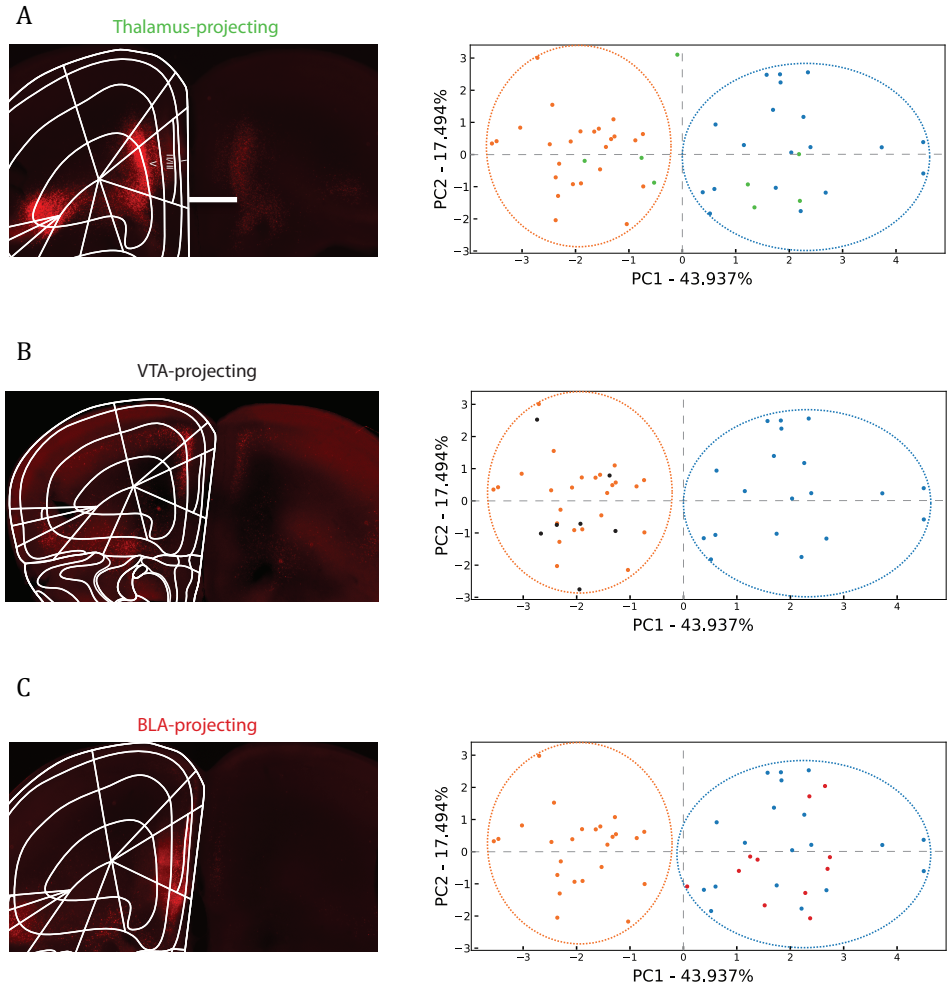

Fig3: Cell-type projection preference through three different brain areas. (A) Thalamus-projecting cells from PL (left). Scale bar = 500 µm. PCA of thalamus-projecting cells (green) combined with D1R (blue) and D2R (orange) WT cells already characterized (right). (B) VTA-projecting cells from PL (left). PCA of VTA-projecting cells (black) combined with D1R (blue) and D2R (orange) WT cells already characterized (right). (C) BLA-projecting cells from PL (left). PCA of BLA-projecting cells (red) combined with D1R (blue) and D2R (orange) WT cells already characterized (right).

Preferential subtypes projecting to specific brain areas in WT

PL cortex is connected to different brain areas. We decided to take three of them related to diverse functions. After CTB555 injections into thalamus, ventral tegmental area (VTA) and basolateral amygdala (BLA), we decided to perform whole cell recordings and identify if one cell-type was more engaged in a specific brain area.

First, we observed a difference in terms of localization following the brain area where they are projecting. Thalamus-projecting neurons seem to be more localized in layer 5 and 6 (Fig3A, left). VTA-projecting neurons look like specifically focused in layer 5 (Fig3B, left) and BLA-projecting neurons are sparsely localized in layer 2/3 and 5 (Fig3C, left).

Second, after PCA analysis we observed that thalamus-projecting cells were both D1R and D2R cell type without any type preference (Fig3A, right). VTA-projecting neurons recorded were presenting similar intrinsic properties than D2R cell-type (Fig3B, right), suggesting a specific target of D2R neurons projecting to VTA. BLA-projecting neurons were closer to D1R intrinsic properties (Fig3C, right) suggesting a specific modulation of D1R cell-type when BLA-PL stream is engaged in a specific behavior such as fear memory formation.

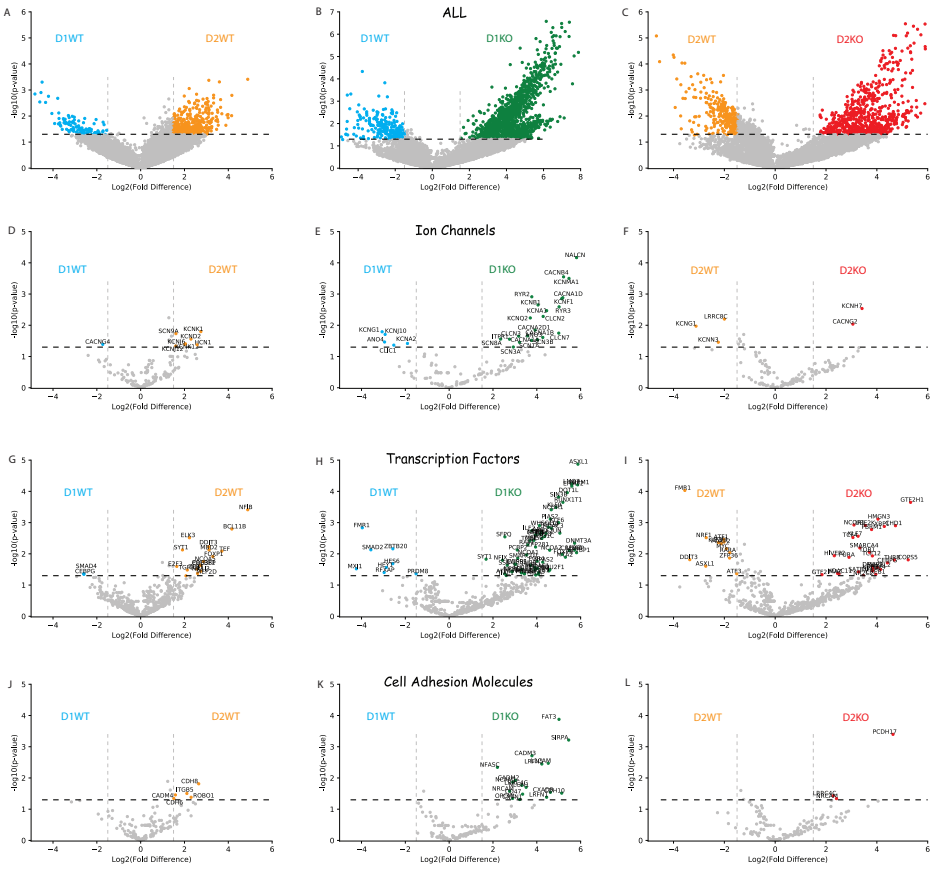

Fig4: Volcano plot illustrating genes enriched in D2R or D1R cells and significantly different (colored dots) for different gene categories (Overall view, Ion channels, Transcription factors, Cell Adhesion molecules (CAM)). (A), (B) and (C) Volcano plot showing an overall view of the genes detected after single-cell RNA sequencing between D1R (blue) and D2R (orange) WT (A), D1R WT (blue) and D1R KO (green) (B), D2R WT (orange) and D2R KO (red) (C). (D), (E) and (F) Volcano plot showing the ion channels genes detected after single-cell RNA sequencing between D1R (blue) and D2R (orange) WT (D), D1R WT (blue) and D1R KO (green) (E), D2R WT (orange) and D2R KO (red) (F). (G), (H) and (I) Volcano plot showing the transcription factors genes detected after single-cell RNA sequencing between D1R (blue) and D2R WT (orange) (G), D1R WT (blue) and D1R KO (green) (H), D2R WT (orange) and D2R KO (red) (I). (J), (K) and (L) Volcano plot showing the CAM genes detected after single-cell RNA sequencing between D1R (blue) and D2R (orange) WT (J), D1R WT (blue) and D1R KO (green) (K), D2R WT (orange) and D2R KO (red) (L). Fold enrichment is plotted in linear space to describe how much the expression differs from one group to the other group. Gray dots denote genes with $P \geq 0.05$ or fold enrichment ≤ 1.5.

Overview of single-cell RNAseq between D1R and D2R WT and *Fmr1*-KO mice

In the aim to go deeper in the characterization of D1R and D2R cell-type between WT and *Fmr1*-KO mice, we decided to perform single-cell RNA sequencing. After electrophysiological recordings, we analyzed their transcriptome by aspiration of cytosol followed by single-cell RNAseq. Using this approach, we characterized the transcriptomics of D1R and D2R pyramidal neurons, which have been previously clustered by their electrophysiology profiles (Fig1Q). Upon alignment of sequencing reads and assignment of gene counts for each gene, we applied stringent quality control metrics to each cell. RNAseq data obtained in this manner from 18 D1R WT, 25 D2R WT, 8 D1R KO and 5 D2R KO pyramidal cells passed quality control.

To gain insight into the molecular identity of recorded cells, we examined expression of genes that had been previously associated with pyramidal cells. As expected, Camk2a and Neurod6 were highly expressed in pyramidal cells. Although Gad1 and Gad2 are markers for interneurons, we found 2 cells expressing both. Then, we decided to look for verification of the layer 5 specificity. Studies showed that different genes can act as a layer 5 control and some of them only are present in one subpopulation of the layer 5 such as ER81, Lmo4, Ctip2 and Calretinin (Molnár and Cheung, 2006). At least, one of these four markers are present in our neurons suggesting that they are belonging to the layer 5.

Single-cell RNA sequencing revealed significant differences in 557 gene products (out of 14067 RNAs detected), belonging to many different functional categories between D1R and D2R WT (Fig4A). We observed more genes highly expressed in D2R (orange) than D1R (blue) WT. The RNAseq analysis showed 1546 genes with a significant difference in expression level between D1R WT and D1R KO (Fig4B) divided in different categories. This analysis showed a bigger number of genes highly expressed in D1R KO (green) than D1R WT (blue), suggesting an overexpression of genes potentially due to the lost of FMRP regulation. The overall RNAseq analysis between D2R WT (orange) and D2R KO (red) highlighted 1176 gene products differently expressed and divided in different categories. As for the D1R KO neurons, D2R KO neurons seem to present an overexpression of genes. Interestingly, some genes were exclusively expressed in either one or the other neuron type, providing potential candidates for their specific genetic targeting. These findings provide a specific transcriptomic profile for each subpopulation (Fig4A - C).

Ion channels expression

As previously described, we observed differences in intrinsic properties between each cell-types. Intrinsic properties are directly linked to ion channels and their expression on the cell membrane. For these reasons, we decided to focus our analysis in the expression of ion channels genes (Fig4 D-F). The RNAseq analysis between D1R and D2R WT allowed us to explain some

intrinsic properties features such as the voltage sag almost non-existent in the D1R type or the higher impedance in D1R type. Some studies showed that HCN1 channels which underlie a neuronal hyperpolarization-activated cationic current (I_h) is one of the most important channel involved in sag response and also in the impedance amplitude (Chen et al., 2009). In our study, we can see that HCN1 is highly expressed in D2R than D1R WT confirming the previous literature (Fig4D). Another channel highly expressed in D2R compared to D1R WT is the potassium voltage-gated channel subfamily D member 2 (Kcnd2) (Fig4D). Some studies showed its implication in mediating the transient outward K^+ current which allow a faster repolarization phase (Zhu et al., 1999). Our findings correlate by the fact that AP half-width is lower for D2R than D1R WT meaning a faster repolarization of D2R cell-type. Then, we have a higher ion channel gene expression of G-protein-activated inward rectifier potassium channel 2 (Kcnj6) into D2R than D1R WT (Fig4D). These channels regulate the neuronal excitability and the presence of a high level in D2R compare to D1R WT could explain a higher rheobase in D2R WT neurons.

Our electrophysiological recordings showed that D1R WT and D1R KO were presenting more differences than D2R WT and D2R KO. After RNAseq analysis, we can observe than D1R WT *versus* D1R KO presented higher ion channels gene products differently expressed than D2R WT and D2R KO. This finding suggests that D1R KO intrinsic properties are more affected by the lost of FMRP than D2R KO.

Transcription factors differences between D1R and D2R WT and KO

Our study is a starting point for other studies and we are providing a dataset allowing to manipulate different cell-types into the PL. The transcription factors are proteins that control the rate of transcription of genetic information from DNA to mRNA. Thanks to these transcription factors, we could target genetically one specific subpopulation leading to transgenic mice. Another option is to target one subpopulation using immunohistochemistry because into PL area, the labeling D1R or D2R didn't work for us. For example, we observed a higher expression of the nuclear factor 1B (Nf1b) gene into D2R than D1R WT (Fig4G). One study indicate that Nf1b proteins may play an important role in regulating tissue-specific gene expression during mammalian embryogenesis (Chaudhry et al., 1997).

We also observed than the comparison between WT and *Fmr1*-KO mice from the same cell-type showed a higher expression of transcription factors in *Fmr1*-KO mice (Fig4H, I). These findings suggest a high regulation of the transcription factors by the FMRP protein.

Cell Adhesion Molecules detection after single-cell RNAseq

CAMs are a subset of cell adhesion proteins located on the cell surface involved in binding with other cells or with the extracellular matrix in the process called cell adhesion. We observed 4 genes significantly different between D1R and D2R WT, which can explain the differences in neuronal connectivity at the molecular level. One fact interesting is that D1R KO mice present a higher number of gene products different from D1R WT that D2R KO *versus* D2R WT. This finding could suggest that D1R KO is differently connected to the local network as well as to the overall brain network.

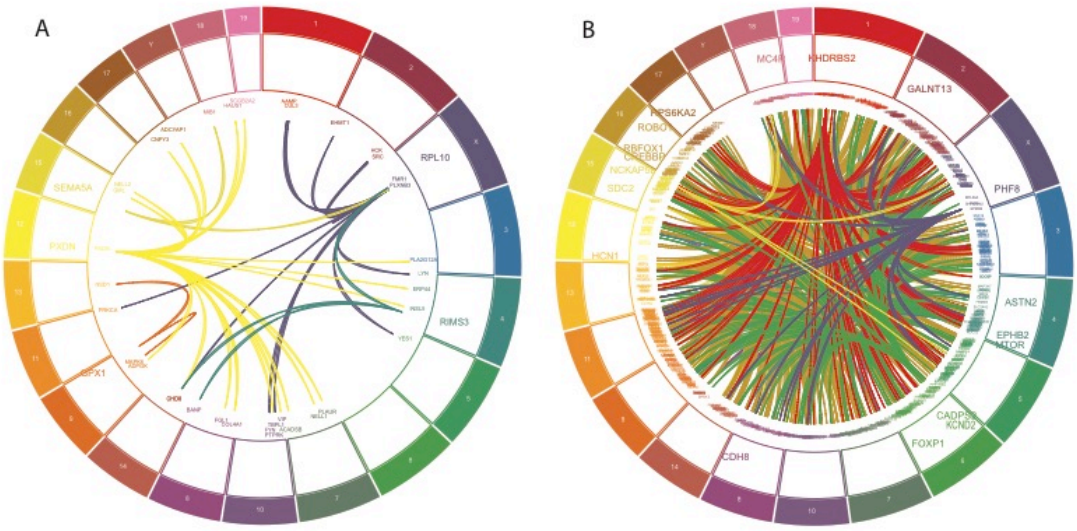

Fig 5: Circa plots of protein-protein interactions (PPI) of mRNA genesets differentially expressed between D1R and D2R WT cell-type. (A) Circa plot showing the PPI of ASD risk genes highly expressed in D1R WT neurons. (B) Circa plot showing the PPI of ASD risk genes highly expressed in D2R WT neurons.

Protein-Protein Interactions (PPI)

The RNA sequencing analysis showed different categories of genes and also genes, which were differently expressed between D1R versus D2R type (557 genes). These data represent a starting point for further studies, especially studies going towards disease model. We decided modeling a PPI only with Autism Spectrum Disorder (ASD) risk genes. Also, for a better understanding, we decided to cluster our PPI in two figures. These figures are showing ASD risk genes highly expressed in D1R or in D2R WT neurons (respectively, Fig5 A and B). This database can also provide us an information about which subpopulation can be more affected by a specific gene mutation involved in ASD mouse model. For example, Pxdn mutation has been detected in ASD patient and an interaction is done with Pxdn in D1R type (Fig5A). This finding can suggest a bigger impact on D1R type cells in the PL for a Pxdn mutation, leading to a dopaminergic modulation deficit and then, to a learning deficit.

Discussion

This study used electrophysiology, morphology, connectivity and mRNA expression profiling to evaluate the divergence between D1R and D2R pyramidal neurons of PL area both in WT and *Fmr1*-KO mice. We first showed a difference in electrophysiological profiles and morphology, followed by a clustering based on the intrinsic properties. Then, we determined a preference of cell-type for three different regions for D1R and D2R WT mice. Therefore, we analyzed the mRNA expressing profiles of D1R and D2R WT and KO into different categories. We finished by a protein-protein interaction analysis based on ASD risk genes expressed into D1R and D2R WT pyramidal neurons. These results expand our understanding of DR pyramidal cells into the PL in WT and *Fmr1*-KO mice, with both important implications for cognitive function impaired in disease and therapeutical target for FXS.

Seong and Carter were not the only authors reporting distinct neuronal populations in the PL cortex. Dembrowet. al. (2010) used retrograde markers, which were injected in the contralateral PL cortex (COM) and the pons (CPn). The two populations showed an interesting overlap with the populations reported by Seong et al. More specifically, the COM neurons showed high R_N, a weak voltage sag ratio and a trend in a hyperpolarized membrane potential compared to CPn neurons. A possibility arises that COM neurons are the same as the D1R neurons reported by Seong and al. Both studies presented morphological data of the recorded neurons, were both the COM and D1R neurons showed significant smaller total apical dendritic length and less complex than CPn and COM neurons, respectively. These properties contrast with D2R neurons, but are similar to other subpopulations of L5 pyramidal neurons in the PFC (Kawaguchi, 1993; Yang et al, 1996) that have unique projection targets (Morishima and Kawaguchi, 2006; Dembrow et al., 2010; Gee et al., 2012). One interesting possibility is that D1R neurons also make distinct connections onto other neurons in the local circuit. This could support the recurrent excitation required for the persistent activity thought to underlie working memory (Goldman-Rakic, 1995; Miller and Cohen, 2001). Our results also indicate a clear clustering between D1R and D2R WT pyramidal neurons based on intrinsic properties indicating differences in ion channels expression. These data allow us to obtain a database and by the fact can help us to determine some deficits in FXS mice.

FMRP is capable of supporting protein-protein interactions, which can directly regulate properties of ion channel proteins, such as the (potassium) K^+ channels Slack and BK (Brown et al., 2010; Deng et al., 2013), as well as calcium (Ca^{2+}) channels (Ferron et al., 2014). FMRP can therefore potentially influence neuronal excitability through multiple mechanisms: by regulating translation of a diverse array of proteins that indirectly set neuronal excitability, and through a translation-independent role by interacting directly with a number of membrane ion channels to alter cellular excitability. Our results show lesser difference between D1R and D2R KO than in WT. The data show a higher number of intrinsic properties differences in D1R KO compared with the same cell-type in WT suggesting a bigger deficit into D1R KO neurons than D2R KO (Wang et al., 2008). These findings indicate a possible impairment in ion channels expression into D1R KO.

Some studies demonstrated that the lost of FMRP can lead to an overexpression of some mRNA (Liu et al., 2018; Thomson et al., 2017). Different studies highlighted the fact that an overexpression of specific transcription factors allow a different cellular differentiation (Hirayama et al., 2017). Then, it is known that CAM are responsible of the cell adhesion into the extracellular matrix and also involved in pre- and post- synaptic formation (Washbourne et al., 2004). Our data indicate an overexpression especially for the D1R KO cell-type for the three main categories that we identified such as ion channels, transcription factors and CAM. This data indicate a possible differentiation of D1R KO cell-type, or a remodeling aspect of this specific cell-type inside the PL and also a modification of the intrinsic properties. These findings seem indicate that D1R KO pyramidal neurons are more affected by the lost of FMRP than D2R KO neurons.

Based in our PPI analysis, it seems to have more probabilities than D2R WT neurons are affected than D1R WT neurons. However, it seems to be the opposite. One explanation could be that there is still a lack in database allowing the construction of this PPI analysis.

In conclusion, our data allow a full classification of D1R and D2R WT neurons of PL. Further, this database can be crucial for disease model comparison as we also used to compare with FXS. Then, the data obtained for D1R and D2R KO can lead to new therapeutic target and allow a possible understanding in the neuronal modulation deficit during memory formation in FXS.

References

Bell, M.V., Hirst, M.C., Nakahori, Y., MacKinnon, R.N., Roche, A., Flint, T.J., Jacobs, P.A., Tommerup, N., Tranebjaerg, L., and Froster-Iskenius, U. (1991). Physical mapping across the fragile X: hypermethylation and clinical expression of the fragile X syndrome. Cell *64*, 861–866.

Bonilha, L., Molnar, C., Horner, M.D., Anderson, B., Forster, L., George, M.S., and Nahas, Z. (2008). Neurocognitive deficits and prefrontal cortical atrophy in patients with schizophrenia. Schizophr. Res. *101*, 142–151.

Bremner, J.D., Narayan, M., Staib, L.H., Southwick, S.M., McGlashan, T., and Charney, D.S. (1999). Neural correlates of memories of childhood sexual abuse in women with and without posttraumatic stress disorder. Am. J. Psychiatry *156*, 1787–1795.

Brown, S.P., and Hestrin, S. (2009). Cell-type identity: a key to unlocking the function of neocortical circuits. Curr. Opin. Neurobiol. *19*, 415–421.

Brown, M.R., Kronengold, J., Gazula, V.-R., Chen, Y., Strumbos, J.G., Sigworth, F.J., Navaratnam, D., and Kaczmarek, L.K. (2010). Fragile X mental retardation protein controls gating of the sodium-activated potassium channel Slack. Nat. Neurosci. *13*, 819–821.

Casey, B.J., Epstein, J.N., Buhle, J., Liston, C., Davidson, M.C., Tonev, S.T., Spicer, J., Niogi, S., Millner, A.J., Reiss, A., et al. (2007). Frontostriatal connectivity and its role in cognitive control in parent-child dyads with ADHD. Am. J. Psychiatry *164*, 1729–1736.

Ceci, A., Brambilla, A., Duranti, P., Grauert, M., Grippa, N., and Borsini, F. (1999). Effect of antipsychotic drugs and selective dopaminergic antagonists on dopamine-induced facilitatory activity in prelimbic cortical pyramidal neurons. An in vitro study. Neuroscience *93*, 107–115.

Claudia Rangel-Barajas, I.C., and Claudia Rangel-Barajas, I.C. (2015). Dopamine Receptors and Neurodegeneration. Aging Dis. *6*, 349–368.

Couey, J.J., Meredith, R.M., Spijker, S., Poorthuis, R.B., Smit, A.B., Brussaard, A.B., and Mansvelder, H.D. (2007). Distributed network actions by nicotine increase the threshold for spike-timing-dependent plasticity in prefrontal cortex. Neuron *54*, 73–87.

Dembrow, N.C., Chitwood, R.A., and Johnston, D. (2010). Projection-Specific Neuromodulation of Medial Prefrontal Cortex Neurons. J. Neurosci. *30*, 16922–16937.

Deng, P.-Y., Rotman, Z., Blundon, J.A., Cho, Y., Cui, J., Cavalli, V., Zakharenko, S.S., and Klyachko, V.A. (2013). FMRP regulates neurotransmitter release and synaptic information transmission by modulating action potential duration via BK channels. Neuron *77*, 696–711.

Dykens, E.M., Hodapp, R.M., and Leckman, J.F. (1987). Strengths and weaknesses in the intellectual functioning of males with fragile X syndrome. Am. J. Ment. Defic. *92*, 234–236.

Ferron, L., Nieto-Rostro, M., Cassidy, J.S., and Dolphin, A.C. (2014). Fragile X mental retardation protein controls synaptic vesicle exocytosis by modulating N-type calcium channel density. Nat. Commun. *5*, 3628.

Gee, S., Ellwood, I., Patel, T., Luongo, F., Deisseroth, K., and Sohal, V.S. (2012). Synaptic activity unmasks dopamine D2 receptor modulation of a specific class of layer V pyramidal neurons in prefrontal cortex. J. Neurosci. *32*, 4959–4971.

Goldman-Rakic, P.S. (1995). Cellular basis of working memory. Neuron *14*, 477–485.

Gross, C., Yao, X., Pong, D.L., Jeromin, A., and Bassell, G.J. (2011). Fragile X Mental Retardation Protein Regulates Protein Expression and mRNA Translation of the Potassium Channel Kv4.2. J. Neurosci. *31*, 5693–5698.

Gulledge, A.T., and Jaffe, D.B. (1998). Dopamine Decreases the Excitability of Layer V Pyramidal Cells in the Rat Prefrontal Cortex. J. Neurosci. *18*, 9139–9151.

Gulledge, A.T., and Stuart, G.J. (2003). Action Potential Initiation and Propagation in Layer 5 Pyramidal Neurons of the Rat Prefrontal Cortex: Absence of Dopamine Modulation. J. Neurosci. *23*, 11363–11372.

Hirayama, M., Ko, S.B.H., Kawakita, T., Akiyama, T., Goparaju, S.K., Soma, A., Nakatake, Y., Sakota, M., Chikazawa-Nohtomi, N., Shimmura, S., et al. (2017). Identification of transcription factors that promote the differentiation of human pluripotent stem cells into lacrimal gland epithelium-like cells. NPJ Aging Mech. Dis. *3*.

Kawaguchi, Y. (1993). Physiological, morphological, and histochemical characterization of three classes of interneurons in rat neostriatum. J. Neurosci. Off. J. Soc. Neurosci. *13*, 4908–4923.

Kruse, M.S., Prémont, J., Krebs, M.-O., and Jay, T.M. (2009). Interaction of dopamine D1 with NMDA NR1 receptors in rat prefrontal cortex. Eur. Neuropsychopharmacol. *19*, 296–304.

Law-Tho, D., Crepel, F., and Hirsch, J.C. (1993). Noradrenaline decreases transmission of NMDA- and non-NMDA-receptor mediated monosynaptic EPSPs in rat prefrontal neurons in vitro. Eur. J. Neurosci. *5*, 1494–1500.

Lewis, D.A., and González-Burgos, G. (2008). Neuroplasticity of neocortical circuits in schizophrenia. Neuropsychopharmacol. Off. Publ. Am. Coll. Neuropsychopharmacol. *33*, 141–165.

Liu, B., Li, Y., Stackpole, E.E., Novak, A., Gao, Y., Zhao, Y., Zhao, X., and Richter, J.D. (2018). Regulatory discrimination of mRNAs by FMRP controls mouse adult neural stem cell differentiation. Proc. Natl. Acad. Sci. U. S. A. *115*, E11397–E11405.

Maes, B., Fryns, J.P., Van Walleghem, M., and Van den Berghe, H. (1994). Cognitive functioning and information processing of adult mentally retarded men with fragile-X syndrome. Am. J. Med. Genet. *50*, 190–200.

Marsh, R., Zhu, H., Wang, Z., Skudlarski, P., and Peterson, B.S. (2007). A developmental fMRI study of self-regulatory control in Tourette's syndrome. Am. J. Psychiatry *164*, 955–966.

Miller, E.K. (2000). The prefrontal cortex and cognitive control. Nat. Rev. Neurosci. *1*, 59–65.

Miller, E.K., and Cohen, J.D. (2001). An integrative theory of prefrontal cortex function. Annu. Rev. Neurosci. *24*, 167–202.

Molnár, Z., and Cheung, A.F.P. (2006). Towards the classification of subpopulations of layer V pyramidal projection neurons. Neurosci. Res. *55*, 105–115.

Morishima, M., and Kawaguchi, Y. (2006). Recurrent Connection Patterns of Corticostriatal Pyramidal Cells in Frontal Cortex. J. Neurosci. *26*, 4394–4405.

Munir, F., Cornish, K.M., and Wilding, J. (2000). Nature of the Working Memory Deficit in Fragile-X Syndrome. Brain Cogn. *44*, 387–401.

Narayanan, N.S., and Laubach, M. (2006). Top-down control of motor cortex ensembles by dorsomedial prefrontal cortex. Neuron *52*, 921–931.

Otsuka, T., and Kawaguchi, Y. (2008). Firing-Pattern-Dependent Specificity of Cortical Excitatory Feed-Forward Subnetworks. J. Neurosci. *28*, 11186–11195.

Ott, T., and Nieder, A. (2019). Dopamine and Cognitive Control in Prefrontal Cortex. Trends Cogn. Sci. *23*, 213–234.

Rosenkranz, J.A., and Johnston, D. (2006). Dopaminergic regulation of neuronal excitability through modulation of Ih in layer V entorhinal cortex. J. Neurosci. Off. J. Soc. Neurosci. *26*, 3229–3244.

Seamans, J.K., and Yang, C.R. (2004). The principal features and mechanisms of dopamine modulation in the prefrontal cortex. Prog. Neurobiol. *74*, 1–58.

Shin, L.M., Orr, S.P., Carson, M.A., Rauch, S.L., Macklin, M.L., Lasko, N.B., Peters, P.M., Metzger, L.J., Dougherty, D.D., Cannistraro, P.A., et al. (2004). Regional cerebral blood flow in the amygdala and medial prefrontal cortex during traumatic imagery in male and female Vietnam veterans with PTSD. Arch. Gen. Psychiatry *61*, 168–176.

Strumbos, J.G., Brown, M.R., Kronengold, J., Polley, D.B., and Kaczmarek, L.K. (2010). Fragile X mental retardation protein is required for rapid experience-dependent regulation of the potassium channel Kv3.1b. J. Neurosci. Off. J. Soc. Neurosci. *30*, 10263–10271.

Thomson, S.R., Seo, S.S., Barnes, S.A., Louros, S.R., Muscas, M., Dando, O., Kirby, C., Wyllie, D.J.A., Hardingham, G.E., Kind, P.C., et al. (2017). Cell-Type-Specific Translation Profiling Reveals a Novel Strategy for Treating Fragile X Syndrome. Neuron *95*, 550-563.e5.

Wang, J., and O'Donnell, P. (2001). D1 Dopamine Receptors Potentiate NMDA-mediated Excitability Increase in Layer V Prefrontal Cortical Pyramidal Neurons. Cereb. Cortex *11*, 452–462.

Wang, H., Wu, L.-J., Kim, S.S., Lee, F.J.S., Gong, B., Toyoda, H., Ren, M., Shang, Y.-Z., Xu, H., Liu, F., et al. (2008). FMRP acts as a key messenger for dopamine modulation in the forebrain. Neuron *59*, 634–647.

Washbourne, P., Dityatev, A., Scheiffele, P., Biederer, T., Weiner, J.A., Christopherson, K.S., and El-Husseini, A. (2004). Cell Adhesion Molecules in Synapse Formation. J. Neurosci. *24*, 9244–9249.

Yang, C.R., and Seamans, J.K. (1996). Dopamine D1 receptor actions in layers V-VI rat prefrontal cortex neurons in vitro: modulation of dendritic-somatic signal integration. J. Neurosci. *16*, 1922–1935.

Yang, C.R., Seamans, J.K., and Gorelova, N. (1996). Electrophysiological and morphological properties of layers V-VI principal pyramidal cells in rat prefrontal cortex in vitro. J. Neurosci. Off. J. Soc. Neurosci. *16*, 1904–1921.

2.2. Intrinsic excitability properties in a BLA-projecting PL neurons

This manuscript allows a better understanding on the processes involved in memory formation occurring into PL area and more precisely in BLA-projecting PL neurons. Fear conditioning induces plasticity of intrinsic excitability in specific neuronal populations of the PL region of the mPFC. The changes occur in neurons projecting to the amygdala, but not in those projecting to the contra-lateral PL. Then, this form of plasticity is dependent on learning.

Manuscript N°2

Manuscript in preparation for submission

Long-Range Connectivity Defines Learning-Induced Intrinsic Plasticity of Prelimbic Neurons

R. De Sa[1*], M. Szlapczynska[1*], L. Zhu[1], A. Frick[1,2]

[1]Inserm u1215, Neurocentre Magendie, Bordeaux 33077, France

[2]University of Bordeaux, Bordeaux 33077, France

Summary

The medial prefrontal cortex plays an important role in the encoding and expression of fear memories, as well as in their extinction. However, the specific way in which information is acquired and stored in the brain depends largely on the functional and anatomical connectivity between various brain regions. More specifically, the long-range connectivity of different neuronal types could cause certain neuronal populations to be preferentially involved in information processing in a learning paradigm. We investigated this hypothesis by studying the plasticity of intrinsic excitability in the prelimbic (PL) part of the mPFC in two defined neuronal groups: those projecting to the ipsilateral amygdala and those projecting to the contralateral mPFC. We used contextual fear conditioning together with retrograde tracing and whole-cell electrophysiological recordings of labeled pyramidal neurons in adult 2-3 month old male C56BL/6J mice. We show that BLA-projecting neurons display learning-dependent changes in neuronal excitability following contextual fear conditioning. In contrast, the excitability of neurons projecting to the contralateral mPFC does not differ between trained and control animals. Together, these results indicate that learning-induced changes in intrinsic excitability are not generalized across all PL neurons but instead are defined by the neurons' long-range projection targets.

Introduction

Associative memories are gradually stored and stabilized within the neocortical circuits during the course of systems-level memory consolidation [1-3]. As such, the medial prefrontal

cortex (mPFC) provides a pivotal role due to its critical involvement in executive processes that include decision-making, goal-oriented action, error detection and memory [4-5]. Moreover, its connectivity with a diversity of subcortical brain regions implicated in the processing of emotional states places it in a strategic position for mediating adaptive behaviour through the control of emotional responses [5]. For example, the mPFC is interconnected with the ventral hippocampus [6] and the basolateral amygdala (BLA; [7-10]), thereby mediating the formation of long-lasting associations between environmental contexts and threatening cues. Indeed, it is now well established that the mPFC plays a critical role in the acquisition, consolidation and storage of fear memories [11-13] as well as in their expression and extinction [14-16].

Learning and memory are typically studied in the context of activity-dependent changes in synaptic strength. However, it is now clear that learning and different patterns of neuronal activity can also induce diverse non-synaptic forms of plasticity such as localized or global changes in the intrinsic excitability of a neuron [17-22]. Learning-induced intrinsic plasticity has been demonstrated in various behavioural tasks [20], including fear conditioning [23-27]. However, despite an increasing interest in learning-induced changes in intrinsic excitability, the identity of the neuronal types and cellular mechanisms underlying fear memory acquisition and expression in the mPFC are still largely unknown. The mPFC contains several distinct populations of neurons that are defined by their projections to different brain areas. This long-range connectivity might therefore determine the way in which mPFC neurons are recruited during learning [28].

To explore this question we used a combination of retrograde labelling, contextual fear conditioning, and whole-cell patch-clamp recordings to characterize properties of defined projection neurons following learning. We focused on the prelimbic cortex (PL), an mPFC region implicated in the acquisition and expression of conditioned fear [5]. We focussed, in particular, on two populations of PL neurons: those projecting to the ipsilateral basolateral amygdala (BLA) and those projecting to the contralateral mPFC. Here, we report that contextual fear conditioning results in learning-dependent changes in the intrinsic properties of PL neurons. Importantly, we demonstrate that intrinsic plasticity does not occur globally in the PL but is instead limited to specific neuronal populations defined by their projection targets.

Results

Learning induced changes in the intrinsic excitability of BLA-projecting PL neurons

The mPFC and the BLA are reciprocally connected and the interaction of the two structures is necessary for the acquisition, expression and extinction of conditioned fear memory [29-37]. In order to investigate the effect of fear conditioning on the intrinsic excitability of the BLA-projecting neurons, we measured the subthreshold properties of these neurons in two groups of mice: COND and CTX (Figure 1 and Supplementary Table 1). We found that neurons from COND mice had more depolarised resting membrane potentials (RMP) compared to those

from CTX mice (p = 0.0016). No differences between the two behavioural groups were present in the neuronal input resistance (R_N; p = 0.53), resonance frequency (f_R; p = 0.28), sag ratio (p = 0.50), membrane time constant (τ) in both the depolarising (p = 0.68) and hyperpolarising directions (p = 0.48) and in the rheobase (p = 0.45).

We then probed changes in the properties of single action potentials (APs; Figure 2*A*). While APs have traditionally been perceived as binary signals that transmit information via their rate and temporal pattern, this view is now being challenged. Emerging evidence suggests that the AP waveform is an important carrier of information. It is responsible for regulating calcium influx and transmitter release at the synapse as well as the temporal pattern of AP firing [38-39]. We found that the BLA-projecting neurons from COND mice fired APs that had a slower initial maximum rate of rise (dV/dt; p = 0.026 and a longer half-width (p = 0.035) than those from CTX mice (Figure 2*B-E*). There was no difference in the AP threshold (p = 0.11) or amplitude (p = 0.37) between these neurons (Supplementary Table 1). Because of these specific changes in AP waveform we probed changes in the first interspike interval (ISI). We observed a strong but not significant trend towards an increased first ISI in COND mice when compared to CTX mice (p = 0.0504; Figure 2*F*) suggesting that the slower AP kinetics of neurons from COND mice could reduce the AP firing frequency in these neurons.

The post-burst afterhyperpolarisation (AHP) is an important regulator of neuronal firing rates [40]. It consists of the medium (mAHP) and slow AHP (sAHP) components, both mediated by Ca^{2+} activated K^+ channels [41-42]. The mAHP is activated within milliseconds following the AP and has a decay time of 50-200 ms. The sAHP on the other hand reaches its maximum peak over several hundred milliseconds and decays over the course of seconds [42]. Learning dependent changes in the post-burst AHP have been shown to be induced by a variety of behavioural tasks including spatial learning and fear conditioning [40-45].

We found that fear conditioning caused an increase in the amplitude of the mAHP in the BLA-projecting neurons at frequencies of 60-100Hz ($p < 0.05$; Figure 2*G,H*). The amplitude of the mAHP depends on the frequency of APs [41]. In agreement with this, we found a significant effect of AP frequency on the amplitude of mAHP regardless of the behavioural condition tested ($p <$ 0.0001). Similarly to the mAHP, the sAHP was significantly increased in BLA-projecting neurons from COND mice when compared to those from CTX mice (p = 0.02; Figure 2*I,J*).

The aforementioned changes in ISI, mAHP, and sAHP would be expected to drive changes in the AP firing patterns of neurons from COND mice. Surprisingly, we found no difference in the number of APs fired by the BLA-projecting neurons at any of the current intensities tested by neurons from COND and CTX mice (p = 0.25; Figure 2*K,L*). Also, no between group differences were observed in the maximum number of APs elicited by these neurons (p = 0.22; Figure 2*M*).

mPFC projecting neurons display no changes following conditioning

The PL is strongly interconnected with other regions of the mPFC [33, 46] and the interhemishperic communication might be important for mediating responses to stressful situations [47]. For this reason we also measured the intrinsic properties of PL neurons projecting to the contralateral mPFC. However, in contrast to the BLA-projecting neurons, we found that the RMP of the mPFC-projecting neurons did not differ between COND and CTX mice (p = 0.73; Supplementary Table 2). We also found no between group differences in the R_N (p = 0.98), f_R (p = 0.89), sag ratio (p = 0.12), membrane τ in both the depolarising (p = 0.75) and hyperpolarising directions (p = 0.06) and in the rheobase (p = 0.32; Supplementary Table 2).

We next investigated the AP properties of mPFC-projecting neurons following fear conditioning. In contrast to the BLA-projecting neurons, fear conditioning did not alter the maximum dV/dt (p = 0.88) or the AP half-width (p = 0.071) of the mPFC-projecting neurons (Figure 3*A-E*). Also the AP threshold (p = 0.17) and amplitude (p = 0.30) (Supplementary Table 2) as well as the first ISI (p = 0.38; Figure 3*F*) did not differ in neurons from COND and CTX mice.

The investigation of the post-burst AHP revealed that the behavioural group had also no effect on the amplitude of the mAHP in the mPFC-projecting neuronal population (p = 0.91; Figure 3*G,H*). However, due to the dependence of mAHP amplitude on AP frequency we found a significant increase in mAHP amplitude with AP frequency (p < 0.0001). No differences in the amplitude of the sAHP were present between COND and CTX mice in the mPFC-projecting neurons (p = 0.60; Figure 3*I,J*). Finally, the analysis of the mPFC-projecting neurons also did not reveal any differences in the number of APs elicited at any current intensity (p = 0.86) or in the maximum number of APs fired by neurons from COND and CTX mice (p = 0.83; Figure 3*K-M*).

These results show that contextual fear conditioning causes neuronal-population specific changes in intrinsic excitability in the PL. These changes suggest an overall reduction in the intrinsic excitability of BLA-projecting neurons, but are absent in mPFC-projecting neurons.

Intrinsic plasticity of BLA-projecting neurons is driven by learning

We found that contextual fear conditioning causes long-lasting changes in the intrinsic excitability of BLA-projecting PL neurons. However, the footshock that the mice are exposed to during training is also a stressful and mildly painful experience. It is, therefore, not clear whether the observed changes in excitability are learning-dependent or whether they could arise from the pain and/or stress associated with the footshock. This is an important consideration given the fact that neurons in the mPFC are known to be required for pain-related aversion learning [36]. Moreover, some mPFC neurons have been shown to respond selectively to the expectation of aversive events [31-41]. In order to control for the aversive effect of the footshock on neuronal excitability we measured the intrinsic excitability in a second control group – the IMM group

(Experimental procedures). In contrast to COND mice, IMM mice do not form an association between the context and the aversive event (as measured by freezing) and this is known as the immediate shock deficit [42-43]. Using this control allowed us to compare the changes in intrinsic plasticity of neurons from mice that had successfully undergone conditioning to those that did not despite having been exposed to the same aversive stimulus (Figure 1*A,B*).

Given that fear conditioning did not induce intrinsic plasticity in the mPFC-projecting neuronal population, we limited our investigation to BLA-projecting neurons. The analyses of the subthreshold parameters of intrinsic excitability revealed that neurons from COND mice had significantly more depolarised RMP compared to those from IMM mice ($p < 0.05$). No statistically significant difference was present between the RMP of CTX and IMM mice ($p \geq 0.05$; **Supplementary Table 3**). We found no significant between-group differences in the: R_N ($p = 0.54$), f_R ($p = 0.40$**)**, sag ratio ($p = 0.76$), membrane τ in both the depolarising ($p = 0.063$) and hyperpolarising directions ($p = 0.79$) and in the rheobase ($p = 0.50$; **Supplementary Table 3**). These results indicate that the depolarised shift in the RMP was specific to neurons from COND mice. On the other hand fear conditioning did not alter any of the other subthreshold parameters measured.

Next, we analysed the AP kinetics (**Figure 4*A***). We found that neurons from the COND mice had a significantly slower maximum *dV/dt* compared to those from the IMM mice ($p < 0.05$). There were no differences between the maximum *dV/dt* of neurons from CTX and IMM mice ($p \geq 0.05$; **Figure 4*B,C***). Additionally we found that neurons from the COND group had significantly longer AP half-widths compared to those from the IMM group ($p < 0.05$). There was no significant difference in the AP half-width between the neurons from CTX and IMM mice ($p \geq 0.05$; **Figure 4*D,E***). Fear conditioning did not alter the AP threshold ($p = 0.068$) or amplitude ($p = 0.51$; **Supplementary Table 3**). Finally, the analysis of the first ISI did not reveal any differences between neurons from IMM, COND and CTX mice although a strong trend towards significant inter-group differences was present ($p = 0.0522$; **Figure 4*F***). These results show that changes in the AP kinetics occur only in neurons from COND mice and are absent in neurons from CTX and IMM mice. Fear conditioning, however has no effect on the AP threshold or amplitude.

We then analysed the amplitude of the mAHP and sAHP (**Figure 4*G,I***). We found that cells from the COND mice had increased mAHP when compared to those from IMM mice at frequencies between 40-100 Hz (40-60 Hz: $p < 0.05$, 80-100 Hz: $p < 0.01$). No significant differences in the mAHP were present between neurons from CTX and IMM mice (**Figure 4*H***). Moreover, as before we found a significant effect of the AP frequency on the amplitude of the mAHP ($p < 0.0001$). Similarly to the mAHP, the sAHP was significantly larger in neurons from COND mice when compared to those from IMM mice ($p < 0.05$). There was no significant difference between the sAHP of neurons from CTX and IMM mice ($p \geq 0.05$; **Figure 4*J***). These results indicate that the increase in the post-bust AHP observed in the BLA-projecting neurons following fear conditioning was learning-dependent.

Finally, as before, we found no effect of contextual fear conditioning on the number of APs fired in response to depolarising steps at any current intensity (p = 0.24; **Figure 4*K,L***). Similarly, the maximum number of APs elicited was comparable in neurons from all three behavioural groups (p = 0.27; **Figure 4*M***).

To summarise, we found that fear conditioning results in learning-dependent changes in the intrinsic properties of PL neurons. These are: a depolarised shift in the RMP, a slower maximum *dV/dt*, a longer AP half-width and an increase in the post-burst AHP. We demonstrate that these changes are learning dependent because they occur only in neurons from COND mice and are absent in those from CTX and IMM mice. Furthermore, we show that changes in intrinsic excitability occur in the BLA-projecting but not in the mPFC-projecting neurons. This indicates that learning-induced intrinsic plasticity does not occur globally in the PL but is instead limited to specific neuronal populations, which can be distinguished based on the neurons' long-range projection targets.

Plasticity modulation in BLA-projecting neurons alters memory retrieval

In order to determine the direct role of this plasticity changes on the behaviour response, we decided to use an excitatory and inhibitory DREADD approach. To specifically target BLA-projecting neurons into the PL, we injected a vector containing a LoxP system into the PL and a retrograde vector belonging a Cre recombinase into the ipsi BLA allowing the expression of hM4Di DREADD into BLA-projecting neurons. After memory retrieval experiments, we observed a significative decrease of freezing response for the mice under CNO injection compared to the ones under saline (Saline: 56.61%, CNO: 34.17%, p = 0.001). These results suggest that an inhibition of the cell activity and plasticity occurring the seven first days after training prevent the formation of the retrieval memory in BLA-projecting neurons.

Then, we used hM3Dq DREADD vector to determine if an enhancement of the memory retrieval would be possible only in modulating the plasticity of BLA-projecting neurons. We observed an increase of freezing response in the animals receiving CNO injections compared to the ones under saline (Saline: 30%, CNO: 53%, p = 0.029). Our results indicate a role crucial of BLA-projecting neurons in the construction and formation of the retrieval memory during the learning phases.

An evaluation of the effect of CNO on the relationship between plasticity and freezing response changes showed that CNO only didn't alters the freezing response compared to the control mice (Saline: 56.61%, CNO: 60.95%, p = 0.127). This finding allows us to conclude that the freezing response effects observed after each DREADD experiments are well due to the modification and alteration of plasticity in BLA-projecting neurons in the early phases after learning.

Discussion

Fear conditioning has been shown to induce intrinsic plasticity in a number of brain regions including the hippocampus [31, 35], the BLA [36, 44], and the infralimbic cortex (IL). Our results confirm that fear conditioning alters neuronal intrinsic excitability and we expand on the above findings by showing that these changes also occur in the PL. More importantly, by investigating two distinct neuronal populations we show that the BLA-projecting but not the mPFC-projecting neurons are altered by fear conditioning. Our findings are in agreement with other recent research showing that fear conditioning preferentially recruits selected neuronal populations within the same brain region based on the neurons' long-range projection targets [44-45].

The PL is bi-directionally connected to the BLA [20, 22, 24] and this pathway is believed to be important for fear learning and expression [27-28, 46-47]. Indeed, fear conditioning has been shown to alter the amplitude of evoked field potentials at the PL-BLA pathway, which then positively correlates with freezing levels during memory retrieval [28]. Furthermore, the disruption of the communication between the PL and the BLA results in impairments in the expression of fear memory [27]. Given the importance of PL-BLA communication, any alteration in the intrinsic excitability of the BLA-projecting PL neurons could in turn influence BLA-mediated fear expression and/or memory allocation to these neurons.

In contrast to the BLA-projecting neurons, we found now no change in the intrinsic excitability of mPFC-projecting neurons. Could this therefore mean that these neurons are not recruited by fear conditioning? Perhaps inter-hemispheric communication between mPFC neurons becomes necessary only in tasks requiring higher cognitive processing such as working memory, error detection or decision-making [48]. Alternatively, mPFC-projecting neurons could still play an important role in fear memory but do so at more remote time points. Indeed, the mPFC has been shown to play a role in the consolidation, storage and retrieval of remote long-term memories [49-53]. A scenario in which the mPFC-projecting neurons are recruited at more remote time points could therefore seem plausible. On the other hand, the early involvement of the BLA-projecting neurons makes sense. Fear memory is available for recall as early as 2 h following conditioning suggesting that the recruitment of the PL-BLA pathway could take place from very early time points.

Most studies that investigated the effect of fear conditioning on intrinsic excitability report an increase in excitability following learning in neurons of the hippocampus and amygdala [31, 35-36, 44]. This is usually manifested by a reduction in the post-burst AHP and/or increased AP firing rates in response to depolarising current injections. In contrast, we observed no change in the overall number of AP fired in response to depolarising current pulses as well as an increase in the post-burst AHP. These findings are therefore surprising and reconciling our

results with previous research presents something of a challenge. One possible reason for the discrepancies could be that the rules governing learning in the PL are different to those for the hippocampus (reviewed in [34]), amygdala [36, 44] or IL. To our knowledge only one previous study investigated the intrinsic excitability of PL neurons following fear conditioning, but found no changes in the excitability of the overall population of PL neurons. However, this is surprising given the well-established role of the PL in fear learning and expression [54-55]. Importantly, our study suggests that changes in the intrinsic excitability only occur in specific neuronal populations of the PL (i.e. the BLA-projecting neurons), and may therefore not be seen at the entire PL population level as investigated in Santini et al.

Another reason for the discrepancies between our and the aforementioned studies regarding the direction of intrinsic excitability (increase versus decrease) could be a methodological one - the type of behavioural protocol used. Most studies investigating learning induced changes in intrinsic excitability used auditory fear conditioning protocols, where the imminent occurrence of the shock is signalled by a tone [31, 35-36, 44]. However, fear learning in paradigms were the footshock is paired with a tone could occur on different rules to the one in which the presentation of the shock is unsignalled. Indeed, the fact that the NMDA (N-methyl-D-aspartate) receptor mediated transmission is necessary for some but not all forms of contextual fear learning in the PL has been demonstrated by Gilmartin & Helmstetter [56]. The blockade of NMDA receptor mediated signalling with APV impairs the acquisition of contextual fear memory when the footshock is paired with a tone. Interestingly, when the tone is presented but it is not paired with the shock, the infusion of APV has no effect on contextual fear acquisition. This unexpected finding shows that mechanisms supporting contextual fear conditioning are not the same across all training paradigms [56].

In summary, our study provides, for the first time, evidence for learning-induced changes in intrinsic excitability in the PL. We show that fear conditioning induces intrinsic plasticity in the PL in a neuronal population specific manner. Moreover, our results add to the growing evidence for the importance of the PL-BLA pathway in fear memory processing. The functional consequences of intrinsic plasticity of the BLA-projecting PL neurons will depend on the identity of their postsynaptic targets (i.e. inhibitory and/or excitatory neurons). For example, intrinsic plasticity in these neurons may impact on memory consolidation by changing the rules for plasticity in their associated neuronal networks (for reviews see [34, 57-59]). In conclusion this work not only demonstrates that contextual fear conditioning induces neuronal population specific changes in intrinsic excitability, it also sets the stage for understanding the functional role of these changes for memory expression.

Experimental Procedures

PL projection neurons were visualised by prior infusions of a retrograde tracer Cholera toxin B (CtB) into the ispilateral BLA and/or the contralateral mPFC of 2-3 month old C57BL/6J mice (Figure 1*C*). Labelled neurons from both projection groups were distributed throughout the superficial layers 2-3 and the deeper layers 5-6 in agreement with previous research [22]; Figure 1*B,* layer 6 not shown). For the purpose of this study we limited our recordings to layers 2/3 and 5.

One week following surgery the mice were trained in a contextual fear conditioning task. The mice were divided into three behavioural groups (Figure 1*A*): i) a conditioned group (COND), where the mice received three unsignaled footshocks (at 1 min intervals) preceded by 2 min of context exploration, ii) a context only group (CTX), where the mice explored the training context but received no footshocks and iii) the immediate shock (IMM), where the mice received three consecutive footshocks (at 1 s intervals) immediately upon placement in the conditioning context. The length of each behavioural session lasted 5 min. Electrophysiological recordings were performed 1-4 days following the behavioural session on neurons from mice that had not undergone memory retrieval. This was done to avoid re-exposing the animals to the training context in the absence of an electric shock. In contextual fear conditioning context re-exposure results in a reduction of freezing responses and reverses learning induced changes in excitability to levels observed in naïve animals [28]. In order to test for fear memory (as measured through freezing) we re-exposed on a subset of mice to the training context 24 h after conditioning. As expected, COND mice showed robust learning by freezing significantly more than both the CTX ($p < 0.001$) and the IMM mice ($p < 0.001$; Figure 1*B*).

Supplementary information

Experimental Procedures

Animals

The mice used in all of the experiments were C57Bl/6J mice obtained from Janvier Labs, France. The mice were group-housed and kept in a temperature-regulated room on a 12 h light/dark schedule with free access to food and water. All the experiments were conducted in the light phase of the cycle and the mice were at least 8 weeks old at the time of any experimental manipulation. All experiments were performed in accordance with the European Directive 2010/63/EU and French law (approved by the Ethics Committee of Bordeaux, authorisation number 5012025-A).

Viral vectors

Two AAV2/1 vectors used in this study were cloned and packaged by the University of Zurich Viral Vector Core. Both vectors were suspended in phosphate buffered saline and stored at −80C until injected. Expression of the hM3Dq DREADD (fused to a mCherry tag) or hM4Di DREADD (fused to a mCherry tag) gene was restricted to neurons in BLA-projecting neurons. This restriction is due to the presence of a LoxP system inside the two vectors. The expression of these vectors is only possible in the presence of the AAV2retrohelper CMV eGFP Cre (2.14^{11} copies/mL) injected into BLA.

Stereotaxic surgery

Mice were anaesthetised with an isoflurane/air mix (4% for initial induction, and 1.5%-2% for maintenance), head-fixed in a stereotaxic apparatus (David Kopf Instruments), and placed on a heating pad (HP-1M, Physitemp Instruments Inc), equipped in a rectal probe (MLT1404, Physitemp Instruments Inc) connected to a controller (TCAT-2LV, Physitemp Instruments Inc) set to maintain the body temperature at 37°C. An eye cream (Lacrigel, Europhta) was applied to prevent the drying of the eyes. The fur on the head was then shaved using an electrical razor and the mice were injected with 0.1 µl of Lurocaïne (Vetoquinol) just underneath the scalp to provide local anaesthesia, and a hole was drilled in the skull. Next, following the set of experiments, vectors previously described or retrograde tracers—the Cholera toxin subunit B (CtB) Alexa Fluor conjugates 488 (CtB 488; C22841, Molecular Probes) and 594 (CtB 594; C-22842, Molecular Probes)—were infused either into the ipsi or contralateral medial prefrontal cortex (Paxinos & Franklin (2001) mouse brain atlas; mPFC; 1.94 mm anterior to bregma, 0.30-0.50 lateral to bregma, 2.50 mm ventral to bregma) and/or into the ipsilateral (left) basolateral amygdala (BLA; 1.46 mm posterior to bregma, 3.40 mm lateral to bregma, 5.00 ventral to bregma). The tracers were infused at the rate of 50 nl/min. After the infusion of 100-200 nl, the infusion rate was reduced to 5 nl/min for 10 min after which the injection needle was removed. Tracer infusions were performed using a Nanofil 33 or 34 gauge bevelled needle (World Precision Instruments) attached to a 10µl-NanoFil microsyringe (NanoFil, World Precision Instruments). The microsyringe was driven by an electronic micro pump system (UltraMicroPump, World Precision Instruments) connected to a microprocessor controller (Micro4, MicroSyringe Pump Controller). Once the infusions were complete the scull was closed, the skin sutured and treated locally with Betadine (10%, MedaPharma) for local disinfection, and the mice were injected subcutaneously with an analgesic Buprenorphine (0.01-0.05 mg/kg, Axience). The mice were allowed to recover for one week before any further experimentation.

Behavioural Apparatus

The mice were fear conditioned in a grey Perspex chamber (length 26 cm, width 18 cm, height: 25 cm, Imetronic, Pessac, France) with a metal grid floor that could be electrified to

deliver a mild scrambled electric shock. The chamber was located inside a sound-attenuating box (length: 55 cm, width: 60 cm, height: 50 cm; Imetronic, Pessac, France) and was illuminated by four small overhead lights. A video camera placed above the conditioning box allowed for the observation and the recording of the animals' behaviour. The mice were tested for memory recall either in the same chamber in which they had been conditioned (SAME) or in a novel context (NOVEL). The NOVEL context was a round cylinder (diameter 20 cm, height 27 cm) with white and grey diagonal stripes. The metal grid floor was replaced with a plastic floor tray covered with sawdust.

Behavioural procedures

The mice were divided into three behavioural groups: conditioned (COND), context only (CTX) and immediate shock (IMM). All mice were handled for five days before the onset of training. On the day of the training the mice were placed in the fear-conditioning chamber for a 5 min long behavioural session. The COND mice were allowed to explore the context for 2 min after which they received three unsignalled footshocks (1 s in duration, 0.5 mA). Each footshock was separated by a 1 min interval. After the delivery of the last shock the COND mice remained in the conditioning chamber for an additional minute before being removed and placed back in their home cage. The CTX mice were also placed in the conditioning chamber but in contrast to the COND mice they did not receive any footshocks and were allowed to freely explore the context for the entire 5 min. The IMM mice received three unsignalled footshocks (1 s in duration, 0.5 mA) immediately upon placement in the conditioning context. Each shock was separated by a 1 s interval. After the delivery of the last shock, the IMM mice remained in the conditioning chamber for the remaining 5 min before being placed back in their home cages. The COND group constituted the learning group whereas the CTX and IMM mice were used as control groups. Between mice, floor trays and shock bars were cleaned with ETOH 70%.

Fear memory was tested on a subset of mice 24 h following training. During the recall phase mice were placed back in the conditioning chamber for 3 min, after which they were returned back to their home cage. All three behavioural groups underwent the same memory recall procedure. Freezing was analysed manually using a custom written analysis programme BehavScor (version 3.0 beta, 2008, by A. Dubreucq). Freezing was classified as complete lack of movement apart from breathing. Every time freezing was observed the experimenter pressed and held down a key on the keyboard. The key was released when the mouse moved again. The time spent freezing was then calculated as a percentage of the total time spent in the chamber.

In order to control for the specificity of the memory, the COND and CTX mice were also tested for memory retrieval 7 days following training. Here, the memory test was performed either in the SAME or in the NOVEL context. As before, the memory retrieval session was 3 min long. In the NOVEL context the sawdust was exchanged between each mouse.

Another set of mice was used to test causality. These mice were injected with hM3Dq or hM4Di vectors into mPFC, eGFP-CRE vector into ipsi BLA and then divided in COND or CTX groups. One to seven days after training, Clozapine N-Oxide (CNO, 0.5mg/mL) was injected intraperitoneally two times per day with 12 hours interval. Then 21 days after training, the memory retrieval was tested in order to determine the freezing rate due only to the same context.

The mice that had undergone stereotaxic surgery and were used for electrophysiological recordings were never tested for memory retrieval. However, a subset of mice was tested regularly for memory recall in order to ensure that no change in the efficacy of the training protocol had taken place. These mice were not used for electrophysiological recordings.

Cortical slice preparation

The mice that were not used for fear memory recall were sacrificed for electrophysiological recordings 1-4 days following the behavioural session. The mice were anaesthetised with isoflurane and intercardiacally perfused with ice-cold (4°C) artificial cerebrospinal fluid (aCSF) consisting of the following (in mM): 2.5 KCl, 1.25 NaH_2PO_4, 25 $NaHCO_3$, 1 $CaCl_2$, 7 $MgCl_2$, 7 D-glucose, 3 kynurenic acid, 200 sucrose, 1.3 ascorbic acid, and 3 sodium pyruvate. The solution was bubbled with 95% O_2 and 5% CO_2 to maintain a pH of ~ 7.4. Following the perfusion, the mice were decapitated, the heads were immersed in ice-cold aCSF and the brains were removed rapidly. Next, the frontal cortex was isolated by making a coronal cut approximately at bregma point to maximise the dendritic projections within the plane of the slice. The second half of the brain, containing the BLA, was preserved and fixed overnight in 4% PFA at 4°C in order to verify the accuracy of the stereotaxic injection. The accuracy of the mPFC injection was readily observable during the electrophysiological experiment. Coronal slices of 300 μm were cut and gently transferred into an incubating chamber filled with aCSF containing (in mM): 100 NaCl, 2.5 KCl, 1.25 NaH_2PO_4, 25 $NaHCO_3$, 1 $CaCl_2$, 7 $MgCl_2$, 7 d-glucose, 3 kynurenic acid, 1.3 ascorbic acid, and 3 sodium pyruvate bubbled with 95% O_2 and 5% CO_2. Following 15-20 min of incubation at 37°C slices were transferred to a second incubation chamber containing (in mM): 125 NaCl, 2.5 KCl, 1.25 NaH_2PO_4, 25 $NaHCO_3$, 2 $CaCl_2$, 1 $MgCl_2$, 10 d-glucose, 1.3 ascorbic acid, and 3 sodium pyruvate bubbled with 95% O_2 and 5% CO_2. The slices were left to incubate for another 20 min at 37°C after which they were stored at room temperature (22°C) until the time of recording. All recordings were performed blind with respect to the behavioural group assignment.

The part of the brain that was preserved after slicing and fixed overnight in 4% PFA was rinsed 3 times in 0.1 M PB. Coronal slices of 100 μm were cut using a vibrating tissue slicer (Leica VT 1000S) and next visualised under standard inverted microscope (Zeiss Axiovert 100) equipped in 470 nm/525 nm and 550nm/605nm excitation/emission filter sets to verify the

accuracy of the BLA injections. Recordings from neurons where the injections were inaccurate or not limited to the BLA were excluded from the analysis.

Whole-cell recordings

Whole-cell current-clamp recordings were performed on slices submerged in a chamber filled with aCSF heated to 32 -34°C via a Scientifica system equipped in a heated perfusion tube (HPT-2, ALA Scientific Instruments). The slices were continuously superfused with aCSF bubbled with a mixture of 95% O_2 and 5% CO_2. The flow rate was set at 1-2 ml/min to ensure sufficient oxygenation but also to minimise mechanical disruption of the recordings. The aCSF was identical to that used during the second incubation. Neurons were visualised using a standard upright microscope (Carl Zeiss Axio Examiner.D1) using the Dodt contrast method, under a 63x water-immersion objective (Zeiss). CtB-labelled neurons were excited via a Compact Light Source HXP 120 (Leistungselektronic JENA GmbH) filtered through 485nm/535nm and 560nm/645nm excitation/emission filters for CtB 488 and for CtB 594 respectively. Neurons were visualised using an Evolve 512 EMCCD Camera (Photometrics). Patch pipettes (4-7 MΩ) were pulled from capillary glass, dimensions: 1.16 x 2.00 x 80.00 mm. (Science Products) using a Flaming/Brown micropipette puller (Model P-97, Sutter Instruments). The pipettes were then filled with internal solution containing the following (in mM): 135 K-gluconate, 10 HEPES, 10 Na_2-Phosphocreatine, 4 KCl, 4 Mg-ATP and 0.3 Na-GTP. Data were acquired using a Dagan BVC-700A amplifier and AxoGraph X (version 1.3.5). Recordings were filtered at 3 kHz and digitised at 20 kHz using an ITC-16 (InstruTech). All recordings were performed in the presence of fast synaptic activity blockers: 50μM of DL-AP5 (DL-2-Amino-5-phosphonopentanoic acid sodium salt, Abcam), 3μM of NBQX (2,3-Dioxo-6-nitro-1,2,3,4-tetrahydrobenzo[f]quinoxaline-7-sulfonamide disodium salt, Abcam), and 10μM of gabazine (2-(3-Carboxypropyl)-3-amino-6-(4 methoxyphenyl)pyridazinium bromide, Abcam). All drugs were made up as 1000x stock solutions in distilled water and were diluted to the desired concentration in aCSF at the start of the experiment. Drugs were allowed 10 min to wash in before taking any measurements. The pipette capacitance was compensated and the bridge was balanced before each recording. Series resistance was measured throughout the experiment. The experiment was terminated if the series resistance was larger than 30 MΩ. Biocytin (Sigma) 1.5-2.5 mg/ml was included in the internal solution for post-hoc morphological identification of the recorded neurons. At the end of the electrophysiological recordings the slices were fixed overnight in 4% paraformaldehyde (PFA) in phosphate buffered saline (PB), pH 7.4. The following day the slices were washed 3 times for 10 min in 0.1 M PB and stored in 0.1M PB at 4°C for up to 2 months.

Biocytin labelling procedure

Biocytin labelling was performed on fixed free-floating 300 µm slices that had been used for electrophysiological recordings. Slices were processed in a 24 well plate each slice occupying one well. Slices were first washed 3 times in 0.1 M PB for 10 min after which they were incubated for 15-30 min in a freshly prepared H_2O_2 solution (3% H_2O_2 in 0.1 M PB) to block any endogenous peroxidase activity. This incubation resulted in the development of oxygen bubbles. Next, the slices were washed 5 times with 0.1 M PB for 10 min. The slices were then permeabilised for 1 h in a 0.1 M PB solution containing 2% Triton X-100 (wt/vol Sigma; e.g 0.4 g Triton X-100 in 20 ml 0.1 M PB). Next, the slices were incubated for at least 2 h at room temperature in the ABC solution (Vectastain Elite kit, avidin-biotin complex, Vector Laboratories, PK-6100) in 0.1 M PB containing 1% Triton X-100 (e.g. 4 drops of #A, 4 drops of #B and 0.2 g of Triton X-100 in 20 ml of 0.1 M PB). Following the incubation, the slices were washed 5 times for 10 min with 0.1 M PB. The chromagenic reaction allowing for biocytin visualisation was started by placing the slices in a solution containing 3,3'-Diaminobenzidine Tetrahydrochloride (DAB, Sigma; taken out of a stock solution of 17.5 mg/ml) and 0.01% H_2O_2 in 0.1 M PB. The slices were incubated in this solution for several minutes and the reaction was observed under a dissection microscope. When the desired contrast between the cell and the slice was reached, the reaction was stopped by transferring the slices into 0.1 M PB. After that the slices were washed 5 times for 10 min.

DAB-processed slices were mounted using polyvinyl alcohol 4-88 (Mowiol 4-88) mounting medium (Fluka) and visualised with a brightfield microscope. Neurons that were not located in the PL or did not have the appearance of pyramidal-shaped neurons were excluded from the analysis. Example neurons were reconstructed using a 100x oil-immersion objective with a computer-controlled system running Neurolucida imaging software (MicroBrightField Bioscience).

Data analysis

All data were acquired and analysed using AxoGraph X. The resting membrane potential (RMP) was recorded after break-in after having allowed several minutes for the cell to stabilise. To examine the effects of behavioural training on membrane excitability, PL neurons were injected with 800 ms current pulses ranging from -200 to 300 pA at 20 pA increments. The input resistance was measured as the slope of the linear fit of the voltage-current plot between -100 pA and -40 pA. The rheobase was defined as the minimum amount of current necessary to evoke the first action potential (AP). The first AP in a train of 4-5 AP was analysed for AP threshold, maximum rate of rise (dV/dt in mV/ms), AP amplitude and AP half-width. Threshold was determined at the point when the dV/dt exceeded 10 mV/ms. AP amplitude was measured from threshold to peak and the half-width was measured at half this distance. The interspike interval (ISI) was measured between the first two APs in a train of 4-5 APs. The number of APs evoked by depolarising current steps as well as the maximum number of APs fired was also measured. The

resonance frequency was measured using sinusoidal current injections of constant amplitude (30-100 pA: adapted to prevent AP firing; average of 3 repetitions) and linearly increasing frequency 0-20 Hz in 20 s. The impedance amplitude profile (ZAP) was determined by taking the ratio of the fast Fourier transform of the voltage response to the fast Fourier transform of the current injection (Ulrich, 2002; Narayanan and Johnston, 2007). The ZAP plot was then fitted with 5-7 exponential fits and the resonance frequency was defined as the peak of the exponential fit. The sag response was measured using hyperpolarising current injections (-100 pA, 800 ms, average of 10 repetitions). In order to calculate the sag, two values were measured: the voltage difference between the RMP and the peak of the hyperpolarisation as well as the voltage difference between the steady-state voltage and the peak of the hyperpolarisation. The sag ratio was then calculated as the ratio of the two values and expressed as a percentage. The membrane time constant was measured through the injection of alternating depolarising and hyperpolarising current pulses (400 pA, 1 ms, 10 repetitions). It was then calculated as the slow component of a double-exponential fit of the average voltage decay in both the depolarising and hyperpolarising directions. The medium afterhyperpolarisation (mAHP) was measured as the maximum negative peak following the last AP in a train of 5 AP evoked at frequencies ranging from 20 to100 Hz (at 20 Hz intervals) by 2 ms current pulses of 2 nA. The slow AHP (sAHP) was measured as the maximum negative peak following the last AP in a train of 15 AP at 50 Hz evoked by 2 ms current pulses of 2 nA.

Statistical analyses were performed using the unpaired student's t-test, a one-way ANOVA or a two-way mixed-design ANOVA. After a significant main effect, post hoc comparisons were performed with the Tukey test, Bonferroni's multiple comparisons test or Dunnett's multiple comparisons test. The group size, mean and the standard error of the mean (SEM), as well as the exact statistical test used for each analysis are provided in the corresponding figure legends.

References

1. Frankland, P. W. & Bontempi, B. The organization of recent and remote memories. Nat Rev Neurosci 6, 119–130 (2005).

2. Tonegawa, S., Morrissey, M.D., Kitamura, T. The role of engram cells in the systems consolidation of memory. Nature Reviews Neuroscience. (2018).

3. Kitamura, T.*, Ogawa, S.K.*, Roy, D.S.*, Okuyama, T., Morrissey, M.D., Smith, L., Redondo, R.L., Tonegawa, S. Engrams and circuits crucial for systems consolidation of a memory. Science. 356: 73-78 (2017).

4. Brown, V. J. & Bowman, E. M. Rodent models of prefrontal cortical function. Trends Neurosci 25, 340–343 (2002).

5. Euston, D. R., Gruber, A. J. & McNaughton, B. L. The role of medial prefrontal cortex in memory and decision making. Neuron 76, 1057–1070 (2012).

6. Thierry, A. M., Gioanni, Y., Dégénétais, E. & Glowinski, J. Hippocampo-prefrontal cortex pathway: anatomical and electrophysiological characteristics. Hippocampus 10, 411–419 (2000).

7. McDonald, A. J. Organization of amygdaloid projections to the prefrontal cortex and associated striatum in the rat. NSC 44, 1–14 (1991).

8. McDonald, A. J., Mascagni, F. & Guo, L. Projections of the medial and lateral prefrontal cortices to the amygdala: a Phaseolus vulgaris leucoagglutinin study in the rat. NSC 71, 55–75 (1996).

9. Vertes, R. P. Differential projections of the infralimbic and prelimbic cortex in the rat. Synapse 51, 32–58 (2004).

10. Likhtik, E., Pelletier, J. G., Paz, R. & Paré, D. Prefrontal control of the amygdala. Journal of Neuroscience 25, 7429–7437 (2005).

11. Frankland, P. W., Bontempi, B., Talton, L. E., Kaczmarek, L. & Silva, A. J. The involvement of the anterior cingulate cortex in remote contextual fear memory. Science 304, 881–883 (2004).

12. Laviolette, S. R., Lipski, W. J. & Grace, A. A. A subpopulation of neurons in the medial prefrontal cortex encodes emotional learning with burst and frequency codes through a dopamine D4 receptor-dependent basolateral amygdala input. Journal of Neuroscience 25, 6066–6075 (2005).

13. Einarsson, E. Ö. & Nader, K. Involvement of the anterior cingulate cortex in formation, consolidation, and reconsolidation of recent and remote contextual fear memory. Learn. Mem. 19, 449–452 (2012).

14. Burgos-Robles, A., Vidal-Gonzalez, I. & Quirk, G. J. Sustained conditioned responses in prelimbic prefrontal neurons are correlated with fear expression and extinction failure. Journal of Neuroscience 29, 8474–8482 (2009).

15. Herry, C. et al. Neuronal circuits of fear extinction. European Journal of Neuroscience 31, 599–612 (2010).

16. Sierra-Mercado, D., Padilla-Coreano, N. & Quirk, G. J. Dissociable roles of prelimbic and infralimbic cortices, ventral hippocampus, and basolateral amygdala in the expression and extinction of conditioned fear. Neuropsychopharmacology 36, 529–538 (2011).

17. Zhang, W. & Linden, D. J. The other side of the engram: experience-driven changes in neuronal intrinsic excitability. Nat Rev Neurosci 4, 885–900 (2003).

18. Frick, A., Magee, J. & Johnston, D. LTP is accompanied by an enhanced local excitability of pyramidal neuron dendrites. Nat Neurosci 7, 126–135 (2004).

19. Frick, A. & Johnston, D. Plasticity of dendritic excitability. J. Neurobiol. 64, 100–115 (2005).

20. Disterhoft, J. F. & Oh, M. M. Learning, aging and intrinsic neuronal plasticity. Trends Neurosci 29, 587–599 (2006).

21. Mozzachiodi, R. & Byrne, J. H. More than synaptic plasticity: role of nonsynaptic plasticity in learning and memory. Trends Neurosci 33, 17–26 (2010).

22. Rogerson, T. et al. Synaptic tagging during memoryallocation. Nat Rev Neurosci 15, 157–169 (2014).

23. Santini, E., Quirk, G. J. & Porter, J. T. Fear conditioning and extinction differentially modify the intrinsic excitability of infralimbic neurons. Journal of Neuroscience 28, 4028–4036 (2008).

24. McKay, B. M., Matthews, E. A., Oliveira, F. A. & Disterhoft, J. F. Intrinsic neuronal excitability is reversibly altered by a single experience in fear conditioning. J Neurophysiol 102, 2763–2770 (2009).

25. Sehgal, M., Ehlers, V. L. & Moyer, J. R. Learning enhances intrinsic excitability in a subset of lateral amygdala neurons. Learn. Mem. 21, 161–170 (2014).

26. Senn, V. et al. Long-range connectivity defines behavioral specificity of amygdala neurons. Neuron 81, 428–437 (2014).

27. Titley, Heather K et al. “Toward a Neurocentric View of Learning.” Neuron vol. 95,1 (2017): 19-32. doi:10.1016/j.neuron.2017.05.02

28. Dembrow, N. C., Chitwood, R. A. & Johnston, D. Projection-specific neuromodulation of medial prefrontal cortex neurons. Journal of Neuroscience 30, 16922–16937 (2010).

29. Zelikowsky, M., Hersman, S., Chawla, M.K., Barnes, C.A., and Fanselow, M.S. (2014). Neuronal Ensembles in Amygdala, Hippocampus, and Prefrontal Cortex Track Differential Components of Contextual Fear. J. Neurosci. *34*, 8462–8466.

30. Asok, A., Schreiber, W.B., Jablonski, S.A., Rosen, J.B., and Stanton, M.E. (2013). Egr-1 increases in the prefrontal cortex following training in the context preexposure facilitation effect (CPFE) paradigm. Neurobiol. Learn. Mem. *106*, 145–153.

31. Chakraborty, T., Asok, A., Stanton, M.E., and Rosen, J.B. (2016). Variants of contextual fear conditioning induce differential patterns of Egr-1 activity within the young adult prefrontal cortex. Behav. Brain Res. *302*, 122–130.

32. Schreiber, W.B., Asok, A., Jablonski, S.A., Rosen, J.B., and Stanton, M.E. (2014). Egr-1 mRNA expression patterns in the prefrontal cortex, hippocampus, and amygdala during variants of contextual fear conditioning in adolescent rats. Brain Res. *1576*, 63–72.

33. Attardo, A., Fitzgerald, J.E., and Schnitzer, M.J. (2015). Impermanence of dendritic spines in live adult CA1 hippocampus. Nature *523*, 592–596.

34. McDonald, A.J. (1991). Organization of amygdaloid projections to the prefrontal cortex and associated striatum in the rat. Neuroscience *44*, 1–14.

35. Bacon, S.J., Headlam, A.J., Gabbott, P.L., and Smith, A.D. (1996). Amygdala input to medial prefrontal cortex (mPFC) in the rat: a light and electron microscope study. Brain Research *720*, 211–219.

36. McDonald, A.J., Mascagni, F., and Guo, L. (1996). Projections of the medial and lateral prefrontal cortices to the amygdala: a Phaseolus vulgaris leucoagglutinin study in the rat. Neuroscience *71*, 55–75.

37. Quirk, G. J., Likhtik, E., Pelletier, J. G., & Paré, D. (2003). Stimulation of medial prefrontal cortex decreases the responsiveness of central amygdala output neurons. Journal of Neuroscience, 23(25), 8800–8807.

38. Vertes, R.P. (2004). Differential projections of the infralimbic and prelimbic cortex in the rat. Synapse *51*, 32–58.

39. Gabbott, P.L.A., Warner, T.A., Jays, P.R.L., Salway, P., and Busby, S.J. (2005). Prefrontal cortex in the rat: projections to subcortical autonomic, motor, and limbic centers. J. Comp. Neurol. *492*, 145–177.

40. Gabbott, P.L.A., Warner, T.A., and Busby, S.J. (2006). Amygdala input monosynaptically innervates parvalbumin immunoreactive local circuit neurons in rat medial prefrontal cortex. Neuroscience *139*, 1039–1048.

41. Stevenson, C.W. (2011). Role of amygdala-prefrontal cortex circuitry in regulating the expression of contextual fear memory. Neurobiology of Learning and Memory *96*, 315–323.

42. Vouimba, R.-M., and Maroun, M. (2011). Learning-induced changes in mPFC-BLA connections after fear conditioning, extinction, and reinstatement of fear. Neuropsychopharmacology *36*, 2276–2285.

43. Debanne, D. (2004). Information processing in the axon. Nat Rev Neurosci *5*, 304–316.

44. Juusola, M., Robinson, H.P.C., and de Polavieja, G.G. (2007). Coding with spike shapes and graded potentials in cortical networks. Bioessays *29*, 178–187.

45. McKay, B.M., Matthews, E.A., Oliveira, F.A., and Disterhoft, J.F. (2009). Intrinsic Neuronal Excitability Is Reversibly Altered by a Single Experience in Fear Conditioning. Journal of Neurophysiology *102*, 2763–2770.

46. Abel, H.J., Lee, J.C.F., Callaway, J.C., and Foehring, R.C. (2004). Relationships between intracellular calcium and afterhyperpolarizations in neocortical pyramidal neurons. Journal of Neurophysiology *91*, 324–335.

47. Stocker, M. (2004). Ca2+-activated K+ channels: molecular determinants and function of the SK family. Nat Rev Neurosci *5*, 758–770.

48. Disterhoft, J.F., and Oh, M.M. (2006). Learning, aging and intrinsic neuronal plasticity. Trends in Neurosciences *29*, 587–599.

49. Song, C., Detert, J.A., Sehgal, M., and Moyer, J.R. (2012). Trace fear conditioning enhances synaptic and intrinsic plasticity in rat hippocampus. Journal of Neurophysiology *107*, 3397–3408.

50. Sehgal, M., Ehlers, V.L., and Moyer, J.R. (2014). Learning enhances intrinsic excitability in a subset of lateral amygdala neurons. Learning & Memory *21*, 161–170.

51. Hoover, W.B., and Vertes, R.P. (2007). Anatomical analysis of afferent projections to the medial prefrontal cortex in the rat. Brain Struct Funct *212*, 149–179.

52. Lupinsky, D., Moquin, L., and Gratton, A. (2010). Interhemispheric Regulation of the Medial Prefrontal Cortical Glutamate Stress Response in Rats. Journal of Neuroscience *30*, 7624–7633.

53. Johansen, J. P., Fields, H. L., & Manning, B. H. (2001). The affective component of pain in rodents: direct evidence for a contribution of the anterior cingulate cortex. Proceedings of the National Academy of Sciences of the United States of America, 98(14), 8077–8082.

54. Baeg, E. H., Kim, Y. B., Jang, J., Kim, H. T., Mook-Jung, I., & Jung, M. W. (2001). Fast spiking and regular spiking neural correlates of fear conditioning in the medial prefrontal cortex of the rat. Cerebral Cortex *11*(5), 441–451.

55. Gilmartin, M. R., & McEchron, M. D. (2005). Single neurons in the medial prefrontal cortex of the rat exhibit tonic and phasic coding during trace fear conditioning. Behavioral Neuroscience, 119(6), 1496–1510.

56. Fanselow, M. S. (1986). Associative vs topographical accounts of the immediate shock-freezing deficit in rats: Implication for the response selection rules governing species-specific defensive reactions. *Learning and Motivation*, 17, 16–39.

57. Landeira-Fernandez, J., DeCola, J.P., Kim, J.J., and Fanselow, M.S. (2006). Immediate Shock Deficit in Fear Conditioning: Effects of Shock Manipulations. Behavioral Neuroscience *120*, 873–879.

58. Senn, V., Wolff, S. B. E., Herry, C., Grenier, F., Ehrlich, I., Gründemann, J., et al. (2014). Long-range connectivity defines behavioral specificity of amygdala neurons. Neuron, 81(2), 428–437.

59. Knapska, E., Macias, M., Mikosz, M., Nowak, A., Owczarek, D., Wawrzyniak, M., et al. (2012). Functional anatomy of neural circuits regulating fear and extinction. Proceedings of the National Academy of Sciences, 109(42), 17093–17098.

60. Corcoran, K. A., & Quirk, G. J. (2007). Activity in prelimbic cortex is necessary for the expression of learned, but not innate, fears. Journal of Neuroscience, *27*(4), 840–844.

61. Orsini, C. A., Kim, J. H., Knapska, E., & Maren, S. (2011). Hippocampal and prefrontal projections to the basal amygdala mediate contextual regulation of fear after extinction. Journal of Neuroscience, 31(47), 17269–17277.

62. Euston, D. R., Gruber, A. J., & McNaughton, B. L. (2012). The role of medial prefrontal cortex in memory and decision making. Neuron, 76(6), 1057–1070.

63. Frankland, P. W., & Bontempi, B. (2005). The organization of recent and remote memories. Nature Reviews Neuroscience, 6(2), 119–130.

64. Restivo, L., Vetere, G., Bontempi, B., & Ammassari-Teule, M. (2009). The formation of recent and remote memory is associated with time-dependent formation of dendritic spines in the hippocampus and anterior cingulate cortex. Journal of Neuroscience, 29(25), 8206–8214.

65. Vetere, G., Restivo, L., Cole, C. J., Ross, P. J., Ammassari-Teule, M., Josselyn, S. A., & Frankland, P. W. (2011). Spine growth in the anterior cingulate cortex is necessary for the consolidation of contextual fear memory. Proceedings of the National Academy of Sciences, 108(20), 8456–8460.

66. Oswald, B. B., Maddox, S. A., Tisdale, N., & Powell, D. A. (2010). Encoding and retrieval are differentially processed by the anterior cingulate and prelimbic cortices: a study based on trace eyeblink conditioning in the rabbit. Neurobiology of Learning and Memory, 93(1), 37–45.

67. Lesburguères, E., Gobbo, O. L., Alaux-Cantin, S., Hambucken, A., Trifilieff, P., & Bontempi, B. (2011). Early tagging of cortical networks is required for the formation of enduring associative memory. Science, 331(6019), 924–928.

68. Choi, D. C., Maguschak, K. A., Ye, K., Jang, S.-W., Myers, K. M., & Ressler, K. J. (2010). Prelimbic cortical BDNF is required for memory of learned fear but not extinction or innate fear. Proceedings of the National Academy of Sciences, 107(6), 2675–2680.

69. Sotres-Bayon, F., & Quirk, G. J. (2010). Prefrontal control of fear: more than just extinction. Current Opinion in Neurobiology, 20(2), 231–235.

70. Gilmartin, M. R., & Helmstetter, F. J. (2010). Trace and contextual fear conditioning require neural activity and NMDA receptor-dependent transmission in the medial prefrontal cortex. Learning & Memory 17(6), 289–296.

71. Frick, A., & Johnston, D. (2005). Plasticity of dendritic excitability. Journal of Neurobiology, 64(1), 100–115.

72. Mozzachiodi, R., & Byrne, J. H. (2010). More than synaptic plasticity: role of nonsynaptic plasticity in learning and memory. Trends in Neurosciences, 33(1), 17–26.

73. Szlapczynska, M., Bonnan, A., Ginger, M., and Frick, A. (2014). Plasticity and pathology of dendritic intrinsic excitability. Book chapter in 'Horizons in Neuroscience Research. Volume 14.' Nova Science Publishers, Inc, New York, USA. ISBN: 978-1-63117-401-8.

Figure legends

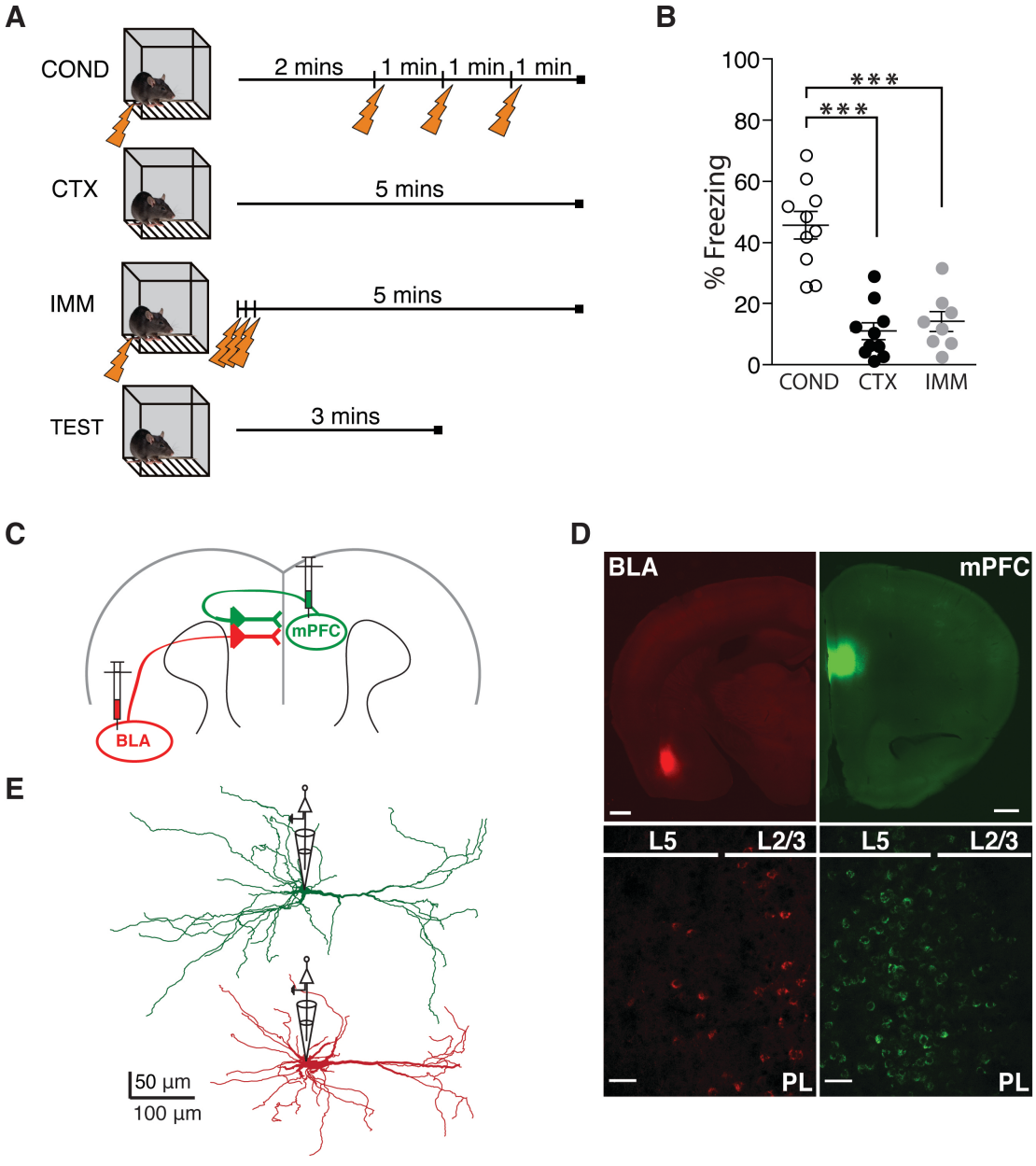

Figure 1: Contextual fear conditioning and retrograde labelling. *A*, Three experimental groups were studied. In the conditioned group (COND), mice explored the context for 2 min after which they received 3 unsignalled footshocks (each 1 min apart). In the control group (CTX) mice explored the context without receiving any footshocks. In the immediate shock group (IMM) mice received three consecutive unsignalled footshocks immediately upon placement in the context. All behavioural sessions lasted 5 min. The memory was tested 24 h after conditioning for 3 min. *B*, Mean percentage of freezing across all behavioural groups. COND mice (45.61 ± 4.48%, $n = 10$) froze significantly more than CTX (10.96 ± 2.81%, $n = 10$, $p < 0.001$) and IMM mice (14.15 ± 3.23%, $n = 10$ $p < 0.001$; $F_{2,25} = 28.80$, $p < 0.0001$). *C,* Schematic of stereotaxic injections strategy. Alexa Fluor conjugates of cholera toxin B (CtB) were infused into the ipsilateral BLA (Alexa 594) and/or into the ipsilateral mPFC (Alexa 488). *D,* Representative coronal slices displaying the site of the Ctb injections (BLA injection, top left; mPFC injection, top right) and the resulting labelling in the PL (BLA injection, bottom left; mPFC injection, bottom right). Scale bars represent 500 μm (top) 50 μm (bottom). *E,* Representative reconstructions from biocytin filled and DAB processed BLA- (red) and mPFC-projecting (green) neurons. Data are shown as the mean ± SEM, ***$p < 0.001$. Statistical significance was calculated using a one-way ANOVA with a Tukey post-hoc test (*B*).

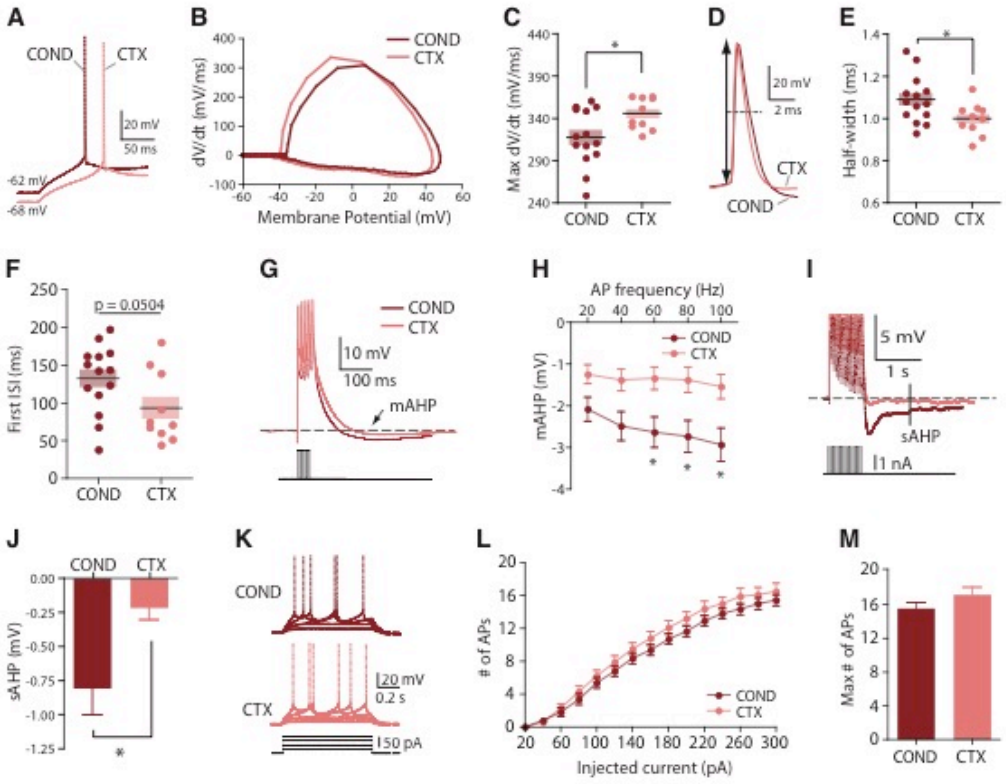

Figure 2: Fear conditioning induced plasticity of intrinsic excitability in BLA-projecting neurons *A,* Example traces showing the first AP fired by BLA-projecting neurons from both COND and CTX mice in response to an 800 ms step current injection sufficient to evoke 4 APs. *B,* Phase plots for the corresponding APs shown in (*A*). Maximum *dV/dt* was measured as the maximum peak of the phase plot. *C,* Fear conditioning resulted in BLA-projecting neurons from COND mice (318 ± 9.06 mV/ms, $n = 14$) having a significantly slower maximum *dV/dt* than those from CTX mice (346 ± 5.89 mV/ms, $n = 10$; $t(22) = 2.38$, $p = 0.026$). *D,* Example traces showing the AP half-width measured at half the distance between the AP threshold and peak for BLA-projecting neurons from both COND and CTX mice. *E,* BLA-projecting neurons from COND mice (1.09 ± 0.03 ms, $n = 14$) had increased AP half-width when compared to those from CTX mice (1.00 ± 0.02 ms, $n = 10$; $t(22) = 2.24$, $p = 0.035$). *F,* Strong but not significant trend towards a longer first ISI in neurons from COND mice when compared to CTX mice (COND, 133 ± 12 ms, $n = 14$; CTX, 93 ± 15 ms, $n = 10$; $t(22) = 2.07$, $p = 0.0504$). *G,* Example traces of AP trains at 100 Hz in neurons from COND and CTX mice (traces are shown as an

average of 3 repetitions, APs are truncated). The mAHP was measured as the maximum negative peak following the last AP in train (black arrow). *H,* Fear conditioning increased the amplitude of the mAHP in the BLA-projecting neurons ($F_{1,76}$ = 6.52; p = 0.0194). This difference was most pronounced at frequencies between 60-100 Hz (p < 0.05). *I,* Example traces showing 15 APs at 50 Hz in neurons from COND and CTX mice (APs are truncated). The sAHP was measured at 1 s following the last AP in train (black line). *J,* Group data showing an increase in sAHP (-0.81 ± 0.20 mV, n = 11) in COND mice when compared to those from CTX mice (-0.22 ± 0.09 mV, n = 9, t(18) = 2.55, p = 0.02). *K,* Example traces of repetitive AP firing. *L,* Number of APs plotted as function of current injected reveal no difference between neurons from COND and CTX mice (COND: n = 14, CTX: n = 10; $F_{1,308}$ = 1.38, p = 0.25). *M,* No significant difference in the maximum number of APs (COND, 16 ± 0.72, n = 14; CTX, 17 ± 0.87, n = 10; t(22) = 1.27, p = 0.22). Data are shown as the mean ± SEM. Statistical significance was calculated with an unpaired student's t-test (*C, E, F, J, M*), or a two-way mixed-design ANOVA (*H, L*) with Bonferroni's multiple comparisons test (*H*). *p < 0.05.

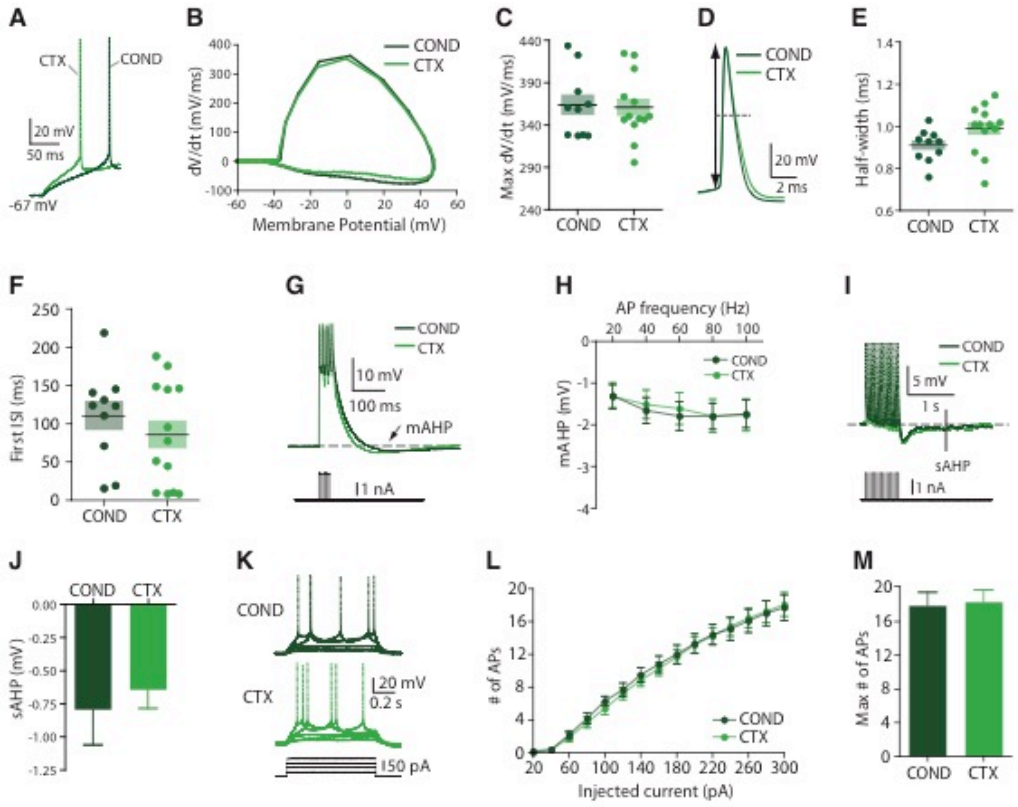

Figure 3: Lack of plasticity of the intrinsic excitability in mPFC-projecting neurons. *A,* Example traces showing the first AP fired by mPFC-projecting neurons from both COND and CTX mice in response to an 800 ms step current injection sufficient to evoke 4 APs. *B,* Phase plots for the corresponding APs shown in (*A*). *C,* Fear conditioning did not alter the maximum *dV/dt* of the mPFC-projecting neurons (COND, 364 ± 12.34 mV/ms, n = 10; CTX, 361.1 ± 10.65 mV/ms, n = 13, t(21) = 0.16, p = 0.88). *D,* Example traces showing the AP half-width for neurons from both COND and CTX mice. *E,* The AP half-width of mPFC neurons from COND (0.91 ± 0.02 ms, n = 10) and CTX (0.99 ± 0.03 ms, n = 13) mice did not differ (t(21) = 1.90, p = 0.071). *F,* Fear conditioning did not alter the first ISI (COND, 110 ± 19 ms, n = 10; CTX, 86 ± 19 ms, n = 13; t(21) = 0.90, p = 0.38). *G,* Example traces showing AP trains at 100 Hz (averages of 3 repetitions, APs are truncated). The mAHP was measured as the maximum negative peak following the last AP in train (black arrow). *H,* Fear conditioning had no effect on the amplitude of the mAHP ($F_{1,84}$ = 0.01; p = 0.91). *I,* Example traces showing 15 APs at 50 Hz in neurons from COND and CTX mice (APs are truncated). The sAHP was measured at 1 s following the last AP in train (black line). *J,* There was no difference in the sAHP between COND (-0.79 ± 0.27, n = 9) and CTX (-0.64 ± 0.14, n = 12) neurons (t(19) = 0.53, p = 0.60). *K,* Example traces of repetitive AP firing. *L,* Fear conditioning had no effect on the number of APs fired in

response to depolarising steps of different current intensities (COND: n = 10, CTX: n = 13; $F_{1,294}$ = 0.03, p = 0.86). *M,* The maximum number of APs fired did not differ (COND, 18 ± 1.57, n = 10; CTX, 18 ± 1.43, n = 13; $t(21)$ = 0.21, p = 0.83). Data are shown as the mean ± SEM. Statistical significance was calculated with an unpaired student's t-test (*C, E, F, J, M*), a two-way mixed-design ANOVA (*H, L*).

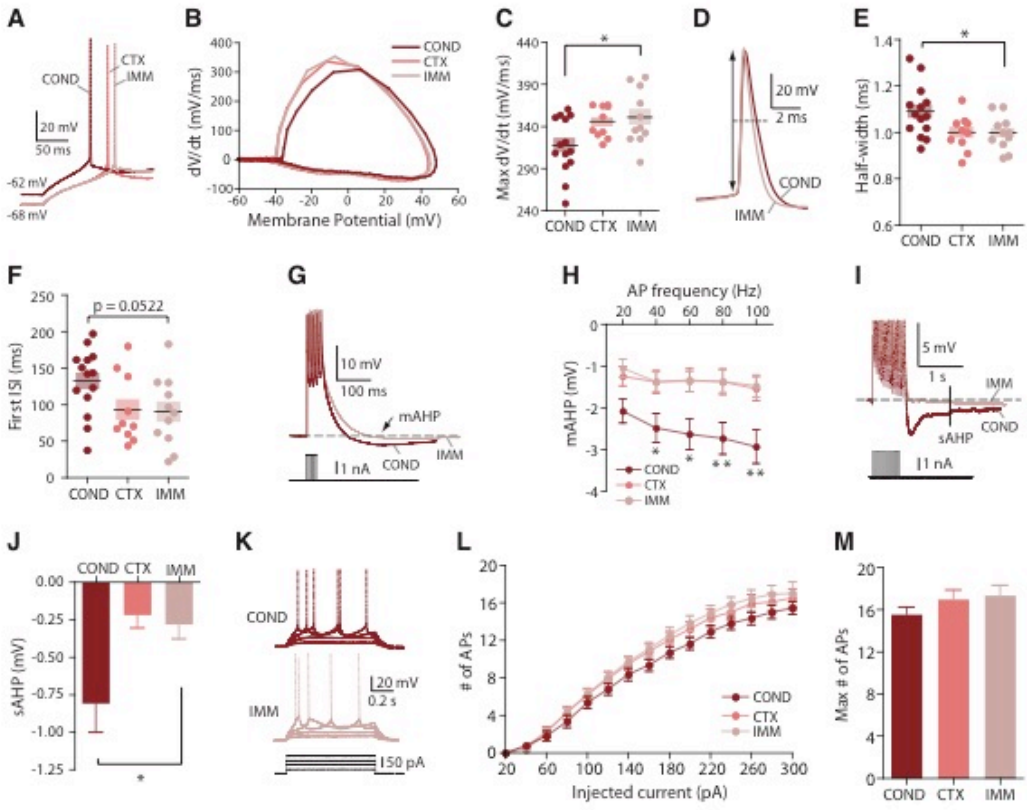

Figure 4: Plasticity of intrinsic excitability in BLA-projecting neurons is learning-dependent. *A,* Example traces of the first AP fired in BLA-projecting neurons from both COND and IMM mice. *B,* Phase plot for the corresponding APs shown in (*A*). *C,* The maximum *dV/dt* was reduced in neurons from COND mice (318 ± 9.06 mV/ms, n = 14) when compared to those from IMM mice (351 ± 9.91 mV/ms, n = 11; p < 0.05). There was no difference in the maximum *dV/dt* between neurons from CTX (346 ± 5.89 mV/ms, n = 10) and IMM mice (p ≥ 0.05; $F_{2,32}$ = 4.54, p = 0.02) *D,* Example traces of the AP half-width for BLA-projecting neurons from both COND and IMM mice. *E,* The AP half-width differed significantly between COND (1.09 ± 0.03 ms, n = 14), CTX (1.00 ± 0.02 ms, n = 10) and IMM mice (1.00 ± 0.02; n = 14) following fear conditioning ($F_{2,32}$ = 4.25, p = 0.02). Neurons from COND mice had significantly increased AP half-widths when compared to those from IMM mice (p < 0.05). No difference was present in the AP half-width of neurons from CTX and IMM mice (p ≥ 0.05). *F,* Fear conditioning did not alter the first ISI of neurons from COND (133 ± 12 ms, n = 14), CTX (93 ± 15 ms, n = 10) and IMM mice (90 ± 15 ms, n = 11) although a strong trend towards significantly different group means was present ($F_{2,32}$ = 3.24, p = 0.0522). *G,* Example traces showing a train of APs fired at a 100 Hz by BLA-projecting neurons from COND and IMM mice (averages of 3 repetitions, APs are truncated). The mAHP was measured as the maximum negative peak (black arrow). *H,* Mean amplitude of the mAHP across 20-100 AP frequencies for all behavioural groups. The amplitude of the mAHP was significantly larger in neurons from COND mice when compared to those from IMM mice at AP frequencies between 40-100 Hz (40-60 Hz: p < 0.05, 80-100 Hz: p < 0.01). No significant differences in the amplitude of the mAHP were present between neurons from CTX and IMM mice (p ≥ 0.05; $F_{2,116}$ = 5.85; p = 0.0073). *I,* Example traces showing 15 APs at 50 Hz in the BLA-projecting neurons from COND and IMM mice (APs are truncated). The sAHP was measured at 1s following the last AP in train (black line). *J,* The sAHP in neurons from COND mice (-0.81 ± 0.20 mV, n = 11) was larger when compared to that from IMM mice (-0.28 ± 0.10 mV, p < 0.05). No difference in the sAHP amplitude

was present in neurons from CTX (-0.22 ± 0.09 mV, n = 9) and IMM mice ($p \geq 0.05$; $F_{2,28} = 5.32$, $p = 0.011$). *K,* Example traces for repetitive AP firing induced in COND and IMM neurons. *L,* No significant difference in the number of APs evoked as function of injected current in COND, CTX and IMM mice ($F_{2,448} = 1.50$, $p = 0.24$). *M,* The maximum number of APs elicited did not differ between neurons from COND (16 ± 0.72, n = 14), CTX (17 ± 0.87, n = 10) and IMM mice (17 ± 0.99, n = 11; $F_{2,32} = 1.35$, $p = 0.27$). Data are shown as the mean ± SEM. Statistical significance was calculated using a one-way between-subjects ANOVA with Dunnett's multiple comparisons test (*C, E, F,* IMM compared to COND and CTX), a two-way mixed-design ANOVA (*H, L*) with Bonferroni's multiple comparisons tests (*H*) or a one-way between-subjects ANOVA (*J, M*) with Dunnett's multiple comparisons test (IMM compared to COND and CTX; *J*), *$p < 0.05$, **$p < 0.01$ (IMM compared to COND). Data for COND and CTX mice are the same as those presented in Figure 1.

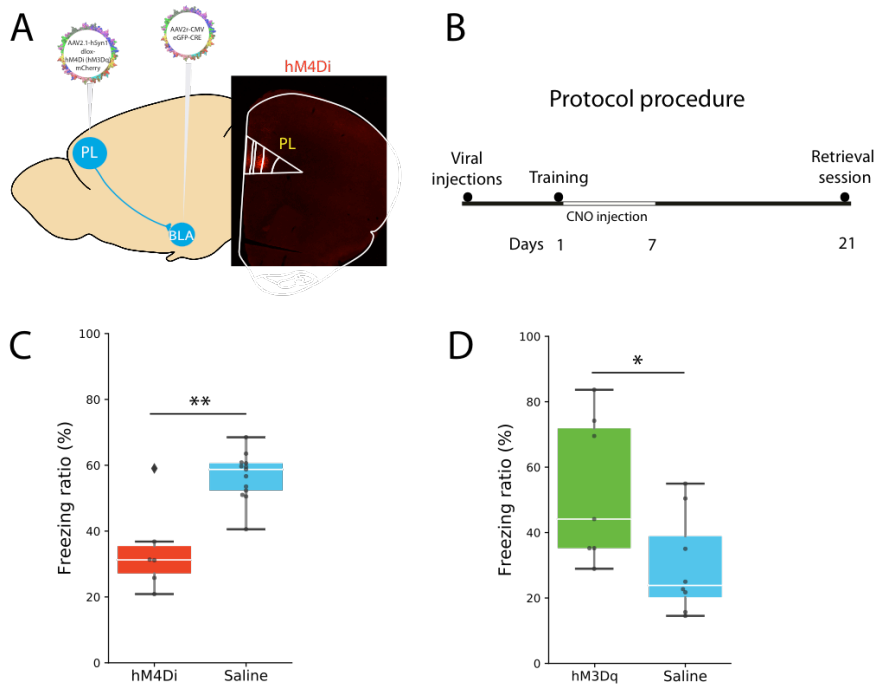

Figure 5: Plasticity modulation in BLA-projecting neurons alters freezing response. A, Schematic of vectors microinjection and efferent connections from PL to others brain regions such as BLA. B, Experimental procedure used to test retrieval memory (21 days after training) after pharmacogenetic modulation (1 to 7 days after training) of BLA-projecting neurons. C, Time spent freezing during retrieval session was decreased by inhibition of BLA-projecting neurons in the CNO injected group (34.17%, n = 6) compared to saline group (56.61%, n = 13, $p = 0.001$). D, Freezing response during retrieval session was increased by increasing the excitability of BLA-projecting neurons in the CNO injected group (53%, n = 7) compared to saline group (30%, n = 8, $p = 0.029$).

3. Discussion and perspectives

The first aim of this project was to characterize and identify 2 different subpopulations (D1R and D2R) into the PL in WT and *Fmr1*-KO mice. For this purpose we combined electrophysiological recordings, morphology analysis, connectivity and single-cell RNA sequencing. We demonstrated that: (1) in WT mice, D1R and D2R neurons own distinct features as well as intrinsic properties that morphology or connectivity, (2) these characteristics are

changed in *Fmr1*-KO mice and D1R KO neurons are more impaired in terms of intrinsic properties changes compare to D1R WT, (3) RNAseq analysis showed differences in gene expression between each cell-type in different gene categories such as ion channels, transcription factors or CAM. Our data suggest that D1R KO neurons seem more affected by the lost of FMRP into the PL area. The second aim of the project was was to explore whether learning alters the intrinsic excitability of the prelimbic neurons (PL) that project to the ipsilateral basolateral amygdala (BLA) or to the contralateral medial prefrontal cortex (mPFC). For this purpose we combined contextual fear conditioning with retrograde labelling and patch-clamp electrophysiology. We demonstrated that: (1) contextual fear conditioning does alter the intrinsic excitability of PL neurons, (2) these changes are neuronal population specific - plasticity occurred in the BLA-projecting neurons but was absent in the mPFC-projecting neurons. These findings therefore indicate that learning in a contextual fear-conditioning task induces intrinsic plasticity of PL neurons that is not generalized across all neurons but is instead limited to specific neuronal populations.

3.1. D1R and D2R WT present different characteristic allowing a distinct clustering

Cell type classification remains one major goal in neuroscience and nowadays thanks to new approaches, it can be more and more complete (Markram et al., 2015; Oberlaender et al., 2011; Radnikow and Feldmeyer, 2018). One important aspect of the classification is the nomenclature used and into the mPFC it is a major problem (Laubach et al., 2018). Some studies showed a controversial modulation effect of DA into the mPFC area but few studies really characterized the precise location of these modulated neurons (Puig et al., 2014; Seamans and Yang, 2004; Seong and Carter, 2012; Yang and Seamans, 1996). Seong and Carter were not the only authors reporting distinct neuronal populations in the PL cortex. Dembrowet. al. (2010) used retrograde markers, which were injected in the contralateral PL cortex (COM) and the pons (CPn). The two populations showed an interesting overlap with the populations reported by Seong et al. More specifically, the COM neurons showed high R_N, a weak voltage sag ratio and a trend in a hyperpolarized membrane potential compared to CPn neurons. A possibility arises that COM neurons are the same as the D1R neurons reported by Seong and al. Both studies presented morphological data of the recorded neurons, were both the COM and D1R neurons showed significant smaller total apical dendritic length and less complex than CPn and COM neurons, respectively. These properties contrast with D2R neurons, but are similar to other subpopulations of L5 pyramidal neurons in the PFC (Kawaguchi, 1993; Yang et al., 1996b) that have unique projection targets (Dembrow et al., 2010; Gee et al., 2012; Morishima and Kawaguchi, 2006). One interesting possibility is that D1R neurons also make distinct connections onto other neurons in the local circuit. This could support the recurrent excitation required for the persistent activity thought to underlie working memory (Goldman-Rakic, 1995; Miller and Cohen, 2001).

3.2. Intrinsic properties of D1R and D2R KO are affected by the lost of FMRP

FMRP is capable of supporting protein-protein interactions, which can directly regulate properties of ion channel proteins, such as the (potassium) K^+ channels Slack and BK (Brown et al., 2010; Deng et al., 2013), as well as calcium (Ca^{2+}) channels (Ferron et al., 2014). FMRP can therefore potentially influence neuronal excitability through multiple mechanisms: by regulating translation of a diverse array of proteins that indirectly set neuronal excitability, and through a translation-independent role by interacting directly with a number of membrane ion channels to alter cellular excitability. Our results show lesser difference between D1R and D2R KO than in WT. The data show a higher number of intrinsic properties differences in D1R KO compared with the same cell-type in WT suggesting a bigger deficit into D1R KO neurons than D2R KO (Wang et al., 2008). These findings indicate a preferentially impairment in ion channels expression into D1R KO. FMRP regulates local protein synthesis in dendritic spines (Bear et al., 2004; Garber et al., 2008; Grossman et al., 2006). Previous studies suggested that FMRP phosphorylation might be a key regulator for activity-dependent protein synthesis (Ceman et al., 2003; Narayanan et al., 2007, 2008). D1R WT stimulation could cause dynamic changes of FMRP phosphorylation at serine residues in PFC slices. The changes of FMRP phosphorylation correspond to the temporal pattern of SAPAP3 after D1R stimulation. This suggests that FMRP could be involved in DA mediated synapse-associated protein expression. A study showed that FMRP plays key roles for DA modulation in forebrain neurons (Wang et al., 2008). In this study, they found that DA D1 receptor-mediated SAPAP3 expression was abolished in *Fmr1* KO PFC neurons. It indicates the requirement of FMRP for DA D1 receptor-induced synapse-associated protein synthesis and by the consequence, the lost of FMRP could impaired the function of D1R neurons (Wang et al., 2010).

3.3. RNAseq revealed differences in gene expression for different categories into each cell-type in WT and *Fmr1*-KO mice

Using translating ribosome affinity purification (TRAP), a recent study found altered translation of 120 mRNAs and down-regulated expression of FMRP target mRNAs as a group in *Fmr1* KO CA1 pyramidal neurons (Heiman et al., 2008; Thomson et al., 2017). FMRP is an RNA binding protein that is highly expressed in the brain and largely functions as a translational repressor (Darnell and Klann, 2013). It is also known that FMRP amino terminus is capable of supporting protein-protein interactions which can directly regulate properties of ion channel proteins, such as the (potassium) K^+ channels Slack and BK (Brown et al., 2010; Deng et al., 2013) while the carboxyl-terminus of FMRP is able to directly interact with calcium (Ca^{2+}) channels (Ferron et al., 2014). FMRP can therefore potentially influence neuronal excitability through multiple mechanisms: by regulating translation of a diverse array of proteins that indirectly set neuronal excitability, and through a translation-independent role by interacting directly with a number of

membrane ion channels to alter cellular excitability. A study showed that FMRP target mRNAs are genes encoding for proteins mostly involved in synaptic activity, cell adhesion, and cytoskeleton structure and remodeling, suggesting that dysregulation of these processes is responsible for the neurological phenotypes of FXS. Our data revealed that D1R KO and D2R KO transcriptome profiles were different from the WT condition. These differences were in a higher number of genes differently expressed coding for different categories such as ion channels, transcription factors or CAM. However, after deeper analysis it seems that D1R KO neurons are more affected by the lost of FMRP than D2R KO neurons due to a higher overexpression of genes compare to the same cell-type in WT.

3.4. Fear conditioning induces intrinsic plasticity in the BLA-projecting PL neurons

Fear conditioning has been shown to induce intrinsic plasticity in a number of brain regions including the hippocampus (McKay et al., 2009; Song et al., 2012), the BLA (Sehgal et al., 2014; Senn et al., 2014), and the infralimbic cortex (IL; (Santini et al., 2008)). Our results confirm that fear conditioning alters neuronal intrinsic excitability and we expand on the above findings by showing that these changes also occur in the PL. More importantly, by investigating two distinct neuronal populations we show that the BLA-projecting but not the mPFC-projecting neurons are altered by fear conditioning. This finding is in agreement with other research showing that fear conditioning preferentially recruits selected neuronal populations within the same brain region based on the neurons' long-range projection targets (Knapska et al., 2012; Senn et al., 2014). The mPFC is an important region for the acquisition and storage of long-term fear memories (Einarsson and Nader, 2012; Frankland et al., 2004) as well as the executive control over emotional responses (Euston et al., 2012). While individual mPFC subregions contribute differently to the processing of fear memories and extinction, the PL seems to be of particular importance for mediating the expression of learned fear (Burgos-Robles et al., 2009; Corcoran and Quirk, 2007; Laurent and Westbrook, 2008; Vidal-Gonzalez et al., 2006). Consequently, any change in the intrinsic properties of PL neurons could alter the manner in which fear responses are generated. This is particularly relevant in the context of the BLA-projecting neurons. The PL is bi-directionally connected to the BLA (Vertes, 2004) and this pathway is important for fear learning and expression (Corcoran and Quirk, 2007; Stevenson, 2011; Vouimba and Maroun, 2011). Indeed, fear conditioning has been shown to increase the amplitude of evoked field potentials at the PL-BLA pathway and this increase correlates positively with freezing levels during memory retrieval (Vouimba and Maroun, 2011). Furthermore, the disruption of the communication between the PL and the BLA results in impairments in the expression of fear memory (Stevenson, 2011). Finally, the BLA-projecting PL neurons have been shown to be preferentially recruited during states of high fear (Orsini et al., 2011). Given the above evidence, any alteration in the excitability of the BLA-projecting PL

neurons could therefore influence BLA-mediated fear expression and/or memory allocation to these neurons.

3.5. Fear conditioning causes a depolarized shift in the resting membrane potential

Our results show that BLA-projecting neurons display more depolarized resting membrane potentials (RMP) following fear conditioning, while no changes are present in other subthreshold membrane parameters. This change in RMP is in agreement with other studies that have found a positive shift in the RMP following associative learning (Gainutdinov et al., 1998; Kemenes et al., 2006). The RMP is an important mediator of the overall neuronal excitability. For example, more depolarized RMP can enhance cell excitability by bringing the membrane potential closer to the action potential (AP) firing threshold, which results in an increased AP discharge to a given current injection. Moreover, because voltage-gated ion channels depend on the membrane voltage, a shift in the RMP can produce changes in the neuronal input resistance and enhance neuronal firing independently of the AP threshold (Dougherty et al., 2012). However, in our study the depolarized shift in the RMP was not accompanied by changes in other subthreshold membrane parameters or by an increase in neuronal firing. Interestingly, similar results have been reported in a study on the cerebral giant cells of a snail, where a single-trial associative learning paradigm resulted in a depolarized shift in the RMP that emerged between 16-24 h following conditioning and persisted for at least 14 days. At baseline conditions, this depolarization was not accompanied by changes in neuronal input resistance or firing frequency. However, upon exposure to the conditioned stimulus (CS) the depolarized RMP caused an increase in neuronal firing, showing that a change in the RMP was sufficient to drive an increase in the network's response to the CS (Kemenes et al., 2006). In the context of our paradigm, it could therefore be hypothesized that the depolarized RMP could contribute to/drive increased firing upon re-exposure to the conditioning environment. Another possible function for a shift in the RMP is to regulate subsequent neuronal excitability and synaptic plasticity. For example, prolonged AP firing of lateral amygdala (LA) neurons can rapidly decrease membrane excitability in vivo by reducing the number of APs evoked by subsequent depolarizing current steps. Interestingly, this reduction in excitability is sensitive to shifts in the membrane potential. When LA neurons are stimulated at more hyperpolarized RMPs to induce bursting in the theta rhythm, the observed decrease in excitability is only transient. However, when the membrane potential is depolarized to more physiological levels, the same stimulation results in a robust decrease of excitability. This decrease in intrinsic excitability reduces the efficacy of subsequently induced synaptic LTP (Rosenkranz, 2011). Given the fact that changes in intrinsic excitability can readily control the induction of synaptic plasticity in vivo what role could this serve in the intact brain? A possible physiological function for this phenomenon is to reduce subsequent associative learning while leaving previous plasticity intact. This would have important implications for the formation

of long-term memories and could act as a mechanism that is used during heightened periods of activity (Rosenkranz, 2011), such as fear conditioning.

3.6. Fear conditioning increases the post-burst afterhyperpolorisation

Our results showed that contextual fear conditioning increases the afterhyperpolarisation (AHP) occurring after a train of APs. This was manifested by an increase in both the medium (mAHP) and slow (sAHP) component. Unexpectedly, our results do not support previous findings, most of which consistently show a decrease of postburst AHP following learning in a variety of behavioural paradigms including trace-eyelid conditioning (Kuo et al., 2008; Moyer et al., 1996; Oh et al., 2009; Thompson et al., 1996), spatial learning in the Morris water maze (Oh et al., 2003), operant conditioning (Saar et al., 1998) as well as fear conditioning (McKay et al., 2009; Song et al., 2012; Sehgal et al., 2014). In fact, the post-burst AHP is considered to be a marker for successful learning and a lack of decrease has been associated with a failure to acquire the task (Moyer et al., 1996; Oh et al., 2003; Song et al., 2012). Both mAHP and sAHP are generated by Ca2+ dependent K+ currents that are activated by a Ca2+ influx that occurs during a train of APs (Abel et al., 2004; Sah and Faber, 2002). The pharmacological block of the small conductance Ca2+ activated K+ channels (SK) facilitates learning (Criado-Marrero et al., 2014; Deschaux et al., 1997; Messier et al., 1991; van der Staay et al., 1999; Stackman et al., 2002). Moreover, the pharmacological activation or the genetic overexpression of SK2 channels - the specific channels underlying mAHP - reduce spontaneous firing rates in vivo and impair memory acquisition over a range of behavioural tasks, including contextual fear conditioning (Hammond et al., 2006; Vick et al., 2010). In slices, the activation or overexpression of SK2 channels increases the mAHP, decreases the number of APs as well as the synapatically evoked glutamatergic EPSPs, and attenuates LTP (Hammond et al., 2006; Criado-Marrero et al., 2014). The exact effect of sAHP modulation on behaviour has been investigated to a lesser degree because the specific Ca2+ activated K+ channels generating the current responsible for sAHP have yet to be identified (Sah & Faber, 2002). It is known however, that the sAHP plays a role in the late phase spike frequency adaptation leading to a strong reduction in AP firing and it might impair NMDA receptor mediated responses (Disterhoft et al., 2004). The channels mediating sAHP are thought to be important for memory encoding and a baseline increase in the sAHP in ageing animals is believed to underpin learning deficits (Disterhoft et al., 2004). If the increase in post-burst AHP is learning-specific, what could be its physiological role? First of all, it is worth noting that the AHP plays an active role in regulating firing frequency – a reduction in AHP increases neuronal firing, whereas an increase in AHP causes a marked decrease in firing (Moyer et al., 1996; Thompson et al., 1996; Kuo et al., 2008; McKay et al., 2009; Song et al., 2012; Sehgal et al., 2014; McKay et al., 2012; Criado-Marrero et al., 2014). Surprisingly, in our study we find no difference in number of AP fired in response to depolarizing current pulses. However, given the fact that the effect of the post-burst AHP on regulating

neuronal firing is well established (Sah & Faber, 2002), it seems likely that in our study, the AHP could still have reduced neuronal firing. Instead of causing a marked reduction in the number of AP it might have alternatively acted as a feedback mechanism to compensate for neuronal overexcitability by bringing the firing rates down to control levels. Indeed, Ca2+ entry during repetitive firing provides the cell with a simple and precise indicator of its recent activity and can act as a negative feedback system by activating AHP conductances. Additionally, apart from mediating post-bust AHP, SK channels also play an important role in regulating synaptic transmission and plasticity in the prefrontal cortex (Faber & Sah, 2007). During basal synaptic transmission they are activated by Ca2+ influx through NMDA receptors as well as voltage-gated Ca2+ channels. Their activation results in the attenuation of excitatory synaptic transmission (Faber, 2010). The activation of SK channels could therefore act as a filtering mechanism to reduce unnecessary or conflicting synaptic input. Another reason for the activation of the Ca2+-depenent K+ channels in our study could be linked to the specific role played by the PL in fear conditioning. Given the well-established role of the PL in mediating the expression of conditioned fear (Vidal-Gonzales et al., 2006; Corcoran and Quirk, 2007; Laurent and Westbrook, 2009; Sierra-Mercado et al., 2011), the activation of Ca2+-depenent K+ channels could act as a balancing force to prevent fear expression outside of the conditioning context. This mechanism would be of particular importance in the PL-BLA pathway, which mediates fear learning and expression (Stevenson, 2011; Vouimba and Maroun, 2011; Orsini et al., 2011).

3.7. Implications of changes in intrinsic excitability

The study of intrinsic plasticity is particularly useful in the context of learning and memory because it can affect a wide range of neuronal functions including the presynaptic release of neurotransmitters, the way synaptic inputs are integrated, the AP output at the soma and the active back-flow of information into the dendrites. Furthermore, it could act as a regulator of synaptic plasticity, support rule learning, or in some cases serve as part of the memory trace itself (Zhang and Linden, 2003; Frick et al., 2004; Frick and Johnston, 2005; Disterhoft and Oh, 2006; Szlapczynska et al., 2014). The functional consequences of intrinsic plasticity for memory formation will depend on the nature of the change (e.g. increase or decrease in excitability), its cellular localization (e.g. neuron-wide or global versus individual dendritic branch), or its time course (transient, long-term). Several learning paradigms (including trace eyelid conditioning, olfactory discrimination, and fear conditioning) have been used to demonstrate a neuron-wide change in intrinsic excitability (Moyer et al., 1996; Saar et al., 1998; Kuo et al., 2008; McKay et al., 2009; Oh et al., 2009; Sehgal et al., 2014). The significance of a global increase in neuronal excitability is not clear, but it may promote memory consolidation by (i) reducing the threshold for the induction of other forms of plasticity such as synaptic or structural plasticity, (ii) enhancing the likelihood that these neurons will be engaged in memory encoding, or (iii) enabling the selective reactivation of these neurons during post-training rest/sleep (Zhang and Linden, 2003; Frick and Johnston, 2005; Disterhoft and Oh, 2006; Euston

et al., 2007; Zhou et al., 2009;; Szlapczynska et al., 2014). The fact that an increase in intrinsic excitability could for example promote memory allocation to specific neurons is an interesting concept. Zhou et al., (2009) experimentally manipulated levels of the cellular trasciption factor CREB (cyclic adenosine 3′,5′-monophosphate response element binding protein) in lateral amygdala (LA) neurons. They found that neurons expressing higher levels of CREB were more excitable and because of this they were more likely to get activated during fear conditioning and be recuited into storing the conditioning episode (Zhou et al., 2009). Intrinsic plasticity is also closely coupled to synaptic plasticity and has been suggested to act as a possible substrate for metaplasticity (Frick and Johnston, 2005; Chen et al., 2006). Metaplasticity is a phenomenon whereby the neuron's ability to undergo synaptic plasticity is subject to the character of previously induced neuronal changes (Abraham and Bear, 1996). Therefore, any long-term change in intrinsic properties that occurs as a consequence of behavioural learning or neuronal activity could in turn modulate the rules governing the induction of synaptic plasticity (Johnston et al., 2003; Sjöström et al., 2008). Indeed, activity induced alteration in the voltage-gated ion channel function is bound to influence the manner in which future synaptic inputs are integrated (Magee, 2000; Magee and Johnston, 2005). Moreover, when backpropagating AP are paired with local EPSPs, this can result in increased Ca2+ influx the induction of NMDA receptor dependent LTP (Sjöström et al., 2008). Interestingly, depending on the exact timing of the backpropagation APs and the location of the activated synapses, the backpropagating AP can act as a bidirectional switch promoting the induction of either LTP or LTD. Finally, short trains of backpropagating APs have also been shown to cause an enduring depression of R-type Ca2+ channels in individual dendritic spines, which in turn inhibits the induction of synaptic plasticity (Yasuda et al., 2003). Another possible function of intrinsic plasticity is the homeostatic regulation of neuronal activity (Desai et al., 1999; Grubb and Burrone, 2010; O'Leary et al., 2010; Pratt and Aizenman, 2007; Turrigiano et al., 1994). It could serve as a feedback mechanism that would allow the network to remain stable following for example Hebbian plasticity or acute changes in neuronal excitability (Frick et al., 2004; Narayanan and Johnston, 2007; Brown and Randall, 2009). Intrinisic plasticity is well suited for this role because it plays a part in the regulation of neuronal firing rates (Frick & Johnston, 2005). Indeed, it has been shown that sustained alterations in neuronal activity can alter the expression of voltage-gated ion channels responsible for shaping firing patterns. For example, the long-term blocking (several days) of neuronal activity in cultured cortical pyramidal neurons can result in the upregulation of Na+ channels and a downregulation of sustained K+ currents. This in turn results in a lower threshold for AP initiation as well as increased firing frequency upon stimuluation (Desai et al., 1999). Another example comes from the studies on crustaceans models. The lobster stomatogastric ganglion (STG) neurons fire in bursts upon synaptic and modulatory stimulation but fire tonically when pharmacologically isolated. However, 3-4 days of isolation of these neurons in culture results in a change of their firing pattern from tonic to bursting upon depolarisation. This is a consequence of an increase in Ca2+ and decrease in K+ conducatances that compensate for the absence of their normal synaptic inputs (Turrigiano et al., 1994). In contrast, exposing cultured hippocampal neurons to periods of

sustained depolarisation by using a medium containing high KCl levels, results in a hyperpolarising shift in the RMP direction. Interestingly, the shift in the RMP becomes more hyperpolarized as KCl treatment concentration is increased. Importantly, however, when these cells are then reexposed to high KCl conditions they compensate by depolarising less than would be predicted for untreated cells (O'Leary et al., 2010). Blocking neuronal activity with glutamatergic antagonists CNQX and APV also results in a homeostatic increase in excitability through an increase in the number of AP. This effect is bidirectional because treatement with bicuculline - The GABAA receptor antagonist causes a decrease in neuronal excitability (Karmarkar and Buonomano, 2006).

3.8. Future perspectives

Based on our findings we suggest the following long-term experimental plan:

(1) In order to better categorize D1R and D2R WT, one solution should to perform single-cell RNAseq on labeled cells projecting to different brain areas. However, mRNA is very sensitive and any cytotoxicity due to a labeling lead to changes in transcriptome profile, so for the moment this approach is restricted. Another plan, should be to create a new transgenic mouse line targeting only D1R or D2R neurons into the PL area allowing a specific targeting of these cells engaged in modulation of memory for example. A last thing could be to determine a therapeutic target in the entire database that we got from the Fmr1-KO mice. Then, test this target on mice performing a task where they are presenting deficit and see the performance can be rescue to normal phenotype.

(2) For future research would be to use pharmacological approaches to better understand the channels mediating the learning-induced changes in excitability that we observed. Because we found a reduction in the maximum *dV/dt*, an increase in AP half-width and an increase in the post-bust AHP, the most obvious candidates for investigation would include: i) Na^+ channels that mediate the depolarising phase of the AP, ii) BK and/or Kv4 channels which control AP repolarisation and iii) SK channels underlying the post-burst AHP. Moreover, by using drug infusions in vivo as well as genetic overexpression/knockout approaches it might be possible to elucidate the importance of these channels for mediating fear expression and memory.

4. References

Abel, H.J., Lee, J.C.F., Callaway, J.C., and Foehring, R.C. (2004). Relationships between intracellular calcium and afterhyperpolarizations in neocortical pyramidal neurons. J. Neurophysiol. *91*, 324–335.

Abitbol, M., Menini, C., Delezoide, A.-L., Rhyner, T., Vekemans, M., and Mallet, J. (1993). Nucleus basalis magnocellularis and hippocampus are the major sites of FMR-1 expression in the human fetal brain. Nat. Genet. *4*, 147.

Abraham, W.C., and Bear, M.F. (1996). Metaplasticity: the plasticity of synaptic plasticity. Trends Neurosci. *19*, 126–130.

Adinolfi, S., Bagni, C., Musco, G., Gibson, T., Mazzarella, L., and Pastore, A. (1999). Dissecting FMR1, the protein responsible for fragile X syndrome, in its structural and functional domains. RNA *5*, 1248–1258.

van Aerde, K.I., and Feldmeyer, D. (2015). Morphological and physiological characterization of pyramidal neuron subtypes in rat medial prefrontal cortex. Cereb. Cortex N. Y. N 1991 *25*, 788–805.

Agulhon, C., Blanchet, P., Kobetz, A., Marchant, D., Faucon, N., Sarda, P., Moraine, C., Sittler, A., Biancalana, V., Malafosse, A., et al. (1999). Expression of FMR1, FXR1, and FXR2 Genes in Human Prenatal Tissues. J. Neuropathol. Exp. Neurol. *58*, 867–880.

Ährlund-Richter, S., Xuan, Y., van Lunteren, J.A., Kim, H., Ortiz, C., Pollak Dorocic, I., Meletis, K., and Carlén, M. (2019). A whole-brain atlas of monosynaptic input targeting four different cell types in the medial prefrontal cortex of the mouse. Nat. Neurosci. *22*, 657–668.

Akimoto, M., Selvaratnam, R., McNicholl, E.T., Verma, G., Taylor, S.S., and Melacini, G. (2013). Signaling through dynamic linkers as revealed by PKA. Proc. Natl. Acad. Sci. U. S. A. *110*, 14231–14236.

Altschuler, D.L., Peterson, S.N., Ostrowski, M.C., and Lapetina, E.G. (1995). Cyclic AMP-dependent activation of Rap1b. J. Biol. Chem. *270*, 10373–10376.

Andrade, R., Foehring, R.C., and Tzingounis, A.V. (2012). The calcium-activated slow AHP: cutting through the Gordian knot. Front. Cell. Neurosci. *6*, 47.

Antar, L.N., Afroz, R., Dictenberg, J.B., Carroll, R.C., and Bassell, G.J. (2004). Metabotropic glutamate receptor activation regulates fragile x mental retardation protein and FMR1 mRNA localization differentially in dendrites and at synapses. J. Neurosci. Off. J. Soc. Neurosci. *24*, 2648–2655.

Antar, L.N., Dictenberg, J.B., Plociniak, M., Afroz, R., and Bassell, G.J. (2005). Localization of FMRP-associated mRNA granules and requirement of microtubules for activity-dependent trafficking in hippocampal neurons. Genes Brain Behav. *4*, 350–359.

Arisawa, M., Makino, T., Izumi, S., and Iizuka, R. (1983). Effect of prostaglandin D2 on gonadotropin release from rat anterior pituitary in vitro. Fertil. Steril. *39*, 93–96.

Arnsten, A.F.T. (1997). Catecholamine regulation of the prefrontal cortex. J. Psychopharmacol. (Oxf.) *11*, 151–162.

Arnsten, A.F.T. (1998). Catecholamine modulation of prefrontal cortical cognitive function. Trends Cogn. Sci. *2*, 436–447.

Ashley, C.T., Wilkinson, K.D., Reines, D., and Warren, S.T. (1993). FMR1 protein: conserved RNP family domains and selective RNA binding. Science *262*, 563–566.

Bacon, S.J., Headlam, A.J., Gabbott, P.L., and Smith, A.D. (1996). Amygdala input to medial prefrontal cortex (mPFC) in the rat: a light and electron microscope study. Brain Res. *720*, 211–219.

Bassell, G.J., and Warren, S.T. (2008). Fragile X Syndrome: Loss of Local mRNA Regulation Alters Synaptic Development and Function. Neuron *60*, 201–214.

Bear, M.F., Huber, K.M., and Warren, S.T. (2004). The mGluR theory of fragile X mental retardation. Trends Neurosci. *27*, 370–377.

Bechara, A., and Damasio, A.R. (2005). The somatic marker hypothesis: A neural theory of economic decision. Games Econ. Behav. *52*, 336–372.

Bekkers, J.M., and Delaney, A.J. (2001). Modulation of excitability by alpha-dendrotoxin-sensitive potassium channels in neocortical pyramidal neurons. J. Neurosci. Off. J. Soc. Neurosci. *21*, 6553–6560.

Benhassine, N., and Berger, T. (2005). Homogeneous distribution of large-conductance calcium-dependent potassium channels on soma and apical dendrite of rat neocortical layer 5 pyramidal neurons. Eur. J. Neurosci. *21*, 914–926.

Benito, E., and Barco, A. (2010). CREB's control of intrinsic and synaptic plasticity: implications for CREB-dependent memory models. Trends Neurosci. *33*, 230–240.

Beom, S., Cheong, D., Torres, G., Caron, M.G., and Kim, K.-M. (2004). Comparative studies of molecular mechanisms of dopamine D2 and D3 receptors for the activation of extracellular signal-regulated kinase. J. Biol. Chem. *279*, 28304–28314.

Berger, B., Thierry, A.M., Tassin, J.P., and Moyne, M.A. (1976). Dopaminergic innervation of the rat prefrontal cortex: A fluorescence histochemical study. Brain Res. *106*, 133–145.

Bibb, J.A., Snyder, G.L., Nishi, A., Yan, Z., Meijer, L., Fienberg, A.A., Tsai, L.H., Kwon, Y.T., Girault, J.A., Czernik, A.J., et al. (1999). Phosphorylation of DARPP-32 by Cdk5 modulates dopamine signalling in neurons. Nature *402*, 669–671.

Bolduc, F.V., Bell, K., Cox, H., Broadie, K., and Tully, T. (2008). Excess protein synthesis in Drosophila Fragile X mutants impairs long-term memory. Nat. Neurosci. *11*, 1143–1145.

Bonilha, L., Molnar, C., Horner, M.D., Anderson, B., Forster, L., George, M.S., and Nahas, Z. (2008). Neurocognitive deficits and prefrontal cortical atrophy in patients with schizophrenia. Schizophr. Res. *101*, 142–151.

Bontempi, B., Laurent-Demir, C., Destrade, C., and Jaffard, R. (1999). Time-dependent reorganization of brain circuitry underlying long-term memory storage. Nature *400*, 671–675.

Bos, J.L., de Rooij, J., and Reedquist, K.A. (2001). Rap1 signalling: adhering to new models. Nat. Rev. Mol. Cell Biol. *2*, 369–377.

Botvinick, M.M., Cohen, J.D., and Carter, C.S. (2004). Conflict monitoring and anterior cingulate cortex: an update. Trends Cogn. Sci. *8*, 539–546.

Boyson, S.J., McGonigle, P., and Molinoff, P.B. (1986). Quantitative autoradiographic localization of the D1 and D2 subtypes of dopamine receptors in rat brain. J. Neurosci. Off. J. Soc. Neurosci. *6*, 3177–3188.

Brager, D.H., Akhavan, A.R., and Johnston, D. (2012). Impaired Dendritic Expression and fmr1−/y Plasticity of h-Channels in the Mouse Model of Fragile X Syndrome. Cell Rep. *1*, 225–233.

Brami-Cherrier, K., Valjent, E., Garcia, M., Pagès, C., Hipskind, R.A., and Caboche, J. (2002). Dopamine induces a PI3-kinase-independent activation of Akt in striatal neurons: a new route to cAMP response element-binding protein phosphorylation. J. Neurosci. Off. J. Soc. Neurosci. *22*, 8911–8921.

Bremner, J.D., Narayan, M., Staib, L.H., Southwick, S.M., McGlashan, T., and Charney, D.S. (1999). Neural correlates of memories of childhood sexual abuse in women with and without posttraumatic stress disorder. Am. J. Psychiatry *156*, 1787–1795.

Brennan, A.R., Dolinsky, B., Vu, M.-A.T., Stanley, M., Yeckel, M.F., and Arnsten, A.F.T. (2008). Blockade of IP3-mediated SK channel signaling in the rat medial prefrontal cortex improves spatial working memory. Learn. Mem. Cold Spring Harb. N *15*, 93–96.

Bromberg-Martin, E.S., Matsumoto, M., and Hikosaka, O. (2010). Dopamine in Motivational Control: Rewarding, Aversive, and Alerting. Neuron *68*, 815–834.

Brown, D.A., and Passmore, G.M. (2009). Neural KCNQ (Kv7) channels. Br. J. Pharmacol. *156*, 1185–1195.

Brown, S.P., and Hestrin, S. (2009). Cell-type identity: a key to unlocking the function of neocortical circuits. Curr. Opin. Neurobiol. *19*, 415–421.

Brown, M.R., Kronengold, J., Gazula, V.-R., Chen, Y., Strumbos, J.G., Sigworth, F.J., Navaratnam, D., and Kaczmarek, L.K. (2010). Fragile X mental retardation protein controls gating of the sodium-activated potassium channel Slack. Nat. Neurosci. *13*, 819–821.

Brown, V., Jin, P., Ceman, S., Darnell, J.C., O'Donnell, W.T., Tenenbaum, S.A., Jin, X., Feng, Y., Wilkinson, K.D., Keene, J.D., et al. (2001). Microarray identification of FMRP-associated brain mRNAs and altered mRNA translational profiles in fragile X syndrome. Cell *107*, 477–487.

Brozoski, T.J., Brown, R.M., Rosvold, H.E., and Goldman, P.S. (1979). Cognitive deficit caused by regional depletion of dopamine in prefrontal cortex of rhesus monkey. Science *205*, 929–932.

Budygin, E.A., Park, J., Bass, C.E., Grinevich, V.P., Bonin, K.D., and Wightman, R.M. (2012). Aversive stimulus differentially triggers subsecond dopamine release in reward regions. Neuroscience *201*, 331–337.

Burgos-Robles, A., Vidal-Gonzalez, I., Santini, E., and Quirk, G.J. (2007). Consolidation of fear extinction requires NMDA receptor-dependent bursting in the ventromedial prefrontal cortex. Neuron *53*, 871–880.

Burgos-Robles, A., Vidal-Gonzalez, I., and Quirk, G.J. (2009). Sustained conditioned responses in prelimbic prefrontal neurons are correlated with fear expression and extinction failure. J. Neurosci. Off. J. Soc. Neurosci. *29*, 8474–8482.

Cadet, J.L., Jayanthi, S., McCoy, M.T., Beauvais, G., and Cai, N.S. (2010). Dopamine D1 receptors, regulation of gene expression in the brain, and neurodegeneration. CNS Neurol. Disord. Drug Targets *9*, 526–538.

Cadwell, C.R., Palasantza, A., Jiang, X., Berens, P., Deng, Q., Yilmaz, M., Reimer, J., Shen, S., Bethge, M., Tolias, K.F., et al. (2016). Electrophysiological, transcriptomic and morphologic profiling of single neurons using Patch-seq. Nat. Biotechnol. *34*, 199–203.

Cai, X., Liang, C.W., Muralidharan, S., Muralidharan, S., Kao, J.P.Y., Tang, C.-M., and Thompson, S.M. (2004). Unique roles of SK and Kv4.2 potassium channels in dendritic integration. Neuron *44*, 351–364.

Cantrell, A.R., and Catterall, W.A. (2001). Neuromodulation of Na+ channels: an unexpected form of cellular plasticity. Nat. Rev. Neurosci. *2*, 397–407.

Carr, D.B., and Sesack, S.R. (2000a). GABA-containing neurons in the rat ventral tegmental area project to the prefrontal cortex. Synapse *38*, 114–123.

Carr, D.B., and Sesack, S.R. (2000b). Projections from the Rat Prefrontal Cortex to the Ventral Tegmental Area: Target Specificity in the Synaptic Associations with Mesoaccumbens and Mesocortical Neurons. J. Neurosci. *20*, 3864–3873.

Casey, B.J., Epstein, J.N., Buhle, J., Liston, C., Davidson, M.C., Tonev, S.T., Spicer, J., Niogi, S., Millner, A.J., Reiss, A., et al. (2007). Frontostriatal connectivity and its role in cognitive control in parent-child dyads with ADHD. Am. J. Psychiatry *164*, 1729–1736.

Catterall, W.A. (2000). Structure and regulation of voltage-gated Ca2+ channels. Annu. Rev. Cell Dev. Biol. *16*, 521–555.

Catterall, W.A. (2011). Voltage-gated calcium channels. Cold Spring Harb. Perspect. Biol. *3*, a003947.

Catterall, W.A., Raman, I.M., Robinson, H.P.C., Sejnowski, T.J., and Paulsen, O. (2012). The Hodgkin-Huxley heritage: from channels to circuits. J. Neurosci. Off. J. Soc. Neurosci. *32*, 14064–14073.

Ceman, S., O'Donnell, W.T., Reed, M., Patton, S., Pohl, J., and Warren, S.T. (2003). Phosphorylation influences the translation state of FMRP-associated polyribosomes. Hum. Mol. Genet. *12*, 3295–3305.

Chang, Y.-M., and Luebke, J.I. (2007). Electrophysiological diversity of layer 5 pyramidal cells in the prefrontal cortex of the rhesus monkey: in vitro slice studies. J. Neurophysiol. *98*, 2622–2632.

Chaudhry, A.Z., Lyons, G.E., and Gronostajski, R.M. (1997). Expression patterns of the four nuclear factor I genes during mouse embryogenesis indicate a potential role in development. Dev. Dyn. Off. Publ. Am. Assoc. Anat. *208*, 313–325.

Chen, L., Yun, S.W., Seto, J., Liu, W., and Toth, M. (2003). The fragile X mental retardation protein binds and regulates a novel class of mRNAs containing U rich target sequences. Neuroscience *120*, 1005–1017.

Chen, X., Yuan, L.-L., Zhao, C., Birnbaum, S.G., Frick, A., Jung, W.E., Schwarz, T.L., Sweatt, J.D., and Johnston, D. (2006). Deletion of Kv4.2 gene eliminates dendritic A-type K+ current and enhances induction of long-term potentiation in hippocampal CA1 pyramidal neurons. J. Neurosci. Off. J. Soc. Neurosci. *26*, 12143–12151.

Chen, X., Shu, S., and Bayliss, D.A. (2009). HCN1 channel subunits are a molecular substrate for hypnotic actions of ketamine. J. Neurosci. Off. J. Soc. Neurosci. *29*, 600–609.

Cianchetti, C., Sannio-Fancello, G., Fratta, A.L., Manconi, F., Orano, A., Pischedda, M.P., Pruna, D., Spinicci, G., Archidiacono, N., and Filippi, G. (1991). Neuropsychological, psychiatric, and physical manifestations in 149 members from 18 fragile X families. Am. J. Med. Genet. *40*, 234–243.

Civelli, O., Bunzow, J.R., and Grandy, D.K. (1993). Molecular diversity of the dopamine receptors. Annu. Rev. Pharmacol. Toxicol. *33*, 281–307.

Claudia Rangel-Barajas, I.C., and Claudia Rangel-Barajas, I.C. (2015). Dopamine Receptors and Neurodegeneration. Aging Dis. *6*, 349–368.

Coffee, R.L., Williamson, A.J., Adkins, C.M., Gray, M.C., Page, T.L., and Broadie, K. (2012). In vivo neuronal function of the fragile X mental retardation protein is regulated by phosphorylation. Hum. Mol. Genet. *21*, 900–915.

Collo, G., Zanetti, S., Missale, C., and Spano, P. (2008). Dopamine D3 receptor-preferring agonists increase dendrite arborization of mesencephalic dopaminergic neurons via extracellular signal-regulated kinase phosphorylation. Eur. J. Neurosci. *28*, 1231–1240.

Collo, G., Bono, F., Cavalleri, L., Plebani, L., Merlo Pich, E., Millan, M.J., Spano, P.F., and Missale, C. (2012). Pre-synaptic dopamine D(3) receptor mediates cocaine-induced structural plasticity in mesencephalic dopaminergic neurons via ERK and Akt pathways. J. Neurochem. *120*, 765–778.

Connors, B.W., and Gutnick, M.J. (1990). Intrinsic firing patterns of diverse neocortical neurons. Trends Neurosci. *13*, 99–104.

Contractor, A. (2013). Broadening roles for FMRP: big news for big potassium (BK) channels. Neuron *77*, 601–603.

Cooper, D.M.F. (2003). Regulation and organization of adenylyl cyclases and cAMP. Biochem. J. *375*, 517–529.

Cooper, D.M., Mons, N., and Karpen, J.W. (1995). Adenylyl cyclases and the interaction between calcium and cAMP signalling. Nature *374*, 421–424.

Corbin, F., Bouillon, M., Fortin, A., Morin, S., Rousseau, F., and Khandjian, E.W. (1997). The Fragile X Mental Retardation Protein is Associated with Poly(A)+ mRNA in Actively Translating Polyribosomes. Hum. Mol. Genet. *6*, 1465–1472.

Corcoran, K.A., and Quirk, G.J. (2007). Activity in prelimbic cortex is necessary for the expression of learned, but not innate, fears. J. Neurosci. Off. J. Soc. Neurosci. *27*, 840–844.

Cornish, K.M., Munir, F., and Cross, G. (1998). The nature of the spatial deficit in young females with Fragile-X syndrome: a neuropsychological and molecular perspective. Neuropsychologia *36*, 1239–1246.

Cornish, K.M., Munir, F., and Cross, G. (1999). Spatial cognition in males with Fragile-X syndrome: evidence for a neuropsychological phenotype. Cortex J. Devoted Study Nerv. Syst. Behav. *35*, 263–271.

Costa, A., and Villalba, E. (2013). Horizons in neuroscience research (Hauppauge, NY: Nova Science Publishers).

Courtin, J., Bienvenu, T.C.M., Einarsson, E.Ö., and Herry, C. (2013). Medial prefrontal cortex neuronal circuits in fear behavior. Neuroscience *240*, 219–242.

Criado-Marrero, M., Santini, E., and Porter, J.T. (2014). Modulating fear extinction memory by manipulating SK potassium channels in the infralimbic cortex. Front. Behav. Neurosci. *8*, 96.

Crill, W.E. (1996). Persistent sodium current in mammalian central neurons. Annu. Rev. Physiol. *58*, 349–362.

Darnell, J.C., and Klann, E. (2013). The Translation of Translational Control by FMRP: Therapeutic Targets for Fragile X Syndrome. Nat. Neurosci. *16*, 1530–1536.

Darnell, J.C., Van Driesche, S.J., Zhang, C., Hung, K.Y.S., Mele, A., Fraser, C.E., Stone, E.F., Chen, C., Fak, J.J., Chi, S.W., et al. (2011). FMRP stalls ribosomal translocation on mRNAs linked to synaptic function and autism. Cell *146*, 247–261.

Dégenètais, E., Thierry, A.-M., Glowinski, J., and Gioanni, Y. (2002). Electrophysiological properties of pyramidal neurons in the rat prefrontal cortex: an in vivo intracellular recording study. Cereb. Cortex N. Y. N 1991 *12*, 1–16.

Dembrow, N.C., Chitwood, R.A., and Johnston, D. (2010). Projection-Specific Neuromodulation of Medial Prefrontal Cortex Neurons. J. Neurosci. *30*, 16922–16937.

DeNardo, L.A., Berns, D.S., DeLoach, K., and Luo, L. (2015). Connectivity of Mouse Somatosensory and Prefrontal Cortex Examined with Trans-synaptic Tracing. Nat. Neurosci. *18*, 1687–1697.

Deng, P.-Y., Rotman, Z., Blundon, J.A., Cho, Y., Cui, J., Cavalli, V., Zakharenko, S.S., and Klyachko, V.A. (2013). FMRP regulates neurotransmitter release and synaptic information transmission by modulating action potential duration via BK channels. Neuron *77*, 696–711.

Desai, N.S., Rutherford, L.C., and Turrigiano, G.G. (1999). Plasticity in the intrinsic excitability of cortical pyramidal neurons. Nat. Neurosci. *2*, 515–520.

Desai, N.S., Casimiro, T.M., Gruber, S.M., and Vanderklish, P.W. (2006). Early postnatal plasticity in neocortex of Fmr1 knockout mice. J. Neurophysiol. *96*, 1734–1745.

Deschaux, O., Bizot, J.C., and Goyffon, M. (1997). Apamin improves learning in an object recognition task in rats. Neurosci. Lett. *222*, 159–162.

Devys, D., Lutz, Y., Rouyer, N., Bellocq, J.-P., and Mandel, J.-L. (1993). The FMR–1 protein is cytoplasmic, most abundant in neurons and appears normal in carriers of a fragile X premutation. Nat. Genet. *4*, 335.

Dictenberg, J.B., Swanger, S.A., Antar, L.N., Singer, R.H., and Bassell, G.J. (2008). A Direct Role for FMRP in Activity-Dependent Dendritic mRNA Transport Links Filopodial-Spine Morphogenesis to Fragile X Syndrome. Dev. Cell *14*, 926–939.

Disterhoft, J.F., and Oh, M.M. (2006). Learning, aging and intrinsic neuronal plasticity. Trends Neurosci. *29*, 587–599.

Disterhoft, J.F., Wu, W.W., and Ohno, M. (2004). Biophysical alterations of hippocampal pyramidal neurons in learning, ageing and Alzheimer's disease. Ageing Res. Rev. *3*, 383–406.

Doble, B.W., and Woodgett, J.R. (2003). GSK-3: tricks of the trade for a multi-tasking kinase. J. Cell Sci. *116*, 1175–1186.

Dölen, G., Osterweil, E., Shankaranarayana Rao, B.S., Smith, G.B., Auerbach, B.D., Chattarji, S., and Bear, M.F. (2007). Correction of fragile X syndrome in mice. Neuron *56*, 955–962.

Douglas, R.J., and Martin, K.A.C. (2004). Neuronal circuits of the neocortex. Annu. Rev. Neurosci. *27*, 419–451.

Douglas, R.J., Martin, K.A.C., and Whitteridge, D. (1989). A Canonical Microcircuit for Neocortex. Neural Comput *1*, 480–488.

Durstewitz, D., Seamans, J.K., and Sejnowski, T.J. (2000). Dopamine-Mediated Stabilization of Delay-Period Activity in a Network Model of Prefrontal Cortex. J. Neurophysiol. *83*, 1733–1750.

Dykens, E.M., Hodapp, R.M., and Leckman, J.F. (1987). Strengths and weaknesses in the intellectual functioning of males with fragile X syndrome. Am. J. Ment. Defic. *92*, 234–236.

Economo, M.N., Clack, N.G., Lavis, L.D., Gerfen, C.R., Svoboda, K., Myers, E.W., and Chandrashekar, J. (2016). A platform for brain-wide imaging and reconstruction of individual neurons. ELife *5*, e10566.

Egan, M.F., and Weinberger, D.R. (1997). Neurobiology of schizophrenia. Curr. Opin. Neurobiol. *7*, 701–707.

Einarsson, E.Ö., and Nader, K. (2012). Involvement of the anterior cingulate cortex in formation, consolidation, and reconsolidation of recent and remote contextual fear memory. Learn. Mem. Cold Spring Harb. N *19*, 449–452.

Emamian, E.S. (2012). AKT/GSK3 signaling pathway and schizophrenia. Front. Mol. Neurosci. *5*, 33.

Euston, D.R., Gruber, A.J., and McNaughton, B.L. (2012). The Role of Medial Prefrontal Cortex in Memory and Decision Making. Neuron *76*, 1057–1070.

Faber, E.S.L. (2010). Functional interplay between NMDA receptors, SK channels and voltage-gated Ca2+ channels regulates synaptic excitability in the medial prefrontal cortex. J. Physiol. *588*, 1281–1292.

Faber, E.S.L., and Sah, P. (2003). Calcium-activated potassium channels: multiple contributions to neuronal function. Neurosci. Rev. J. Bringing Neurobiol. Neurol. Psychiatry *9*, 181–194.

Feldmeyer, D. (2012). Excitatory neuronal connectivity in the barrel cortex. Front. Neuroanat. *6*, 24.

Feldmeyer, D., Lübke, J., Silver, R.A., and Sakmann, B. (2002). Synaptic connections between layer 4 spiny neurone-layer 2/3 pyramidal cell pairs in juvenile rat barrel cortex: physiology and anatomy of interlaminar signalling within a cortical column. J. Physiol. *538*, 803–822.

Fellows, L.K. (2007). Advances in understanding ventromedial prefrontal function: the accountant joins the executive. Neurology *68*, 991–995.

Feng, Y., Gutekunst, C.-A., Eberhart, D.E., Yi, H., Warren, S.T., and Hersch, S.M. (1997a). Fragile X Mental Retardation Protein: Nucleocytoplasmic Shuttling and Association with Somatodendritic Ribosomes. J. Neurosci. *17*, 1539–1547.

Feng, Y., Absher, D., Eberhart, D.E., Brown, V., Malter, H.E., and Warren, S.T. (1997b). FMRP Associates with Polyribosomes as an mRNP, and the I304N Mutation of Severe Fragile X Syndrome Abolishes This Association. Mol. Cell *1*, 109–118.

Ferron, L., Nieto-Rostro, M., Cassidy, J.S., and Dolphin, A.C. (2014). Fragile X mental retardation protein controls synaptic vesicle exocytosis by modulating N-type calcium channel density. Nat. Commun. *5*, 3628.

Fishell, G., and Heintz, N. (2013). The Neuron Identity Problem: Form Meets Function. Neuron *80*, 602–612.

Floresco, S.B., and Phillips, A.G. (2001). Delay-dependent modulation of memory retrieval by infusion of a dopamine D_1 agonist into the rat medial prefrontal cortex. Behav. Neurosci. *115*, 934–939.

Földy, C., Darmanis, S., Aoto, J., Malenka, R.C., Quake, S.R., and Südhof, T.C. (2016). Single-cell RNAseq reveals cell adhesion molecule profiles in electrophysiologically defined neurons. Proc. Natl. Acad. Sci. U. S. A. *113*, E5222-5231.

Forn, J., Krueger, B.K., and Greengard, P. (1974). Adenosine 3',5'-monophosphate content in rat caudate nucleus: demonstration of dopaminergic and adrenergic receptors. Science *186*, 1118–1120.

Frankland, P.W., and Bontempi, B. (2005). The organization of recent and remote memories. Nat. Rev. Neurosci. *6*, 119–130.

Frankland, P.W., Bontempi, B., Talton, L.E., Kaczmarek, L., and Silva, A.J. (2004). The involvement of the anterior cingulate cortex in remote contextual fear memory. Science *304*, 881–883.

Freund, L.S., and Reiss, A.L. (1991). Cognitive profiles associated with the fra(X) syndrome in males and females. Am. J. Med. Genet. *38*, 542–547.

Frick, A., and Johnston, D. (2005). Plasticity of dendritic excitability. J. Neurobiol. *64*, 100–115.

Frick, A., Magee, J., Koester, H.J., Migliore, M., and Johnston, D. (2003). Normalization of Ca2+ signals by small oblique dendrites of CA1 pyramidal neurons. J. Neurosci. Off. J. Soc. Neurosci. *23*, 3243–3250.

Frick, A., Magee, J., and Johnston, D. (2004). LTP is accompanied by an enhanced local excitability of pyramidal neuron dendrites. Nat. Neurosci. *7*, 126–135.

Frick, A., Feldmeyer, D., Helmstaedter, M., and Sakmann, B. (2008). Monosynaptic connections between pairs of L5A pyramidal neurons in columns of juvenile rat somatosensory cortex. Cereb. Cortex N. Y. N 1991 *18*, 397–406.

Fuzik, J., Zeisel, A., Máté, Z., Calvigioni, D., Yanagawa, Y., Szabó, G., Linnarsson, S., and Harkany, T. (2016). Integration of electrophysiological recordings with single-cell RNA-seq data identifies neuronal subtypes. Nat. Biotechnol. *34*, 175–183.

Gabbott, P.L.A., Warner, T.A., Jays, P.R.L., Salway, P., and Busby, S.J. (2005). Prefrontal cortex in the rat: projections to subcortical autonomic, motor, and limbic centers. J. Comp. Neurol. *492*, 145–177.

Gabel, L.A., Won, S., Kawai, H., McKinney, M., Tartakoff, A.M., and Fallon, J.R. (2004). Visual experience regulates transient expression and dendritic localization of fragile X mental retardation protein. J. Neurosci. Off. J. Soc. Neurosci. *24*, 10579–10583.

Garber, K., Smith, K.T., Reines, D., and Warren, S.T. (2006). Transcription, translation and fragile X syndrome. Curr. Opin. Genet. Dev. *16*, 270–275.

Garber, K.B., Visootsak, J., and Warren, S.T. (2008). Fragile X syndrome. Eur. J. Hum. Genet. EJHG *16*, 666–672.

Gee, S., Ellwood, I., Patel, T., Luongo, F., Deisseroth, K., and Sohal, V.S. (2012). Synaptic activity unmasks dopamine D2 receptor modulation of a specific class of layer V pyramidal neurons in prefrontal cortex. J. Neurosci. *32*, 4959–4971.

Gibson, J.R., Bartley, A.F., Hays, S.A., and Huber, K.M. (2008). Imbalance of neocortical excitation and inhibition and altered UP states reflect network hyperexcitability in the mouse model of fragile X syndrome. J. Neurophysiol. *100*, 2615–2626.

Golding, N.L., Kath, W.L., and Spruston, N. (2001). Dichotomy of action-potential backpropagation in CA1 pyramidal neuron dendrites. J. Neurophysiol. *86*, 2998–3010.

Goldman-Rakic, P.S. (1995). Cellular basis of working memory. Neuron *14*, 477–485.

Gong, H., Zeng, S., Yan, C., Lv, X., Yang, Z., Xu, T., Feng, Z., Ding, W., Qi, X., Li, A., et al. (2013). Continuously tracing brain-wide long-distance axonal projections in mice at a one-micron voxel resolution. NeuroImage *74*, 87–98.

Granon, S., Passetti, F., Thomas, K.L., Dalley, J.W., Everitt, B.J., and Robbins, T.W. (2000). Enhanced and Impaired Attentional Performance After Infusion of D1 Dopaminergic Receptor Agents into Rat Prefrontal Cortex. J. Neurosci. *20*, 1208–1215.

Graybiel, A.M., Aosaki, T., Flaherty, A.W., and Kimura, M. (1994). The basal ganglia and adaptive motor control. Science *265*, 1826–1831.

Greengard, P., Allen, P.B., and Nairn, A.C. (1999). Beyond the dopamine receptor: the DARPP-32/protein phosphatase-1 cascade. Neuron *23*, 435–447.

Grewe, B.F., Bonnan, A., and Frick, A. (2010). Back-Propagation of Physiological Action Potential Output in Dendrites of Slender-Tufted L5A Pyramidal Neurons. Front. Cell. Neurosci. *4*, 13.

Gross, C., Yao, X., Pong, D.L., Jeromin, A., and Bassell, G.J. (2011). Fragile X mental retardation protein regulates protein expression and mRNA translation of the potassium channel Kv4.2. J. Neurosci. Off. J. Soc. Neurosci. *31*, 5693–5698.

Grossman, A.W., Aldridge, G.M., Weiler, I.J., and Greenough, W.T. (2006). Local protein synthesis and spine morphogenesis: Fragile X syndrome and beyond. J. Neurosci. Off. J. Soc. Neurosci. *26*, 7151–7155.

Grubb, M.S., and Burrone, J. (2010). Activity-dependent relocation of the axon initial segment fine-tunes neuronal excitability. Nature *465*, 1070–1074.

Guan, D., Lee, J.C.F., Higgs, M.H., Spain, W.J., and Foehring, R.C. (2007a). Functional roles of Kv1 channels in neocortical pyramidal neurons. J. Neurophysiol. *97*, 1931–1940.

Guan, D., Tkatch, T., Surmeier, D.J., Armstrong, W.E., and Foehring, R.C. (2007b). Kv2 subunits underlie slowly inactivating potassium current in rat neocortical pyramidal neurons. J. Physiol. *581*, 941–960.

Guan, D., Higgs, M.H., Horton, L.R., Spain, W.J., and Foehring, R.C. (2011). Contributions of Kv7-mediated potassium current to sub- and suprathreshold responses of rat layer II/III neocortical pyramidal neurons. J. Neurophysiol. *106*, 1722–1733.

Guan, D., Armstrong, W.E., and Foehring, R.C. (2013). Kv2 channels regulate firing rate in pyramidal neurons from rat sensorimotor cortex. J. Physiol. *591*, 4807–4825.

Gulledge, A.T., and Jaffe, D.B. (1998). Dopamine Decreases the Excitability of Layer V Pyramidal Cells in the Rat Prefrontal Cortex. J. Neurosci. *18*, 9139–9151.

Gulledge, A.T., and Stuart, G.J. (2003). Action Potential Initiation and Propagation in Layer 5 Pyramidal Neurons of the Rat Prefrontal Cortex: Absence of Dopamine Modulation. J. Neurosci. *23*, 11363–11372.

Gulledge, A.T., Park, S.B., Kawaguchi, Y., and Stuart, G.J. (2007). Heterogeneity of phasic cholinergic signaling in neocortical neurons. J. Neurophysiol. *97*, 2215–2229.

Gunaydin, L.A., Grosenick, L., Finkelstein, J.C., Kauvar, I.V., Fenno, L.E., Adhikari, A., Lammel, S., Mirzabekov, J.J., Airan, R.D., Zalocusky, K.A., et al. (2014). Natural Neural Projection Dynamics Underlying Social Behavior. Cell *157*, 1535–1551.

Gutman, G.A., Chandy, K.G., Grissmer, S., Lazdunski, M., McKinnon, D., Pardo, L.A., Robertson, G.A., Rudy, B., Sanguinetti, M.C., Stühmer, W., et al. (2005). International Union of Pharmacology. LIII. Nomenclature and molecular relationships of voltage-gated potassium channels. Pharmacol. Rev. *57*, 473–508.

Ha, C.M., Park, D., Han, J.-K., Jang, J., Park, J.-Y., Hwang, E.M., Seok, H., and Chang, S. (2012). Calcyon forms a novel ternary complex with dopamine D1 receptor through PSD-95 protein and plays a role in dopamine receptor internalization. J. Biol. Chem. *287*, 31813–31822.

Hagenston, A.M., Fitzpatrick, J.S., and Yeckel, M.F. (2008). MGluR-mediated calcium waves that invade the soma regulate firing in layer V medial prefrontal cortical pyramidal neurons. Cereb. Cortex N. Y. N 1991 *18*, 407–423.

Hagerman, R.J., Leehey, M., Heinrichs, W., Tassone, F., Wilson, R., Hills, J., Grigsby, J., Gage, B., and Hagerman, P.J. (2001). Intention tremor, parkinsonism, and generalized brain atrophy in male carriers of fragile X. Neurology *57*, 127–130.

Hammond, R.S., Bond, C.T., Strassmaier, T., Ngo-Anh, T.J., Adelman, J.P., Maylie, J., and Stackman, R.W. (2006). Small-conductance Ca2+-activated K+ channel type 2 (SK2) modulates hippocampal learning, memory, and synaptic plasticity. J. Neurosci. Off. J. Soc. Neurosci. *26*, 1844–1853.

Harris, J.A., Hirokawa, K.E., Sorensen, S.A., Gu, H., Mills, M., Ng, L.L., Bohn, P., Mortrud, M., Ouellette, B., Kidney, J., et al. (2014). Anatomical characterization of Cre driver mice for neural circuit mapping and manipulation. Front. Neural Circuits *8*.

Heidbreder, C.A., and Groenewegen, H.J. (2003). The medial prefrontal cortex in the rat: evidence for a dorso-ventral distinction based upon functional and anatomical characteristics. Neurosci. Biobehav. Rev. *27*, 555–579.

Heiman, M., Schaefer, A., Gong, S., Peterson, J., Day, M., Ramsey, K.E., Suárez-Fariñas, M., Schwarz, C., Stephan, D.A., Surmeier, D.J., et al. (2008). Development of a BACarray translational profiling approach for the molecular characterization of CNS cell types. Cell *135*, 738–748.

Herry, C., Ciocchi, S., Senn, V., Demmou, L., Müller, C., and Lüthi, A. (2008). Switching on and off fear by distinct neuronal circuits. Nature *454*, 600–606.

Hirayama, M., Ko, S.B.H., Kawakita, T., Akiyama, T., Goparaju, S.K., Soma, A., Nakatake, Y., Sakota, M., Chikazawa-Nohtomi, N., Shimmura, S., et al. (2017). Identification of transcription factors that promote the differentiation of human pluripotent stem cells into lacrimal gland epithelium-like cells. NPJ Aging Mech. Dis. *3*.

Hodgkin, A.L., and Huxley, A.F. (1952). A quantitative description of membrane current and its application to conduction and excitation in nerve. J. Physiol. *117*, 500–544.

Hoeffer, C.A., and Klann, E. (2010). mTOR signaling: at the crossroads of plasticity, memory and disease. Trends Neurosci. *33*, 67–75.

Hoffman, D.A., and Johnston, D. (1998). Downregulation of transient K+ channels in dendrites of hippocampal CA1 pyramidal neurons by activation of PKA and PKC. J. Neurosci. Off. J. Soc. Neurosci. *18*, 3521–3528.

Hoffman, D.A., and Johnston, D. (1999). Neuromodulation of dendritic action potentials. J. Neurophysiol. *81*, 408–411.

Holloway, C.M., and McIntyre, C.K. (2011). Post-training disruption of Arc protein expression in the anterior cingulate cortex impairs long-term memory for inhibitory avoidance training. Neurobiol. Learn. Mem. *95*, 425–432.

Holroyd, C.B., Coles, M.G.H., and Nieuwenhuis, S. (2002). Medial prefrontal cortex and error potentials. Science *296*, 1610-1611 author reply 1610-1611.

Hoover, W.B., and Vertes, R.P. (2007). Anatomical analysis of afferent projections to the medial prefrontal cortex in the rat. Brain Struct. Funct. *212*, 149–179.

Irwin, S.A., Swain, R.A., Christmon, C.A., Chakravarti, A., Weiler, I.J., and Greenough, W.T. (2000). Evidence for altered Fragile-X mental retardation protein expression in response to behavioral stimulation. Neurobiol. Learn. Mem. *74*, 87–93.

Johnston, D., and Narayanan, R. (2008). Active dendrites: colorful wings of the mysterious butterflies. Trends Neurosci. *31*, 309–316.

Johnston, D., Christie, B.R., Frick, A., Gray, R., Hoffman, D.A., Schexnayder, L.K., Watanabe, S., and Yuan, L.-L. (2003). Active dendrites, potassium channels and synaptic plasticity. Philos. Trans. R. Soc. Lond. B. Biol. Sci. *358*, 667–674.

Karmarkar, U.R., and Buonomano, D.V. (2006). Different forms of homeostatic plasticity are engaged with distinct temporal profiles. Eur. J. Neurosci. *23*, 1575–1584.

Kates, W.R., Abrams, M.T., Kaufmann, W.E., Breiter, S.N., and Reiss, A.L. (1997). Reliability and validity of MRI measurement of the amygdala and hippocampus in children with fragile X syndrome. Psychiatry Res. *75*, 31–48.

Kawaguchi, Y. (1993). Physiological, morphological, and histochemical characterization of three classes of interneurons in rat neostriatum. J. Neurosci. Off. J. Soc. Neurosci. *13*, 4908–4923.

Kawasaki, H., Springett, G.M., Mochizuki, N., Toki, S., Nakaya, M., Matsuda, M., Housman, D.E., and Graybiel, A.M. (1998). A family of cAMP-binding proteins that directly activate Rap1. Science *282*, 2275–2279.

Kebabian, J.W., and Greengard, P. (1971). Dopamine-sensitive adenyl cyclase: possible role in synaptic transmission. Science *174*, 1346–1349.

Kepecs, A., and Fishell, G. (2014). Interneuron cell types are fit to function. Nature *505*, 318–326.

Kim, G.E., and Kaczmarek, L.K. (2014). Emerging role of the KCNT1 Slack channel in intellectual disability. Front. Cell. Neurosci. *8*, 209.

Kim, C., Vigil, D., Anand, G., and Taylor, S.S. (2006). Structure and dynamics of PKA signaling proteins. Eur. J. Cell Biol. *85*, 651–654.

Kim, G.E., Kronengold, J., Barcia, G., Quraishi, I.H., Martin, H.C., Blair, E., Taylor, J.C., Dulac, O., Colleaux, L., Nabbout, R., et al. (2014a). Human slack potassium channel mutations increase positive cooperativity between individual channels. Cell Rep. *9*, 1661–1672.

Kim, J., Jung, S.-C., Clemens, A.M., Petralia, R.S., and Hoffman, D.A. (2007). Regulation of dendritic excitability by activity-dependent trafficking of the A-type K+ channel subunit Kv4.2 in hippocampal neurons. Neuron *54*, 933–947.

Kim, S.-Y., Burris, J., Bassal, F., Koldewyn, K., Chattarji, S., Tassone, F., Hessl, D., and Rivera, S.M. (2014b). Fear-Specific Amygdala Function in Children and Adolescents on the Fragile X Spectrum: A Dosage Response of the FMR1 Gene. Cereb. Cortex N. Y. NY *24*, 600–613.

Kiss, T. (2008). Persistent Na-channels: origin and function. A review. Acta Biol. Hung. *59 Suppl*, 1–12.

Knapska, E., Macias, M., Mikosz, M., Nowak, A., Owczarek, D., Wawrzyniak, M., Pieprzyk, M., Cymerman, I.A., Werka, T., Sheng, M., et al. (2012). Functional anatomy of neural circuits regulating fear and extinction. Proc. Natl. Acad. Sci. U. S. A. *109*, 17093–17098.

Koekkoek, S.K.E., Yamaguchi, K., Milojkovic, B.A., Dortland, B.R., Ruigrok, T.J.H., Maex, R., De Graaf, W., Smit, A.E., VanderWerf, F., Bakker, C.E., et al. (2005). Deletion of FMR1 in Purkinje cells enhances parallel fiber LTD, enlarges spines, and attenuates cerebellar eyelid conditioning in Fragile X syndrome. Neuron *47*, 339–352.

Kole, M.H.P., Hallermann, S., and Stuart, G.J. (2006). Single Ih channels in pyramidal neuron dendrites: properties, distribution, and impact on action potential output. J. Neurosci. Off. J. Soc. Neurosci. *26*, 1677–1687.

Kole, M.H.P., Letzkus, J.J., and Stuart, G.J. (2007). Axon initial segment Kv1 channels control axonal action potential waveform and synaptic efficacy. Neuron *55*, 633–647.

Krishnan, V., Graham, A., Mazei-Robison, M.S., Lagace, D.C., Kim, K.-S., Birnbaum, S., Eisch, A.J., Han, P.-L., Storm, D.R., Zachariou, V., et al. (2008). Calcium-sensitive adenylyl cyclases in depression and anxiety: behavioral and biochemical consequences of isoform targeting. Biol. Psychiatry *64*, 336–343.

Krueger, D.D., Osterweil, E.K., Chen, S.P., Tye, L.D., and Bear, M.F. (2011). Cognitive dysfunction and prefrontal synaptic abnormalities in a mouse model of fragile X syndrome. Proc. Natl. Acad. Sci. U. S. A. *108*, 2587–2592.

Kuo, A.G., Lee, G., McKay, B.M., and Disterhoft, J.F. (2008). Enhanced neuronal excitability in rat CA1 pyramidal neurons following trace eyeblink conditioning acquisition is not due to alterations in I M. Neurobiol. Learn. Mem. *89*, 125–133.

Kwon, H., Menon, V., Eliez, S., Warsofsky, I.S., White, C.D., Dyer-Friedman, J., Taylor, A.K., Glover, G.H., and Reiss, A.L. (2001). Functional neuroanatomy of visuospatial working memory in fragile X syndrome: relation to behavioral and molecular measures. Am. J. Psychiatry *158*, 1040–1051.

Lai, H.C., and Jan, L.Y. (2006). The distribution and targeting of neuronal voltage-gated ion channels. Nat. Rev. Neurosci. *7*, 548–562.

Larkum, M.E., Waters, J., Sakmann, B., and Helmchen, F. (2007). Dendritic spikes in apical dendrites of neocortical layer 2/3 pyramidal neurons. J. Neurosci. Off. J. Soc. Neurosci. *27*, 8999–9008.

Larkum, M.E., Nevian, T., Sandler, M., Polsky, A., and Schiller, J. (2009). Synaptic integration in tuft dendrites of layer 5 pyramidal neurons: a new unifying principle. Science *325*, 756–760.

Laubach, M., Amarante, L.M., Swanson, K., and White, S.R. (2018). What, If Anything, Is Rodent Prefrontal Cortex? ENeuro *5*.

Laurent, V., and Westbrook, R.F. (2008). Distinct contributions of the basolateral amygdala and the medial prefrontal cortex to learning and relearning extinction of context conditioned fear. Learn. Mem. Cold Spring Harb. N *15*, 657–666.

LeDoux, J. (2003). The emotional brain, fear, and the amygdala. Cell. Mol. Neurobiol. *23*, 727–738.

Lee, H.Y., Ge, W.-P., Huang, W., He, Y., Wang, G.X., Rowson-Baldwin, A., Smith, S.J., Jan, Y.N., and Jan, L.Y. (2011). Bidirectional regulation of dendritic voltage-gated potassium channels by the fragile X mental retardation protein. Neuron *72*, 630–642.

Lefkowitz, R.J., and Shenoy, S.K. (2005). Transduction of receptor signals by beta-arrestins. Science *308*, 512–517.

Lesburguères, E., Gobbo, O.L., Alaux-Cantin, S., Hambucken, A., Trifilieff, P., and Bontempi, B. (2011). Early Tagging of Cortical Networks Is Required for the Formation of Enduring Associative Memory. Science *331*, 924–928.

Lewis, A.S., and Chetkovich, D.M. (2011). HCN channels in behavior and neurological disease: too hyper or not active enough? Mol. Cell. Neurosci. *46*, 357–367.

Lewis, D.A., and González-Burgos, G. (2008). Neuroplasticity of neocortical circuits in schizophrenia. Neuropsychopharmacol. Off. Publ. Am. Coll. Neuropsychopharmacol. *33*, 141–165.

Li, J., Pelletier, M.R., Perez Velazquez, J.-L., and Carlen, P.L. (2002). Reduced cortical synaptic plasticity and GluR1 expression associated with fragile X mental retardation protein deficiency. Mol. Cell. Neurosci. *19*, 138–151.

Liao, L., Park, S.K., Xu, T., Vanderklish, P., and Yates, J.R. (2008). Quantitative proteomic analysis of primary neurons reveals diverse changes in synaptic protein content in fmr1 knockout mice. Proc. Natl. Acad. Sci. U. S. A. *105*, 15281–15286.

Little, J.P., and Carter, A.G. (2012). Subcellular synaptic connectivity of layer 2 pyramidal neurons in the medial prefrontal cortex. J. Neurosci. Off. J. Soc. Neurosci. *32*, 12808–12819.

Liu, B., Li, Y., Stackpole, E.E., Novak, A., Gao, Y., Zhao, Y., Zhao, X., and Richter, J.D. (2018). Regulatory discrimination of mRNAs by FMRP controls mouse adult neural stem cell differentiation. Proc. Natl. Acad. Sci. U. S. A. *115*, E11397–E11405.

Loos, M., Pattij, T., Janssen, M.C.W., Counotte, D.S., Schoffelmeer, A.N.M., Smit, A.B., Spijker, S., and van Gaalen, M.M. (2010). Dopamine receptor D1/D5 gene expression in the medial prefrontal cortex predicts impulsive choice in rats. Cereb. Cortex N. Y. N 1991 *20*, 1064–1070.

Lozano, R., Azarang, A., Wilaisakditipakorn, T., and Hagerman, R.J. (2016). Fragile X syndrome: A review of clinical management. Intractable Rare Dis. Res. *5*, 145–157.

Lubs, H.A. (1969). A marker X chromosome. Am. J. Hum. Genet. *21*, 231–244.

Luedtke, R.R., Mishra, Y., Wang, Q., Griffin, S.A., Bell-Horner, C., Taylor, M., Vangveravong, S., Dillon, G.H., Huang, R.-Q., Reichert, D.E., et al. (2012). Comparison of the binding and functional

properties of two structurally different D2 dopamine receptor subtype selective compounds. ACS Chem. Neurosci. *3*, 1050–1062.

Luján, R. (2010). Organisation of potassium channels on the neuronal surface. J. Chem. Neuroanat. *40*, 1–20.

Maes, B., Fryns, J.P., Van Walleghem, M., and Van den Berghe, H. (1994). Cognitive functioning and information processing of adult mentally retarded men with fragile-X syndrome. Am. J. Med. Genet. *50*, 190–200.

Magee, J.C. (2000). Dendritic integration of excitatory synaptic input. Nat. Rev. Neurosci. *1*, 181–190.

Magee, J.C., and Johnston, D. (2005). Plasticity of dendritic function. Curr. Opin. Neurobiol. *15*, 334–342.

Malin, S.A., and Nerbonne, J.M. (2002). Delayed rectifier K+ currents, IK, are encoded by Kv2 alpha-subunits and regulate tonic firing in mammalian sympathetic neurons. J. Neurosci. Off. J. Soc. Neurosci. *22*, 10094–10105.

Mamiya, N., Fukushima, H., Suzuki, A., Matsuyama, Z., Homma, S., Frankland, P.W., and Kida, S. (2009). Brain region-specific gene expression activation required for reconsolidation and extinction of contextual fear memory. J. Neurosci. Off. J. Soc. Neurosci. *29*, 402–413.

Mannoury la Cour, C., Salles, M.-J., Pasteau, V., and Millan, M.J. (2011). Signaling pathways leading to phosphorylation of Akt and GSK-3β by activation of cloned human and rat cerebral $D_2$and D_3 receptors. Mol. Pharmacol. *79*, 91–105.

Maren, S., and Quirk, G.J. (2004). Neuronal signalling of fear memory. Nat. Rev. Neurosci. *5*, 844–852.

Mark, M.D., and Herlitze, S. (2000). G-protein mediated gating of inward-rectifier K+ channels. Eur. J. Biochem. *267*, 5830–5836.

Markram, H., Toledo-Rodriguez, M., Wang, Y., Gupta, A., Silberberg, G., and Wu, C. (2004). Interneurons of the neocortical inhibitory system. Nat. Rev. Neurosci. *5*, 793–807.

Markram, H., Muller, E., Ramaswamy, S., Reimann, M.W., Abdellah, M., Sanchez, C.A., Ailamaki, A., Alonso-Nanclares, L., Antille, N., Arsever, S., et al. (2015). Reconstruction and Simulation of Neocortical Microcircuitry. Cell *163*, 456–492.

Marsh, R., Zhu, H., Wang, Z., Skudlarski, P., and Peterson, B.S. (2007). A developmental fMRI study of self-regulatory control in Tourette's syndrome. Am. J. Psychiatry *164*, 955–966.

Martin, J.P., and Bell, J. (1943). A PEDIGREE OF MENTAL DEFECT SHOWING SEX-LINKAGE. J. Neurol. Psychiatry *6*, 154–157.

Maviel, T., Durkin, T.P., Menzaghi, F., and Bontempi, B. (2004). Sites of Neocortical Reorganization Critical for Remote Spatial Memory. Science *305*, 96–99.

Mazzocco, M.M., Hagerman, R.J., Cronister-Silverman, A., and Pennington, B.F. (1992). Specific frontal lobe deficits among women with the fragile X gene. J. Am. Acad. Child Adolesc. Psychiatry *31*, 1141–1148.

McCary, L.M., and Roberts, J.E. (2013). Early identification of autism in fragile X syndrome: a review. J. Intellect. Disabil. Res. JIDR *57*, 803–814.

McKay, B.M., Matthews, E.A., Oliveira, F.A., and Disterhoft, J.F. (2009). Intrinsic Neuronal Excitability Is Reversibly Altered by a Single Experience in Fear Conditioning. J. Neurophysiol. *102*, 2763–2770.

Meredith, R.M., Holmgren, C.D., Weidum, M., Burnashev, N., and Mansvelder, H.D. (2007). Increased threshold for spike-timing-dependent plasticity is caused by unreliable calcium signaling in mice lacking fragile X gene FMR1. Neuron *54*, 627–638.

Messier, C., Mourre, C., Bontempi, B., Sif, J., Lazdunski, M., and Destrade, C. (1991). Effect of apamin, a toxin that inhibits Ca(2+)-dependent K+ channels, on learning and memory processes. Brain Res. *551*, 322–326.

Migliore, M., and Shepherd, G.M. (2002). Emerging rules for the distributions of active dendritic conductances. Nat. Rev. Neurosci. *3*, 362–370.

Miller, E.K. (2000a). The prefrontal cortex and cognitive control. Nat. Rev. Neurosci. *1*, 59–65.

Miller, E.K. (2000b). The prefrontal cortex and cognitive control. Nat. Rev. Neurosci. *1*, 59–65.

Miller, E.K., and Cohen, J.D. (2001). An integrative theory of prefrontal cortex function. Annu. Rev. Neurosci. *24*, 167–202.

Miller, K.D., Pinto, D.J., and Simons, D.J. (2001). Processing in layer 4 of the neocortical circuit: new insights from visual and somatosensory cortex. Curr. Opin. Neurobiol. *11*, 488–497.

Missale, C., Nash, S.R., Robinson, S.W., Jaber, M., and Caron, M.G. (1998). Dopamine receptors: from structure to function. Physiol. Rev. *78*, 189–225.

Miyashiro, K.Y., Beckel-Mitchener, A., Purk, T.P., Becker, K.G., Barret, T., Liu, L., Carbonetto, S., Weiler, I.J., Greenough, W.T., and Eberwine, J. (2003). RNA Cargoes Associating with FMRP Reveal Deficits in Cellular Functioning in Fmr1 Null Mice. Neuron *37*, 417–431.

Molnár, Z., and Cheung, A.F.P. (2006). Towards the classification of subpopulations of layer V pyramidal projection neurons. Neurosci. Res. *55*, 105–115.

Montell, C. (2005). The TRP superfamily of cation channels. Sci. STKE Signal Transduct. Knowl. Environ. *2005*, re3.

Morishima, M., and Kawaguchi, Y. (2006). Recurrent Connection Patterns of Corticostriatal Pyramidal Cells in Frontal Cortex. J. Neurosci. *26*, 4394–4405.

Moyer, J.R., Thompson, L.T., and Disterhoft, J.F. (1996). Trace eyeblink conditioning increases CA1 excitability in a transient and learning-specific manner. J. Neurosci. Off. J. Soc. Neurosci. *16*, 5536–5546.

Mozzachiodi, R., and Byrne, J.H. (2010). More than synaptic plasticity: role of nonsynaptic plasticity in learning and memory. Trends Neurosci. *33*, 17–26.

Müller, U., Cramon, D.Y. von, and Pollmann, S. (1998). D1- Versus D2-Receptor Modulation of Visuospatial Working Memory in Humans. J. Neurosci. *18*, 2720–2728.

Munir, F., Cornish, K.M., and Wilding, J. (2000). Nature of the Working Memory Deficit in Fragile-X Syndrome. Brain Cogn. *44*, 387–401.

Murphy, B.L., Arnsten, A.F., Goldman-Rakic, P.S., and Roth, R.H. (1996). Increased dopamine turnover in the prefrontal cortex impairs spatial working memory performance in rats and monkeys. Proc. Natl. Acad. Sci. *93*, 1325–1329.

Myrick, L.K., Nakamoto-Kinoshita, M., Lindor, N.M., Kirmani, S., Cheng, X., and Warren, S.T. (2014). Fragile X syndrome due to a missense mutation. Eur. J. Hum. Genet. EJHG *22*, 1185–1189.

Myrick, L.K., Deng, P.-Y., Hashimoto, H., Oh, Y.M., Cho, Y., Poidevin, M.J., Suhl, J.A., Visootsak, J., Cavalli, V., Jin, P., et al. (2015a). Independent role for presynaptic FMRP revealed by an FMR1 missense mutation associated with intellectual disability and seizures. Proc. Natl. Acad. Sci. U. S. A. *112*, 949–956.

Myrick, L.K., Hashimoto, H., Cheng, X., and Warren, S.T. (2015b). Human FMRP contains an integral tandem Agenet (Tudor) and KH motif in the amino terminal domain. Hum. Mol. Genet. *24*, 1733–1740.

Narayanan, N.S., and Laubach, M. (2006). Top-down control of motor cortex ensembles by dorsomedial prefrontal cortex. Neuron *52*, 921–931.

Narayanan, U., Nalavadi, V., Nakamoto, M., Pallas, D.C., Ceman, S., Bassell, G.J., and Warren, S.T. (2007). FMRP phosphorylation reveals an immediate-early signaling pathway triggered by group I mGluR and mediated by PP2A. J. Neurosci. Off. J. Soc. Neurosci. *27*, 14349–14357.

Narayanan, U., Nalavadi, V., Nakamoto, M., Thomas, G., Ceman, S., Bassell, G.J., and Warren, S.T. (2008). S6K1 phosphorylates and regulates fragile X mental retardation protein (FMRP) with the neuronal protein synthesis-dependent mammalian target of rapamycin (mTOR) signaling cascade. J. Biol. Chem. *283*, 18478–18482.

Neves, S.R., Ram, P.T., and Iyengar, R. (2002). G protein pathways. Science *296*, 1636–1639.

Nishi, A., Snyder, G.L., Fienberg, A.A., Fisone, G., Aperia, A., Nairn, A.C., and Greengard, P. (1999a). Requirement for DARPP-32 in mediating effect of dopamine D2 receptor activation. Eur. J. Neurosci. *11*, 2589–2592.

Nishi, A., Snyder, G.L., Nairn, A.C., and Greengard, P. (1999b). Role of calcineurin and protein phosphatase-2A in the regulation of DARPP-32 dephosphorylation in neostriatal neurons. J. Neurochem. *72*, 2015–2021.

Norris, A.J., and Nerbonne, J.M. (2010). Molecular dissection of I(A) in cortical pyramidal neurons reveals three distinct components encoded by Kv4.2, Kv4.3, and Kv1.4 alpha-subunits. J. Neurosci. Off. J. Soc. Neurosci. *30*, 5092–5101.

Notomi, T., and Shigemoto, R. (2004). Immunohistochemical localization of Ih channel subunits, HCN1-4, in the rat brain. J. Comp. Neurol. *471*, 241–276.

Nusser, Z. (2012). Differential subcellular distribution of ion channels and the diversity of neuronal function. Curr. Opin. Neurobiol. *22*, 366–371.

Oberlaender, M., Boudewijns, Z.S.R.M., Kleele, T., Mansvelder, H.D., Sakmann, B., and de Kock, C.P.J. (2011). Three-dimensional axon morphologies of individual layer 5 neurons indicate cell type-specific intracortical pathways for whisker motion and touch. Proc. Natl. Acad. Sci. U. S. A. *108*, 4188–4193.

Oberle, I., Rousseau, F., Heitz, D., Kretz, C., Devys, D., Hanauer, A., Boue, J., Bertheas, M.F., and Mandel, J.L. (1991). Instability of a 550-base pair DNA segment and abnormal methylation in fragile X syndrome. Science *252*, 1097–1102.

Oh, M.M., Kuo, A.G., Wu, W.W., Sametsky, E.A., and Disterhoft, J.F. (2003). Watermaze learning enhances excitability of CA1 pyramidal neurons. J. Neurophysiol. *90*, 2171–2179.

Oh, M.M., McKay, B.M., Power, J.M., and Disterhoft, J.F. (2009). Learning-related postburst afterhyperpolarization reduction in CA1 pyramidal neurons is mediated by protein kinase A. Proc. Natl. Acad. Sci. U. S. A. *106*, 1620–1625.

O'Leary, T., van Rossum, M.C.W., and Wyllie, D.J.A. (2010). Homeostasis of intrinsic excitability in hippocampal neurones: dynamics and mechanism of the response to chronic depolarization. J. Physiol. *588*, 157–170.

Orsini, C.A., Kim, J.H., Knapska, E., and Maren, S. (2011). Hippocampal and prefrontal projections to the basal amygdala mediate contextual regulation of fear after extinction. J. Neurosci. Off. J. Soc. Neurosci. *31*, 17269–17277.

Otsuka, T., and Kawaguchi, Y. (2008). Firing-Pattern-Dependent Specificity of Cortical Excitatory Feed-Forward Subnetworks. J. Neurosci. *28*, 11186–11195.

Ott, T., and Nieder, A. (2019). Dopamine and Cognitive Control in Prefrontal Cortex. Trends Cogn. Sci. *23*, 213–234.

Pape, H.C. (1996). Queer current and pacemaker: the hyperpolarization-activated cation current in neurons. Annu. Rev. Physiol. *58*, 299–327.

Paradee, W., Melikian, H.E., Rasmussen, D.L., Kenneson, A., Conn, P.J., and Warren, S.T. (1999). Fragile X mouse: strain effects of knockout phenotype and evidence suggesting deficient amygdala function. Neuroscience *94*, 185–192.

Peineau, S., Bradley, C., Taghibiglou, C., Doherty, A., Bortolotto, Z.A., Wang, Y.T., and Collingridge, G.L. (2008). The role of GSK-3 in synaptic plasticity. Br. J. Pharmacol. *153 Suppl 1*, S428-437.

Peters, H.C., Hu, H., Pongs, O., Storm, J.F., and Isbrandt, D. (2005). Conditional transgenic suppression of M channels in mouse brain reveals functions in neuronal excitability, resonance and behavior. Nat. Neurosci. *8*, 51–60.

Peters, J., Kalivas, P.W., and Quirk, G.J. (2009). Extinction circuits for fear and addiction overlap in prefrontal cortex. Learn. Mem. Cold Spring Harb. N *16*, 279–288.

Petilla Interneuron Nomenclature Group, Ascoli, G.A., Alonso-Nanclares, L., Anderson, S.A., Barrionuevo, G., Benavides-Piccione, R., Burkhalter, A., Buzsáki, G., Cauli, B., Defelipe, J., et al. (2008). Petilla terminology: nomenclature of features of GABAergic interneurons of the cerebral cortex. Nat. Rev. Neurosci. *9*, 557–568.

Pi, H.-J., Hangya, B., Kvitsiani, D., Sanders, J.I., Huang, Z.J., and Kepecs, A. (2013). Cortical interneurons that specialize in disinhibitory control. Nature *503*, 521–524.

Pieretti, M., Zhang, F., Fu, Y.-H., Warren, S.T., Oostra, B.A., Caskey, C.T., and Nelson, D.L. (1991). Absence of expression of the FMR-1 gene in fragile X syndrome. Cell *66*, 817–822.

Pillai, G., Brown, N.A., McAllister, G., Milligan, G., and Seabrook, G.R. (1998). Human D2 and D4 dopamine receptors couple through betagamma G-protein subunits to inwardly rectifying K+ channels (GIRK1) in a Xenopus oocyte expression system: selective antagonism by L-741,626 and L-745,870 respectively. Neuropharmacology *37*, 983–987.

Popescu, A.T., Zhou, M.R., and Poo, M. (2016). Phasic dopamine release in the medial prefrontal cortex enhances stimulus discrimination. Proc. Natl. Acad. Sci. *113*, E3169–E3176.

Posner, M.I., Rothbart, M.K., Sheese, B.E., and Tang, Y. (2007). The anterior cingulate gyrus and the mechanism of self-regulation. Cogn. Affect. Behav. Neurosci. *7*, 391–395.

Poulin, J.-F., Tasic, B., Hjerling-Leffler, J., Trimarchi, J.M., and Awatramani, R. (2016). Disentangling neural cell diversity using single-cell transcriptomics. Nat. Neurosci. *19*, 1131–1141.

Pratt, K.G., and Aizenman, C.D. (2007). Homeostatic regulation of intrinsic excitability and synaptic transmission in a developing visual circuit. J. Neurosci. Off. J. Soc. Neurosci. *27*, 8268–8277.

Preston, A.R., and Eichenbaum, H. (2013). Interplay of hippocampus and prefrontal cortex in memory. Curr. Biol. CB *23*, R764-773.

Pretto, D., Yrigollen, C.M., Tang, H.-T., Williamson, J., Espinal, G., Iwahashi, C.K., Durbin-Johnson, B., Hagerman, R.J., Hagerman, P.J., and Tassone, F. (2014). Clinical and molecular implications of mosaicism in FMR1 full mutations. Front. Genet. *5*, 318.

Puig, M.V., Rose, J., Schmidt, R., and Freund, N. (2014). Dopamine modulation of learning and memory in the prefrontal cortex: insights from studies in primates, rodents, and birds. Front. Neural Circuits *8*.

Quirk, G.J., and Mueller, D. (2008). Neural mechanisms of extinction learning and retrieval. Neuropsychopharmacol. Off. Publ. Am. Coll. Neuropsychopharmacol. *33*, 56–72.

Radnikow, G., and Feldmeyer, D. (2018). Layer- and Cell Type-Specific Modulation of Excitatory Neuronal Activity in the Neocortex. Front. Neuroanat. *12*, 1.

Rajasethupathy, P., Sankaran, S., Marshel, J.H., Kim, C.K., Ferenczi, E., Lee, S.Y., Berndt, A., Ramakrishnan, C., Jaffe, A., Lo, M., et al. (2015). Projections from neocortex mediate top-down control of memory retrieval. Nature *526*, 653–659.

Reiss, A.L., Lee, J., and Freund, L. (1994). Neuroanatomy of fragile X syndrome: the temporal lobe. Neurology *44*, 1317–1324.

Restivo, L., Vetere, G., Bontempi, B., and Ammassari-Teule, M. (2009). The formation of recent and remote memory is associated with time-dependent formation of dendritic spines in the hippocampus and anterior cingulate cortex. J. Neurosci. Off. J. Soc. Neurosci. *29*, 8206–8214.

Ridderinkhof, K.R., Ullsperger, M., Crone, E.A., and Nieuwenhuis, S. (2004). The role of the medial frontal cortex in cognitive control. Science *306*, 443–447.

Robinson, R.B., and Siegelbaum, S.A. (2003). Hyperpolarization-activated cation currents: from molecules to physiological function. Annu. Rev. Physiol. *65*, 453–480.

Robinson, S.W., and Caron, M.G. (1997). Selective inhibition of adenylyl cyclase type V by the dopamine D3 receptor. Mol. Pharmacol. *52*, 508–514.

Roche, K.W., O'Brien, R.J., Mammen, A.L., Bernhardt, J., and Huganir, R.L. (1996). Characterization of multiple phosphorylation sites on the AMPA receptor GluR1 subunit. Neuron *16*, 1179–1188.

Rogawski, M.A. (2000). KCNQ2/KCNQ3 K+ channels and the molecular pathogenesis of epilepsy: implications for therapy. Trends Neurosci. *23*, 393–398.

Rosenkranz, J.A., Frick, A., and Johnston, D. (2009). Kinase-dependent modification of dendritic excitability after long-term potentiation. J. Physiol. *587*, 115–125.

Routh, B.N., Johnston, D., and Brager, D.H. (2013). Loss of Functional A-Type Potassium Channels in the Dendrites of CA1 Pyramidal Neurons from a Mouse Model of Fragile X Syndrome. J. Neurosci. *33*, 19442–19450.

Runyan, J.D., Moore, A.N., and Dash, P.K. (2004). A role for prefrontal cortex in memory storage for trace fear conditioning. J. Neurosci. Off. J. Soc. Neurosci. *24*, 1288–1295.

Rushworth, M.F.S., Noonan, M.P., Boorman, E.D., Walton, M.E., and Behrens, T.E. (2011). Frontal cortex and reward-guided learning and decision-making. Neuron *70*, 1054–1069.

Saar, D., Grossman, Y., and Barkai, E. (1998). Reduced after-hyperpolarization in rat piriform cortex pyramidal neurons is associated with increased learning capability during operant conditioning. Eur. J. Neurosci. *10*, 1518–1523.

Sah, P., and Faber, E.S.L. (2002). Channels underlying neuronal calcium-activated potassium currents. Prog. Neurobiol. *66*, 345–353.

Sahakian, B.J., Sarna, G.S., Kantamaneni, B.D., Jackson, A., Hutson, P.H., and Curzon, G. (1985). Association between learning and cortical catecholamines in non-drug-treated rats. Psychopharmacology (Berl.) *86*, 339–343.

Sailer, C.A., Kaufmann, W.A., Marksteiner, J., and Knaus, H.-G. (2004). Comparative immunohistochemical distribution of three small-conductance Ca2+-activated potassium channel subunits, SK1, SK2, and SK3 in mouse brain. Mol. Cell. Neurosci. *26*, 458–469.

Salles, M.-J., Hervé, D., Rivet, J.-M., Longueville, S., Millan, M.J., Girault, J.-A., and Mannoury la Cour, C. (2013). Transient and rapid activation of Akt/GSK-3β and mTORC1 signaling by D3 dopamine receptor stimulation in dorsal striatum and nucleus accumbens. J. Neurochem. *125*, 532–544.

Sánchez-Rodríguez, I., Temprano-Carazo, S., Nájera, A., Djebari, S., Yajeya, J., Gruart, A., Delgado-García, J.M., Jiménez-Díaz, L., and Navarro-López, J.D. (2017). Activation of G-protein-gated inwardly rectifying potassium (Kir3/GirK) channels rescues hippocampal functions in a mouse model of early amyloid-β pathology. Sci. Rep. *7*.

Sanes, J.R., and Masland, R.H. (2015). The Types of Retinal Ganglion Cells: Current Status and Implications for Neuronal Classification. Annu. Rev. Neurosci. *38*, 221–246.

Santini, E., and Porter, J.T. (2010). M-type potassium channels modulate the intrinsic excitability of infralimbic neurons and regulate fear expression and extinction. J. Neurosci. Off. J. Soc. Neurosci. *30*, 12379–12386.

Santini, E., Valjent, E., Usiello, A., Carta, M., Borgkvist, A., Girault, J.-A., Hervé, D., Greengard, P., and Fisone, G. (2007). Critical involvement of cAMP/DARPP-32 and extracellular signal-regulated protein kinase signaling in L-DOPA-induced dyskinesia. J. Neurosci. Off. J. Soc. Neurosci. *27*, 6995–7005.

Santini, E., Quirk, G.J., and Porter, J.T. (2008). Fear conditioning and extinction differentially modify the intrinsic excitability of infralimbic neurons. J. Neurosci. Off. J. Soc. Neurosci. *28*, 4028–4036.

Santoro, M.R., Bray, S.M., and Warren, S.T. (2012). Molecular mechanisms of fragile X syndrome: a twenty-year perspective. Annu. Rev. Pathol. *7*, 219–245.

Sausbier, U., Sausbier, M., Sailer, C.A., Arntz, C., Knaus, H.-G., Neuhuber, W., and Ruth, P. (2006). Ca2+ -activated K+ channels of the BK-type in the mouse brain. Histochem. Cell Biol. *125*, 725–741.

Sawaguchi, T., and Goldman-Rakic, P.S. (1991). D1 dopamine receptors in prefrontal cortex: involvement in working memory. Science *251*, 947–950.

Sawaguchi, T., and Goldman-Rakic, P.S. (1994). The role of D1-dopamine receptor in working memory: local injections of dopamine antagonists into the prefrontal cortex of rhesus monkeys performing an oculomotor delayed-response task. J. Neurophysiol. *71*, 515–528.

Sawaguchi, T., Matsumura, M., and Kubota, K. (1990). Effects of dopamine antagonists on neuronal activity related to a delayed response task in monkey prefrontal cortex. J. Neurophysiol. *63*, 1401–1412.

Schaefer, G.B., and Mendelsohn, N.J. (2008). Genetics evaluation for the etiologic diagnosis of autism spectrum disorders. Genet. Med. Off. J. Am. Coll. Med. Genet. *10*, 4–12.

Schiffmann, S.N., Desdouits, F., Menu, R., Greengard, P., Vincent, J.D., Vanderhaeghen, J.J., and Girault, J.A. (1998). Modulation of the voltage-gated sodium current in rat striatal neurons by DARPP-32, an inhibitor of protein phosphatase. Eur. J. Neurosci. *10*, 1312–1320.

Schrader, L.A., Anderson, A.E., Mayne, A., Pfaffinger, P.J., and Sweatt, J.D. (2002). PKA modulation of Kv4.2-encoded A-type potassium channels requires formation of a supramolecular complex. J. Neurosci. Off. J. Soc. Neurosci. *22*, 10123–10133.

Schubert, D., Kötter, R., and Staiger, J.F. (2007). Mapping functional connectivity in barrel-related columns reveals layer- and cell type-specific microcircuits. Brain Struct. Funct. *212*, 107–119.

Seamans, J.K., and Yang, C.R. (2004). The principal features and mechanisms of dopamine modulation in the prefrontal cortex. Prog. Neurobiol. *74*, 1–58.

Seamans, J.K., Floresco, S.B., and Phillips, A.G. (1998). D1 Receptor Modulation of Hippocampal–Prefrontal Cortical Circuits Integrating Spatial Memory with Executive Functions in the Rat. J. Neurosci. *18*, 1613–1621.

Sehgal, M., Ehlers, V.L., and Moyer, J.R. (2014). Learning enhances intrinsic excitability in a subset of lateral amygdala neurons. Learn. Mem. Cold Spring Harb. N *21*, 161–170.

Senn, V., Wolff, S.B.E., Herry, C., Grenier, F., Ehrlich, I., Gründemann, J., Fadok, J.P., Müller, C., Letzkus, J.J., and Lüthi, A. (2014). Long-range connectivity defines behavioral specificity of amygdala neurons. Neuron *81*, 428–437.

Seong, H.J., and Carter, A.G. (2012). D1 receptor modulation of action potential firing in a subpopulation of layer 5 pyramidal neurons in the prefrontal cortex. J. Neurosci. Off. J. Soc. Neurosci. *32*, 10516–10521.

Sesack, S.R., Deutch, A.Y., Roth, R.H., and Bunney, B.S. (1989). Topographical organization of the efferent projections of the medial prefrontal cortex in the rat: an anterograde tract-tracing study with Phaseolus vulgaris leucoagglutinin. J. Comp. Neurol. *290*, 213–242.

Shapiro, E., Biezuner, T., and Linnarsson, S. (2013). Single-cell sequencing-based technologies will revolutionize whole-organism science. Nat. Rev. Genet. *14*, 618–630.

Shin, L.M., Orr, S.P., Carson, M.A., Rauch, S.L., Macklin, M.L., Lasko, N.B., Peters, P.M., Metzger, L.J., Dougherty, D.D., Cannistraro, P.A., et al. (2004). Regional cerebral blood flow in the amygdala and medial prefrontal cortex during traumatic imagery in male and female Vietnam veterans with PTSD. Arch. Gen. Psychiatry *61*, 168–176.

Shu, Y., Yu, Y., Yang, J., and McCormick, D.A. (2007). Selective control of cortical axonal spikes by a slowly inactivating K+ current. Proc. Natl. Acad. Sci. U. S. A. *104*, 11453–11458.

Simon, H. (1981). [Dopaminergic A10 neurons and frontal system (author's transl)]. J. Physiol. (Paris) *77*, 81–95.

Siomi, H., Siomi, M.C., Nussbaum, R.L., and Dreyfuss, G. (1993). The protein product of the fragile X gene, FMR1, has characteristics of an RNA-binding protein. Cell *74*, 291–298.

Sjöström, P.J., Rancz, E.A., Roth, A., and Häusser, M. (2008). Dendritic excitability and synaptic plasticity. Physiol. Rev. *88*, 769–840.

Song, C., Detert, J.A., Sehgal, M., and Moyer, J.R. (2012). Trace fear conditioning enhances synaptic and intrinsic plasticity in rat hippocampus. J. Neurophysiol. *107*, 3397–3408.

Sotres-Bayon, F., and Quirk, G.J. (2010). Prefrontal control of fear: more than just extinction. Curr. Opin. Neurobiol. *20*, 231–235.

Sotres-Bayon, F., Diaz-Mataix, L., Bush, D.E.A., and LeDoux, J.E. (2009). Dissociable roles for the ventromedial prefrontal cortex and amygdala in fear extinction: NR2B contribution. Cereb. Cortex N. Y. N 1991 *19*, 474–482.

Spruston, N., and Johnston, D. (1992). Perforated patch-clamp analysis of the passive membrane properties of three classes of hippocampal neurons. J. Neurophysiol. *67*, 508–529.

van der Staay, F.J., Fanelli, R.J., Blokland, A., and Schmidt, B.H. (1999). Behavioral effects of apamin, a selective inhibitor of the SK(Ca)-channel, in mice and rats. Neurosci. Biobehav. Rev. *23*, 1087–1110.

Stackman, R.W., Hammond, R.S., Linardatos, E., Gerlach, A., Maylie, J., Adelman, J.P., and Tzounopoulos, T. (2002). Small conductance Ca2+-activated K+ channels modulate synaptic plasticity and memory encoding. J. Neurosci. Off. J. Soc. Neurosci. *22*, 10163–10171.

Stevenson, C.W. (2011). Role of amygdala-prefrontal cortex circuitry in regulating the expression of contextual fear memory. Neurobiol. Learn. Mem. *96*, 315–323.

Stocker, M., Hirzel, K., D'hoedt, D., and Pedarzani, P. (2004). Matching molecules to function: neuronal Ca2+-activated K+ channels and afterhyperpolarizations. Toxicon Off. J. Int. Soc. Toxinology *43*, 933–949.

Stuart, G.J., and Sakmann, B. (1994). Active propagation of somatic action potentials into neocortical pyramidal cell dendrites. Nature *367*, 69–72.

Stuart, G., Spruston, N., Sakmann, B., and Häusser, M. (1997a). Action potential initiation and backpropagation in neurons of the mammalian CNS. Trends Neurosci. *20*, 125–131.

Stuart, G., Schiller, J., and Sakmann, B. (1997b). Action potential initiation and propagation in rat neocortical pyramidal neurons. J. Physiol. *505 (Pt 3)*, 617–632.

Sunahara, R.K., and Taussig, R. (2002). Isoforms of mammalian adenylyl cyclase: multiplicities of signaling. Mol. Interv. *2*, 168–184.

Surmeier, D.J., Bargas, J., Hemmings, H.C., Nairn, A.C., and Greengard, P. (1995). Modulation of calcium currents by a D1 dopaminergic protein kinase/phosphatase cascade in rat neostriatal neurons. Neuron *14*, 385–397.

Sutton, M.A., and Schuman, E.M. (2006). Dendritic protein synthesis, synaptic plasticity, and memory. Cell *127*, 49–58.

Svensson, V., Natarajan, K.N., Ly, L.-H., Miragaia, R.J., Labalette, C., Macaulay, I.C., Cvejic, A., and Teichmann, S.A. (2017). Power analysis of single-cell RNA-sequencing experiments. Nat. Methods *14*, 381–387.

Taniguchi, H., He, M., Wu, P., Kim, S., Paik, R., Sugino, K., Kvitsani, D., Fu, Y., Lu, J., Lin, Y., et al. (2011). A Resource of Cre Driver Lines for Genetic Targeting of GABAergic Neurons in Cerebral Cortex. Neuron *71*, 995–1013.

Telias, M., Segal, M., and Ben-Yosef, D. (2013). Neural differentiation of Fragile X human Embryonic Stem Cells reveals abnormal patterns of development despite successful neurogenesis. Dev. Biol. *374*, 32–45.

Tesmer, J.J., Sunahara, R.K., Gilman, A.G., and Sprang, S.R. (1997). Crystal structure of the catalytic domains of adenylyl cyclase in a complex with Gsalpha.GTPgammaS. Science *278*, 1907–1916.

Thompson, L.T., Moyer, J.R., and Disterhoft, J.F. (1996). Transient changes in excitability of rabbit CA3 neurons with a time course appropriate to support memory consolidation. J. Neurophysiol. *76*, 1836–1849.

Thomson, A.M., and Lamy, C. (2007). Functional maps of neocortical local circuitry. Front. Neurosci. *1*, 19–42.

Thomson, S.R., Seo, S.S., Barnes, S.A., Louros, S.R., Muscas, M., Dando, O., Kirby, C., Wyllie, D.J.A., Hardingham, G.E., Kind, P.C., et al. (2017). Cell-Type-Specific Translation Profiling Reveals a Novel Strategy for Treating Fragile X Syndrome. Neuron *95*, 550-563.e5.

Todd, P.K., Malter, J.S., and Mack, K.J. (2003). Whisker stimulation-dependent translation of FMRP in the barrel cortex requires activation of type I metabotropic glutamate receptors. Brain Res. Mol. Brain Res. *110*, 267–278.

Tolmie, J. (2002). Fragile X Syndrome - Diagnosis, Treatment and Research: Third edition. Editors Randi Jenssen Hagerman, Paul J Hagerman. £65.50 HB, £31.00 PB. Baltimore: The Johns Hopkins University Press. 2002. ISBN 0-8018-6844-0. J. Med. Genet. *39*, 783–783.

Trapnell, C. (2015). Defining cell types and states with single-cell genomics. Genome Res. *25*, 1491–1498.

Tremblay, R., Lee, S., and Rudy, B. (2016). GABAergic Interneurons in the Neocortex: From Cellular Properties to Circuits. Neuron *91*, 260–292.

Trimmer, J.S., and Rhodes, K.J. (2004). Localization of voltage-gated ion channels in mammalian brain. Annu. Rev. Physiol. *66*, 477–519.

Tronel, S., and Sara, S.J. (2003). Blockade of NMDA receptors in prelimbic cortex induces an enduring amnesia for odor-reward associative learning. J. Neurosci. Off. J. Soc. Neurosci. *23*, 5472–5476.

Turrigiano, G., Abbott, L.F., and Marder, E. (1994). Activity-dependent changes in the intrinsic properties of cultured neurons. Science *264*, 974–977.

Undieh, A.S. (2010). Pharmacology of signaling induced by dopamine D(1)-like receptor activation. Pharmacol. Ther. *128*, 37–60.

Vacher, H., Mohapatra, D.P., and Trimmer, J.S. (2008). Localization and targeting of voltage-dependent ion channels in mammalian central neurons. Physiol. Rev. *88*, 1407–1447.

Van De Werd, H.J.J.M., Rajkowska, G., Evers, P., and Uylings, H.B.M. (2010). Cytoarchitectonic and chemoarchitectonic characterization of the prefrontal cortical areas in the mouse. Brain Struct. Funct. *214*, 339–353.

Varga, A.W., Yuan, L.-L., Anderson, A.E., Schrader, L.A., Wu, G.-Y., Gatchel, J.R., Johnston, D., and Sweatt, J.D. (2004). Calcium-calmodulin-dependent kinase II modulates Kv4.2 channel expression and upregulates neuronal A-type potassium currents. J. Neurosci. Off. J. Soc. Neurosci. *24*, 3643–3654.

Venkatachalam, K., and Montell, C. (2007). TRP Channels. Annu. Rev. Biochem. *76*, 387–417.

Verkerk, A.J., Pieretti, M., Sutcliffe, J.S., Fu, Y.H., Kuhl, D.P., Pizzuti, A., Reiner, O., Richards, S., Victoria, M.F., and Zhang, F.P. (1991). Identification of a gene (FMR-1) containing a CGG repeat coincident with a breakpoint cluster region exhibiting length variation in fragile X syndrome. Cell *65*, 905–914.

Vertes, R.P. (2004). Differential projections of the infralimbic and prelimbic cortex in the rat. Synap. N. Y. N *51*, 32–58.

Vertes, R.P. (2006). Interactions among the medial prefrontal cortex, hippocampus and midline thalamus in emotional and cognitive processing in the rat. Neuroscience *142*, 1–20.

Vertes, R.P., Hoover, W.B., Szigeti-Buck, K., and Leranth, C. (2007). Nucleus reuniens of the midline thalamus: link between the medial prefrontal cortex and the hippocampus. Brain Res. Bull. *71*, 601–609.

Vick, K.A., Guidi, M., and Stackman, R.W. (2010). In vivo pharmacological manipulation of small conductance Ca(2+)-activated K(+) channels influences motor behavior, object memory and fear conditioning. Neuropharmacology *58*, 650–659.

Vidal-Gonzalez, I., Vidal-Gonzalez, B., Rauch, S.L., and Quirk, G.J. (2006). Microstimulation reveals opposing influences of prelimbic and infralimbic cortex on the expression of conditioned fear. Learn. Mem. Cold Spring Harb. N *13*, 728–733.

Vouimba, R.-M., and Maroun, M. (2011). Learning-induced changes in mPFC-BLA connections after fear conditioning, extinction, and reinstatement of fear. Neuropsychopharmacol. Off. Publ. Am. Coll. Neuropsychopharmacol. *36*, 2276–2285.

Wamsley, J.K., Gehlert, D.R., Filloux, F.M., and Dawson, T.M. (1989). Comparison of the distribution of D-1 and D-2 dopamine receptors in the rat brain. J. Chem. Neuroanat. *2*, 119–137.

Wang, H., Wu, L.-J., Kim, S.S., Lee, F.J.S., Gong, B., Toyoda, H., Ren, M., Shang, Y.-Z., Xu, H., Liu, F., et al. (2008). FMRP acts as a key messenger for dopamine modulation in the forebrain. Neuron *59*, 634–647.

Wang, H., Kim, S.S., and Zhuo, M. (2010). Roles of fragile X mental retardation protein in dopaminergic stimulation-induced synapse-associated protein synthesis and subsequent alpha-amino-3-hydroxyl-5-methyl-4-isoxazole-4-propionate (AMPA) receptor internalization. J. Biol. Chem. *285*, 21888–21901.

Wang, H.S., Pan, Z., Shi, W., Brown, B.S., Wymore, R.S., Cohen, I.S., Dixon, J.E., and McKinnon, D. (1998). KCNQ2 and KCNQ3 potassium channel subunits: molecular correlates of the M-channel. Science *282*, 1890–1893.

Wang, Y., Markram, H., Goodman, P.H., Berger, T.K., Ma, J., and Goldman-Rakic, P.S. (2006). Heterogeneity in the pyramidal network of the medial prefrontal cortex. Nat. Neurosci. *9*, 534–542.

Washbourne, P., Dityatev, A., Scheiffele, P., Biederer, T., Weiner, J.A., Christopherson, K.S., and El-Husseini, A. (2004). Cell Adhesion Molecules in Synapse Formation. J. Neurosci. *24*, 9244–9249.

Wei, A.D., Gutman, G.A., Aldrich, R., Chandy, K.G., Grissmer, S., and Wulff, H. (2005). International Union of Pharmacology. LII. Nomenclature and molecular relationships of calcium-activated potassium channels. Pharmacol. Rev. *57*, 463–472.

Weiler, I.J., Irwin, S.A., Klintsova, A.Y., Spencer, C.M., Brazelton, A.D., Miyashiro, K., Comery, T.A., Patel, B., Eberwine, J., and Greenough, W.T. (1997). Fragile X mental retardation protein is translated near synapses in response to neurotransmitter activation. Proc. Natl. Acad. Sci. *94*, 5395–5400.

Westenbroek, R.E., Merrick, D.K., and Catterall, W.A. (1989). Differential subcellular localization of the RI and RII Na+ channel subtypes in central neurons. Neuron *3*, 695–704.

Williams, G.V., and Goldman-Rakic, P.S. (1995). Modulation of memory fields by dopamine D1 receptors in prefrontal cortex. Nature *376*, 572–575.

Wolff, S.B.E., Gründemann, J., Tovote, P., Krabbe, S., Jacobson, G.A., Müller, C., Herry, C., Ehrlich, I., Friedrich, R.W., Letzkus, J.J., et al. (2014). Amygdala interneuron subtypes control fear learning through disinhibition. Nature *509*, 453–458.

Xu, N., Harnett, M.T., Williams, S.R., Huber, D., O'Connor, D.H., Svoboda, K., and Magee, J.C. (2012). Nonlinear dendritic integration of sensory and motor input during an active sensing task. Nature *492*, 247–251.

Yamada, S.-I., Takechi, H., Kanchiku, I., Kita, T., and Kato, N. (2004). Small-conductance Ca2+-dependent K+ channels are the target of spike-induced Ca2+ release in a feedback regulation of pyramidal cell excitability. J. Neurophysiol. *91*, 2322–2329.

Yang, C.R., and Seamans, J.K. (1996). Dopamine D1 receptor actions in layers V-VI rat prefrontal cortex neurons in vitro: modulation of dendritic-somatic signal integration. J. Neurosci. *16*, 1922–1935.

Yang, C.R., Seamans, J.K., and Gorelova, N. (1996a). Electrophysiological and morphological properties of layers V-VI principal pyramidal cells in rat prefrontal cortex in vitro. J. Neurosci. Off. J. Soc. Neurosci. *16*, 1904–1921.

Yang, C.R., Seamans, J.K., and Gorelova, N. (1996b). Electrophysiological and morphological properties of layers V-VI principal pyramidal cells in rat prefrontal cortex in vitro. J. Neurosci. Off. J. Soc. Neurosci. *16*, 1904–1921.

Yang, S., Tang, C.-M., and Yang, S. (2015). The Shaping of Two Distinct Dendritic Spikes by A-Type Voltage-Gated K+ Channels. Front. Cell. Neurosci. *9*.

Yasuda, R., Sabatini, B.L., and Svoboda, K. (2003). Plasticity of calcium channels in dendritic spines. Nat. Neurosci. *6*, 948–955.

Yu, S., Pritchard, M., Kremer, E., Lynch, M., Nancarrow, J., Baker, E., Holman, K., Mulley, J.C., Warren, S.T., Schlessinger, D., et al. (1991). Fragile X genotype characterized by an unstable region of DNA. Science *252*, 1179–1181.

Yuan, L.-L., and Chen, X. (2006). Diversity of potassium channels in neuronal dendrites. Prog. Neurobiol. *78*, 374–389.

Yuan, L.-L., Adams, J.P., Swank, M., Sweatt, J.D., and Johnston, D. (2002). Protein kinase modulation of dendritic K+ channels in hippocampus involves a mitogen-activated protein kinase pathway. J. Neurosci. Off. J. Soc. Neurosci. *22*, 4860–4868.

Zahrt, J., Taylor, J.R., Mathew, R.G., and Arnsten, A.F.T. (1997). Supranormal Stimulation of D1 Dopamine Receptors in the Rodent Prefrontal Cortex Impairs Spatial Working Memory Performance. J. Neurosci. *17*, 8528–8535.

Zeng, H., and Sanes, J.R. (2017). Neuronal cell-type classification: challenges, opportunities and the path forward. Nat. Rev. Neurosci. *18*, 530–546.

Zhang, W., and Linden, D.J. (2003). The other side of the engram: experience-driven changes in neuronal intrinsic excitability. Nat. Rev. Neurosci. *4*, 885–900.

Zhang, F., Vierock, J., Yizhar, O., Fenno, L.E., Tsunoda, S., Kianianmomeni, A., Prigge, M., Berndt, A., Cushman, J., Polle, J., et al. (2011). The microbial opsin family of optogenetic tools. Cell *147*, 1446–1457.

Zhang, Y., Brown, M.R., Hyland, C., Chen, Y., Kronengold, J., Fleming, M.R., Kohn, A.B., Moroz, L.L., and Kaczmarek, L.K. (2012). Regulation of neuronal excitability by interaction of fragile X mental retardation protein with slack potassium channels. J. Neurosci. Off. J. Soc. Neurosci. *32*, 15318–15327.

Zhang, Y., Bonnan, A., Bony, G., Ferezou, I., Pietropaolo, S., Ginger, M., Sans, N., Rossier, J., Oostra, B., LeMasson, G., et al. (2014). Dendritic channelopathies contribute to neocortical and sensory hyperexcitability in Fmr1(-/y) mice. Nat. Neurosci. *17*, 1701–1709.

Zhao, M.-G., Toyoda, H., Ko, S.W., Ding, H.-K., Wu, L.-J., and Zhuo, M. (2005). Deficits in trace fear memory and long-term potentiation in a mouse model for fragile X syndrome. J. Neurosci. Off. J. Soc. Neurosci. *25*, 7385–7392.

Zhou, Y., Won, J., Karlsson, M.G., Zhou, M., Rogerson, T., Balaji, J., Neve, R., Poirazi, P., and Silva, A.J. (2009). CREB regulates excitability and the allocation of memory to subsets of neurons in the amygdala. Nat. Neurosci. *12*, 1438–1443.

Zhu, X.R., Wulf, A., Schwarz, M., Isbrandt, D., and Pongs, O. (1999). Characterization of human Kv4.2 mediating a rapidly-inactivating transient voltage-sensitive K+ current. Receptors Channels *6*, 387–400.

Zingg, B., Hintiryan, H., Gou, L., Song, M.Y., Bay, M., Bienkowski, M.S., Foster, N.N., Yamashita, S., Bowman, I., Toga, A.W., et al. (2014). Neural networks of the mouse neocortex. Cell *156*, 1096–1111.